Mobility shift-affinity capillary electrophoresis for investigation of protein-metal ion interactions: aspects of method development, validation and high throughput screening

Von der Fakultät für Lebenswissenschaften

der Technischen Universität Carolo-Wilhelmina zu Braunschweig

zur Erlangung des Grades eines

Doktors der Naturwissenschaften

(Dr. rer. nat.)

genehmigte

D i s s e r t a t i o n

von Hassan Ahmad Mohammad Alhazmi
aus Alesha / Saudi Arabia

1. Referent: Professor Dr. Hermann Wätzig
2. Referent: Professor Dr. Ingo Ott
eingereicht am: 20.04.2015
mündliche Prüfung (Disputation) am: 18.06.2015

Druckjahr 2015

Vorveröffentlichungen der Dissertation

Teilergebnisse aus dieser Arbeit wurden mit Genehmigung der Fakultät für Lebenswissenschaften, vertreten durch den Mentor der Arbeit, in folgenden Beiträgen vorab veröffentlicht:

Publikationen

1. Alhazmi, H. A., Nachbar, M., Albishri H. M., Abd El-Hady, D., Redweik, S., El Deeb, S. & Wätzig, H. A comprehensive platform to investigate protein-metal ion interactions by affinity capillary electrophoresis. J. Pharm. Biomed. Anal. 107: 311–317 (2015).
2. Albishri, H. M., El Deeb, S., AlGarabli, N., AlAstal, R., Alhazmi H. A., Nachbar, M., Abd El-Hady, D. & Wätzig, H. Recent advances in affinity capillary electrophoresis for binding studies, Bioanalysis 6: 3369-3392 (2014).
3. Alhazmi, H. A., El Deeb, S, Nachbar, M., Redweik, S., Albishri H. M., Abd El-Hady, D. & Wätzig, H. Affinity capillary electrophoresis: acceleration, method transfer and precision improvement for protein-metal ion interactions. **Submitted to Journal of Separation science (2015).**

Tagungsbeiträge

1- Wätzig, H., Alhazmi, H. A., Nachbar, M., Abd El-Hady D. & Redweik, S.: Fast and validated Affinity Capillary Electrophoresis for routine binding screening assays. (poster) CEPH34-MO. HPLC 2013, Amsterdam (2013).

2- Alhazmi, H. A., Nachbar, M., Albishri H. M., Abd El-Hady, D., El Deeb, S, Redweik, S. & Wätzig, H.: Investigation for successful ACE method transfer. (poster) P7. CE-Forum, Jena (2013).

3- Alhazmi, H. A., Nachbar, M., Albishri H. M., Abd El-Hady, D., El Deeb, S., Redweik, S. & Wätzig, H.: Investigation for successful ACE method transfer. (poster) AC10. DPhG annual meeting, Freiburg (2013).

4- Nachbar, M., Alhazmi, H. A., Abd El-Hady, D., Albishri H. M., Redweik, S. & Wätzig, H.: Fast screening for protein-ion interactions using affinity capillary electrophoresis. (poster) AC05. DPhG annual meeting, Freiburg (2013).

5- Alhazmi, H. A., Nachbar, M., El Deeb, S., Abd El-Hady, D., Albishri H. M. & Wätzig, H.: Investigations of metalloproteins and their interactions by Affinity Capillary Electrophoresis. (oral) OC03. Drug analysis, Liege (2014).
6- Alhazmi, H. A., Nachbar, M., El Deeb, S., Abd El-Hady, D., Albishri H. M. & Wätzig, H.: Affinity Capillary Electrophoresis (ACE) as Reliable Technique for Studying Protein-Metal Interactions. (poster) AS14. Drug analysis, Liege (2014).
7- Alhazmi, H. A., Nachbar, M., Mozafari, M., Redweik, S., El Deeb, S., Abd El-Hady, D., Albishri H. M. & Wätzig, H.: A comprehensive platform to investigate protein-metal ion interactions by affinity capillary electrophoresis (ACE). (oral) OP 37. EuroBIC12, Zurich (2014).
8- Alhazmi, H. A., Nachbar, M., El Deeb, S., Abd El-Hady, D., Albishri H. M. & Wätzig, H.: Affinity Capillary Electrophoresis (ACE) for Fast Prediction of Protein Selectivity to Metal Ions. (poster) P 295. EuroBIC12, Zurich (2014).
9- Alhazmi, H. A., Nachbar, M., Mozafari, M., Redweik, S., El Deeb, S., Abd El-Hady, D., Albishri H. M. & Wätzig, H. Fast Estimation for Cellular Metal Ion Uptake Using Affinity Capillary Electrophoresis (ACE). (poster) MC 24. DPhG annual meeting, Frankfurt (2014).

Audioslides

1- Alhazmi, H. A., El Deeb, S. & Wätzig, H. A comprehensive platform to investigate protein-metal ion interactions by affinity capillary electrophoresis. Elsevier B. V. (2015).

ACKNOWLEDGMENT

I would like to express my deep gratitude to my supervisor Prof. Dr. Hermann Wätzig and my Co-supervisor Dr. Sami Eldeeb at the institute of Medicinal and Pharmaceutical Chemistry, TU-Braunschweig. I am deeply indebted to them for their supervisions, advices, constructive discussions during the progress of the work.

It is also a pleasure to express a deep appreciation and thanks to the members of the examination committee for finding enough time to read and evaluate this work.

I gratefully acknowledge the financial support by the funding of King AbdulAziz University, Jeddah, Saudi Arabia, provided by Vice President Prof. Dr. A. O. AlYoubi. I also thank Jazan University and the Saudi Arabian cultural office in Berlin for supporting our work by an enough grant. Furthermore, we thank Polymicro Technologies for providing the capillaries.

I am deeply thankful to the entire members of Prof. Dr. Hermann Wätzig research group, in particular the members of the ACE subgroup especially Dr. Sabine Redweik and Mr. Markus Nachbar for their kindly help.

I would like to thank all members of the institute of Medicinal and Pharmaceutical Chemistry, TU-Braunschweig, for their help and support during the work.

I would like also to express my deep gratitude to my family, father Ahmad Alhazmi, mother Fatimah Jaboor, wife Asma Alhazmi and children, Fatimah, Abdulrahman and Almotassim Billah for all the sacrifices done for me.

Dedication

To:

My Parents, Wife, Kids,

Sisters and Brother

List of Abbreviations

ACE	affinity capillary electrophoresis
ATM	analytical transfer team
AU	absorption unit
bar	Unit of pressure = 10^5 pascal (Pa) or ≈ 1 atmosphere
BGE	background electrolyte
BSA	bovine serum albumin
β-LG	β-lactoglobulin
CD	circular dichroism (CD) spectroscopy
CCE	chiral capillary electrophoresis
CE	capillary electrophoresis
CGE	capillary gel electrophoresis
CIEF	capillary isoelectric focusing
cm	centimeter = 10^{-2} meter
CN	coordination number
cnf	confidence interval
CZE	capillary zone electrophoresis
µm	micrometer = 10^{-6} meter
Da	dalton
EDTA	ethylenediaminetetraacetic acid
DIMS	direct infusion mass spectrometry
ELISA	enzyme-linked immunosorbent assay
EOF	electro-osmotic flow
ESI	electrospray ionization
FTIR	fourier transform infra-red spectroscopy
g	gram
HD	hummel-dreyer
HPAC	high-performance affinity chromatography
HSA	human serum albumin
HSAB	hard and soft acid and base theory
I.D.	internal diameter
kDa	kilodalton
kV	kilovolt

L	liter
LOD	limit of detection
mAU	milli absorption unit
MB	myoglobin
m	meter
M	molarity
MEKC	micellar electrokinetic capillary chromatography
min	minute
mL	milliliter
MS	mass spectrometry
N	normality
nL	nanoliter = 10^{-9} L
NMR	nuclear magnetic resonance
OVA	ovalbumin
pI	isoelectric point
RSD	relative standard deviation
s	second
SD	Standard deviation
SPR	surface plasmon resonance
tris	tris(hydroxymethyl)aminomethane (2-Amino-2-hydroxymethyl-propane-1,3-diol)
UV/Vis	ultraviolet/visible
VACE	vacancy affinity capillary electrophoresis
VP	vacancy-peak

List of Symbols

$\hat{\sigma}$	standard deviation
$\hat{\sigma}_{total}$	total standard deviation of the two series data
μ_a	electrophoretic mobility of an analyte
μ_{app}	apparent electrophoretic mobility of an analyte
μ_{eff}	effective electrophoretic mobility of an analyte
μ_{eof}	electrophoretic mobility of an EOF marker
μ_{prot}	electrophoretic mobility of a protein
ζ	zeta potential
ε	dielectric constant
ΔP	applied pressure
η	viscosity of the sample solution
A, or Ala	alanine
Ag	silver
Au	gold
Ba	barium
c	sample concentration
°C	centigrade, a unit of measurement for temperature
Cl^-	chloride
CO	carbon monoxide
Co	cobalt
Cr	chromium
Cu	copper
C, or Cys	cysteine
D, or Asp	aspartic acid
E	electric filed strength
E, or Glu	glutamic acid
f	number of freedom
F, or Phe	phenylalanine
F_{el}	electric force
F_s	friction force
Ga	gallium

G, or Gly	glycine
H, or His	histidine
I, Ile	isoleucine
Ir	iridium
K, Lys	lysine
K_b	binding constant
L	capillary total length
l	*capillary effective length*
L, or Leu	leucine
Li	lithium
Mo	molybdenum
M, or Met	methionine
N, or Asn	asparagine
Ni	nickel
NO_3^-	nitrate
NO	nitrogen monoxide
n	number of runs
Na	sodium
Os	osmium
P, or Pro	proline
Pd	palladium
Pt	platinum
pKa	ionization constant
Q, or Gln	glutamine
q	injected amount
q_i	overall charge of an analyte
R, or Arg	arginine
R	mobility ratio
R_f	mobility ratio of an analyte
R_i	mobility ratio of an analyte in presence of a ligand
R_c	mobility ratio of an analyte at saturation concentration of a ligand
ΔR	difference of mobility ratios = R_i- R_f

r	inner radius of the capillary
r_i	hydrodynamic radius of the charged analyte
Rh	rhodium
Ru	ruthenium
S, or Ser	serine
Se	selenium
T, or Thr	threonine
t	time
t_{eff}	effective migration time of an analyte
t_{app}	apparent migration time of an analyte
t_{eof}	migration time of an EOF marker
t_{prot}	migration time of a protein
U, or Sec	selenocysteine
U	Applied voltage
V	vanadium
V, or Val	valine
v	velocity
v_{eff}	effective electrophoretic velocity of the analyte
v_{app}	apparent electrophoretic velocity of the analyte
W, or Trp	tryptophan
$\bar{x}$	mean
Y, or Tyr	tyrosine

1 Introduction

1.1 Proteins

Proteins are essential for cell function [1, 2]. They program certain activities encoded by gene. Many of different proteins are involved in controlling the cell function by suitable coordination and control the intra and extra cellular interaction [1, 2]. Therefore, any defect on the structure or amount of these proteins will disturb the cell work program [3-5]. Diseases, which are caused by proteins, are called protepathy [6]. The aggregate forms of some protein can cause diseases. For example, the fibrils of the aggregate form of alpha-synuclein and Amyloid β peptide can cause the Parkinson's and Alzheimer's diseases, respectively [7, 8]. Furthermore, change in hemoglobin structure causes anemia such as hemoglobin S for sickle cell anemia [9]. In general, abnormal protein depositions have been reported with more than 50 diseases in human brain and other tissues [6]. Biomarker proteins such as antibodies can be used to diagnose several diseases [10]. Furthermore, proteins are increasingly being used as biopharmaceuticals for the treatment of various diseases [11]. Currently, there are different protein drugs available such as insulin, growth hormone erythropoietin and monoclonal antibodies as recombinant human proteins and other viral and bacterial proteins as vaccines [11].

Studying of protein-ligand interaction is interesting since the misfolding of active native protein could be prevented by binding with small molecule [5]. On the other hand, different protein activities could occur depending on the type of ligand, for example stimulation or inhibition of macromolecular receptors [12].

1.1.1 Structure of proteins

It is well known that the activity of a protein relies on its structure and movable parts [1, 2]. A protein is able to do a function, only if it is in a correct conformation. Therefore, knowing about the structure of proteins is important. Proteins are constructed by polymerization of 20 amino acids (Figure 1). In addition to these amino acids, selenocysteine is considered as amino acid, it involves in construction of some enzymes. Each amino acid has a central α -carbon atom linked covalently with hydrogen, amino, carboxylate and one specific group called side chain. The central α -carbon atom in all amino acids is a chiral atom except glycine. All proteins contain only the levo-isomers amino acids, the dextro-isomers are available in very rare cases such as in some bacterial envelopes [2, 13].

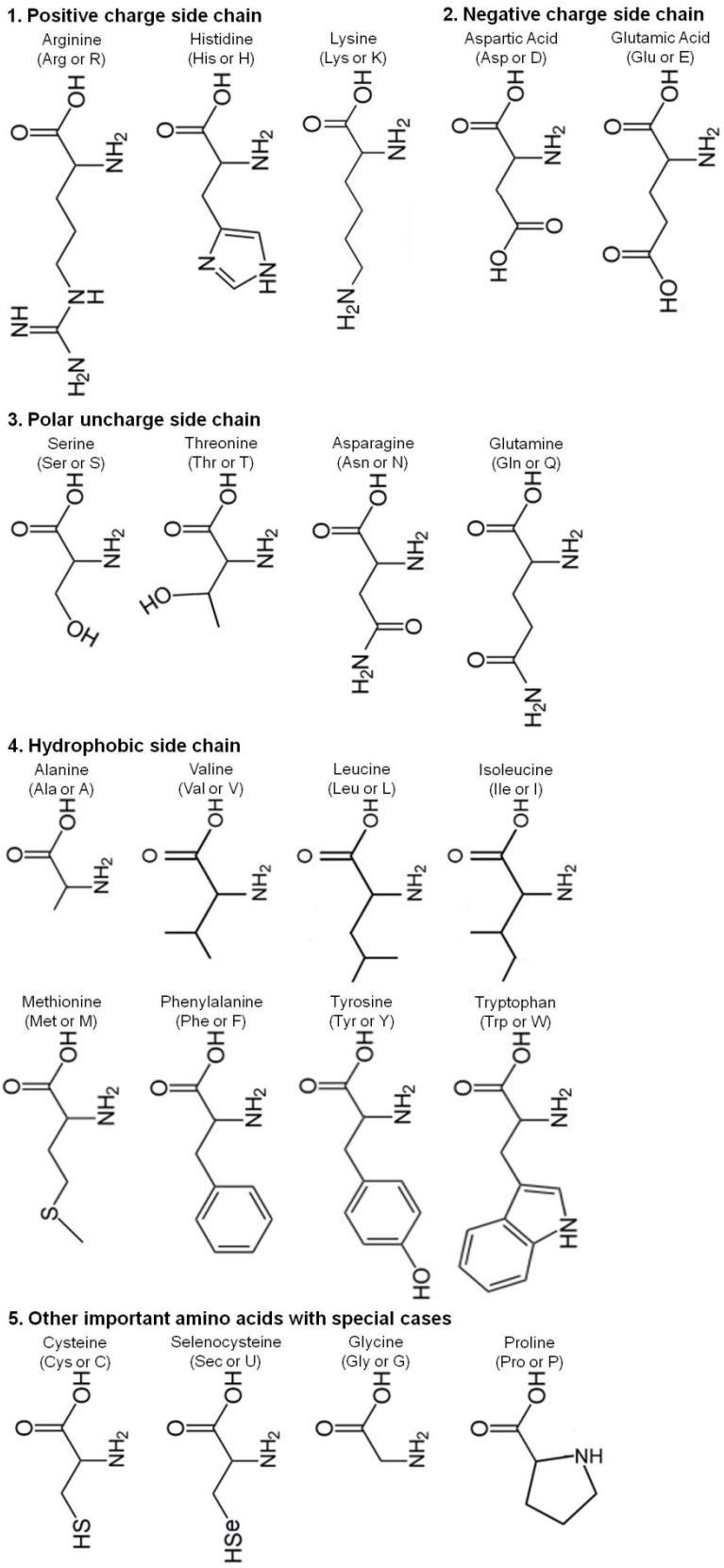

Figure 1. Chemical classifications and structures of 21 amino acids in human.

As shown in Figure 2, a simple protein is selected to explain the different levels of protein structure [14]. The linear chain of amino acids linked by peptide bonds form the primary protein structure. Repeated amides and central α -carbons form the backbone of the protein. Thus, one carboxylate and one amino groups at both ends of the protein and are called C and N-terminus [1, 2]. A further folding of the primary structure by noncovalent bond such as hydrogen bond forms different types of secondary structure such as α helix and β sheet, of course depending on the type of the amino acids in a sequence. A specific combination of different secondary structures build up motifs and then the whole protein as tertiary structure (three-dimensional structure). Motifs are important for protein function since they can bind a cofactor, for example helix-loop-helix (EF hand) for calcium ion and helix-antiparallel β sheets for zinc ion (zinc finger). The tertiary structure is formed when the polypeptide chain undergoes overall conformation through different hydrogen bonds as well as hydrophobic interactions. Quaternary structure (multimeric) is the fourth protein structure level in which two or more proteins or subunits are associated together by noncovalent bonds. The conformation of the quaternary structure and its subunits are critical for cell function. Furthermore, enzymes can act also as subunits of some quaternary proteins within the cell to enhance the pathway operation [1, 2].

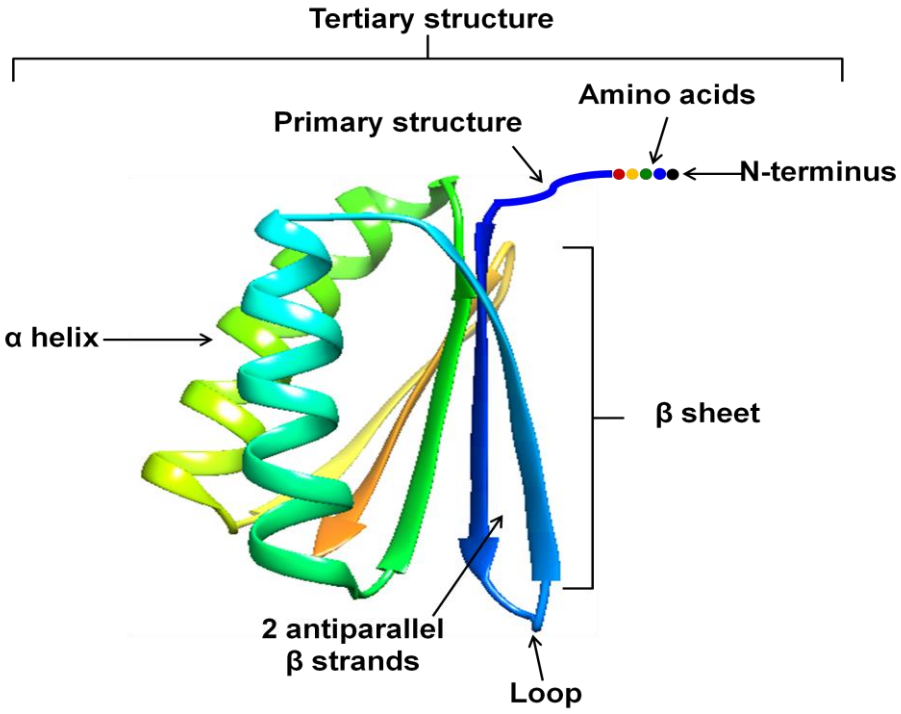

Figure 2. Three-dimensional structure of the simple protein Top 7 (Protein Data Bank ID (www.rcsb.org): 1QYS; [14].

1.1.2 Influence of pH, ionic strength and temperature

The right conformation of a protein is important for its function. Therefore, the environment of a protein has significant influence on its conformation. pH, ionic strength, and temperature are the major factors affecting the protein conformation and function. pH can exert its influence by different mechanisms, 1) changing the ionization of the functional groups at active binging sites, 2) changing the ionization of the substrate, 3) altering the right conformation by changing the ionization of the functional groups of the amino acids residues of a whole protein [15]. The ionic strength has influence on a protein depending on the type of the salt, it has a great influence on the charge-charge interaction capability of the protein, and it can also change the activity of a protein by changing its size and conformation [15, 16]. The environmental temperature plays a major role on the protein reactivity, for example the catalytic activity of the enzymes. It enhances the collision between an enzyme and a substrate and so the rate of interaction increases [15, 16]. However, the reactivity of a protein is increased until a critical temperature since a protein begins to denature through breaking of the intra and inter-molecular bonds [15, 16].

1.1.3 Investigated proteins

1.1.3.1 Serum albumins

Serum albumins often referred to blood albumin. They are the most abundant proteins in the circulation systems of mammals. Bovine serum albumin (BSA) and human serum albumin (HSA) serve as transporters for a variety of inorganic and organic molecules including metal ions such as Cu^{2+} and Zn^{2+}, and biomolecules to their target sites [17]. Furthermore, they have important roles to control the extracellular fluid volume since they can pull water into the circulation system by contributing in colloid osmotic pressure [18]. Both proteins (BSA and HSA) have similar structure since the sequence of BSA is 76% similar to that of HSA [19-21]. BSA consists of 583 amino acids while HSA has additional two amino acids (585). BSA contains two tryptophan residues, rather than only one in HSA [22, 23]. Both have approximately molecular mass of 66.5 kDa and isoelectric point (pI) of 4.7 [23]. Their folded spherical structures (Figure 3) are stabilized by large numbers of disulfide bonds (17) [23]. At neutral pH (7.4), the estimated overall charge at neutral pH is -18 for BSA and -16 for HSA (http://www.scripps.edu/~cdputnam/protcalc.html). The N-terminals of HSA (DAH) and BSA (DTH) usually form copper and nickel

binding pockets [23, 24]. Serum albumins have ability to undergo a reversible conformational modification at different pH, indicate their main physiological role of transporting a variety of metal ions, molecules and biomolecules to their target sites [21]. However, the small difference (≈ 24%) in sequence between BSA and HSA could lead to different behaviours to some ligands. For example, retinol and retinoic acid were bound to BSA and HSA giving different binding constants (K, L mol^{-1}) 3.29 × 10^5 and 2.27 × 10^6 and 1.28 × 10^5 and 5.25 × 10^6, respectively [25]. Furthermore, different displacement results were observed, retinol displaced retinoic acid from BSA and vice versa in case of HSA [25].

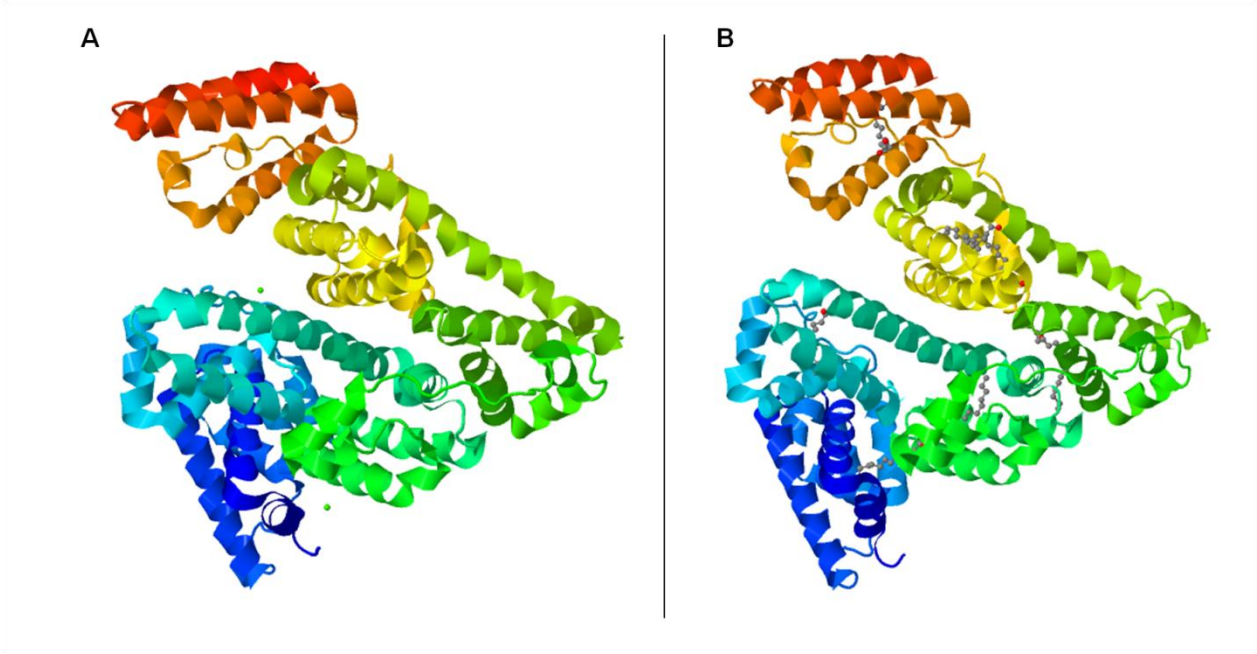

Figure 3: Structures of BSA (A) and HSA (B) (Protein Data Bank ID (www.rcsb.org): 3V03 for BSA and 1E7H for HSA).

1.1.3.2 β-lactoglobulin

β-lactoglobulin (β-LG) is the major composition of the whey proteins in the milk of ruminants and some mammals [26]. It is a small protein, which is highly soluble in water, and normally exists naturally as dimer with a molecular weight of 18.35 KDa [26]. It is stable at acidic and neutral pH (less than pH 7.5). Each monomer consists of 162 amino acids. Furthermore, two disulphide brides and one free cysteine are available within the structure [26]. As shown in Figure 4, β-LG consists of a β barrel (large β sheet) built up from 8 antiparallel β strands, 3-turn α helix and 1 more β

strand [27, 28]. In particular, the position of the EF loop can act as gate for the hydrophobic binding site (see Figure 4). It will exist in open position at high pH and the binding to various ligands contain hydrophobic parts will be possible, while at low pH it is in closed and the binding will be impossible [26-28]. Other proteins from the same family of β-LG (lipocalins) have several series of functions based on ligand binding function [26]. In general, the binding capability of β-LG to different ligands such as organic molecules (vitamins, fatty acids and cholesterol) and metal ions were studied [26]. However, there are no identifiable clear functions for β-LG. Possibly one of its main functions is just to serve as nutrient.

Figure 4: Structures of β-LG (Protein Data Bank ID (www.rcsb.org): 2BLG).

1.1.3.3 Myoglobin

Myoglobin (MB) is one of the respiratory proteins, which can bind oxygen reversibly [29-31]. It is produced in the red muscle in response to the need of muscle cells for oxygen. Different functions for MB were reported [29-31], short and long-term storage of oxygen, improvement of the diffusion of oxygen inside the muscle cells and as biochemical catalyst. Furthermore, it transports the oxygen from the sacolemma to the mitochondria of the red muscle cells and vertebrate heart cell since these muscles are contracting for long periods and need more oxygen [29]. MB is a hemoprotein consisting of 154 amino acids, folded to 8 α helixes (Figure 5) with a

heme residue (a porphyrin ring-iron complex), and has an isoelectric point of 7.2 [31, 32]. The heme residue is located between two histidine (His, 64 and 93) residues to stabilize the MB-heme-iron complex [31]. The iron binds with six ligands, with four nitrogen atoms of the porphyrin and one imidazole group of His 93 [31] As shown in Figure 5, the sixth ligand is for binding with oxygen, or for other ligands such as carbon monoxide (CO) and nitrogen monoxide (NO).

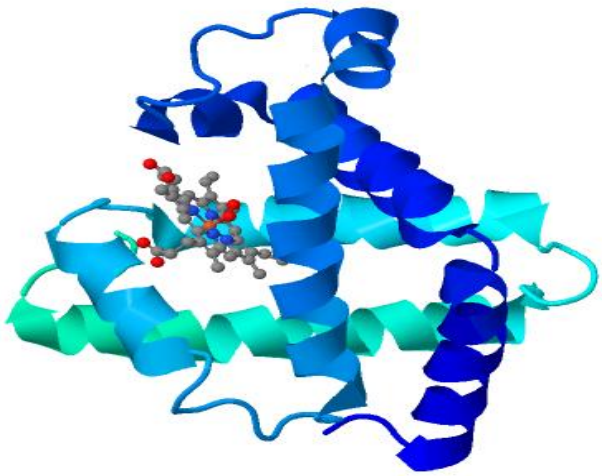

Figure 5: Structure of MB showing binding with oxygen (Protein Data Bank ID (www.rcsb.org): 1MBO).

1.1.3.4 Ovalbumin

Ovalbumin (OVA) is the major protein in the egg-white, which is available in large amounts of 60-65% [33, 34]. It has been used as model for various studies of the structure and properties of proteins, the characterization of protein binding to different ligands, and in some allergy experimental models [33]. It consists of 386 amino acids with a relative molecular mass of 45 KDa and isoelectric point of 4.5 [35, 36]. Six cysteines are available within the sequence, with one disulfide bridge between Cys 74 and Cys 121 [33, 34]. The N terminus is naturally acetylated. The carbohydrate side chain which is covalently bonded to the amide nitrogen of Asn 293 is recognized

by gycosyltransferase, and could be glycosylated [33, 34]. Furthermore, the residues of Ser (69 and 348) are potential sites for phosphorylation [33]. Therefore, the electrophoresis of OVA is highly dependent on the different degrees of phosphorylation of these target sites [33]. As shown if Figure 6, three isoforms of OVA have been detected, this is related to three different cases of phosphorylation, 1) no phosphorylated residue, 2) one phosphorylated residue, 3) two phosphorylated residues. In fact, the native ovalbumin belongs to the serpin protein family, which provides a major function as protease inhibitors of human plasma. Furthermore, OVA has similar folding of serpin with three-turn α helical reactive loop (see Figure 7) [33]. However, OVA is not a protease inhibitor, this is due to the cleavage of the reactive loop which does not offer good incorporation with the β sheet of the four antiparallel β strands [33].

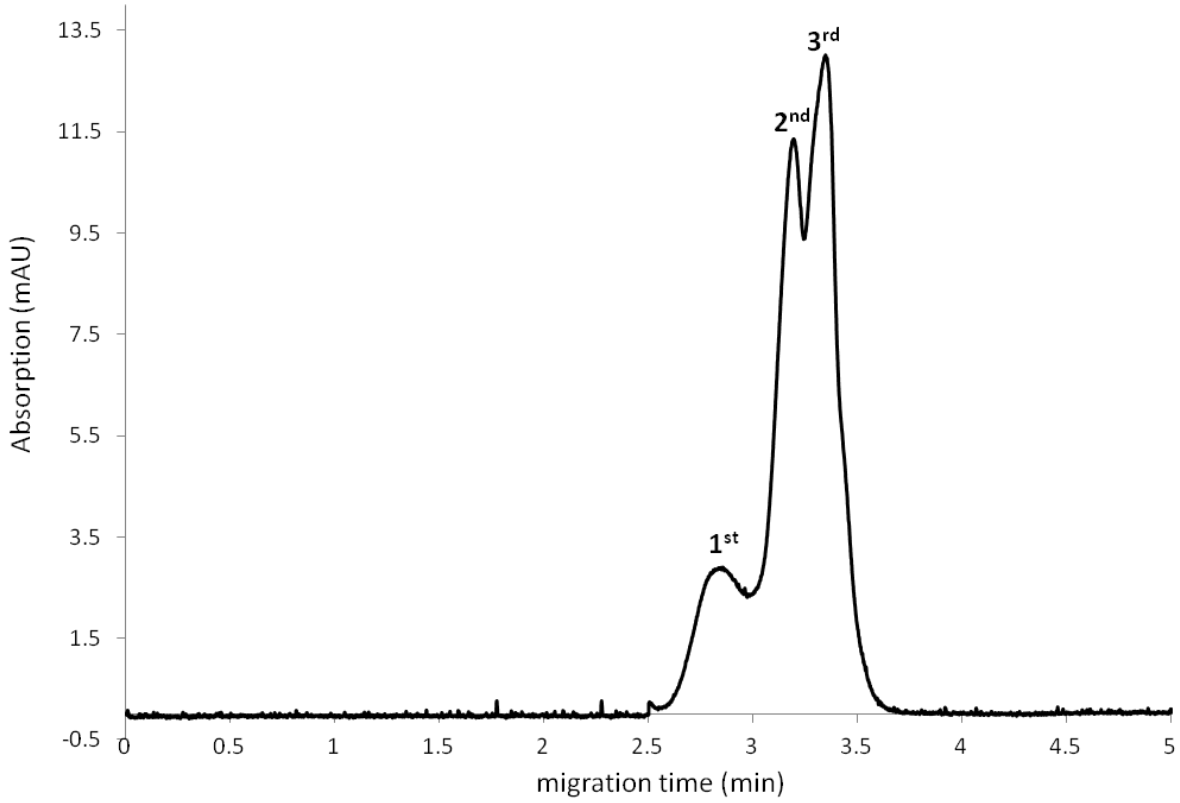

Figure 6. Electrophoretic separation of three OVA isoforms (1st, 2nd and 3rd).

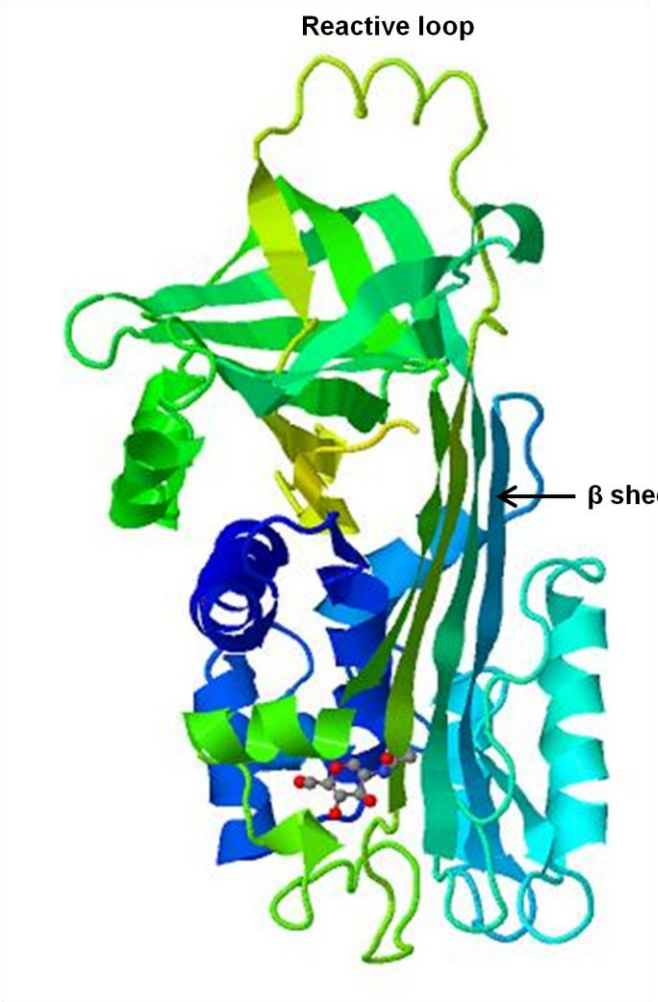

Figure 7: Structure of OVA (Protein Data Bank ID (www.rcsb.org): 1OVA).

1.2 Metalloproteins

Metalloproteins are proteins which contain a specific metal ion as cofactor. Approximately 30% of all proteins are metalloproteins, this means: for all these metals are important for their function [37, 38]. In general, essentially all proteins will interact with metal ions; some of these interactions may later prove to be important as well. On the surface of each protein one will find amino acid residues such as thiolat, carboxylate, imidazole, amines and amides, which will usually bind to existing metal ions [2].

In Figure 8 different functions of a wide variety of metal ion on the biological system have been reported. Popular protein-metal ion interactions are known to produce various crucial biological roles such as storage role as ferritin for Fe^{3+}, metallothionein proteins for Zn^{2+}, Cu^{2+} and other heavy metals, transport role as

transferrin for Fe^{3+} and oxygen transport by bind to Fe^{2+} of heme metalloprotein, cofactor for enzymes e.g. selenium on glutathione peroxidase. Furthermore, Cu^{2+}, Mn^{2+}, Fe^{2+} and Ni^{2+} can be incorporated to form active sites of antioxidant defense enzymes such as superoxide dismutases and Mg can be incorporated for hexokinase [1, 39, 40]. The toxicity of some of the heavy metals such as Hg^{2+} and As^{3+} can be manifested when they bind irreversibly to a variety of selenocystine enzymes [1, 41-43].

On the other hand, the investigation of diagnostic biomarkers for several diseases such as metalloproteins is still growing [37]. Furthermore, a substantial progress in producing organometallic complexes for several disorders such as cancer, inflammation, infection and neurological disorders have been achieved [42-46]. These complexes are generally pro-drugs that can be transformed by ligand exchanges or redox process before metal ion partner reach the target sites. The influences of metal ion partner should be investigated prior to developing new pro-drugs. Therefore, the characterization of interactions between proteins and metal ions are important.

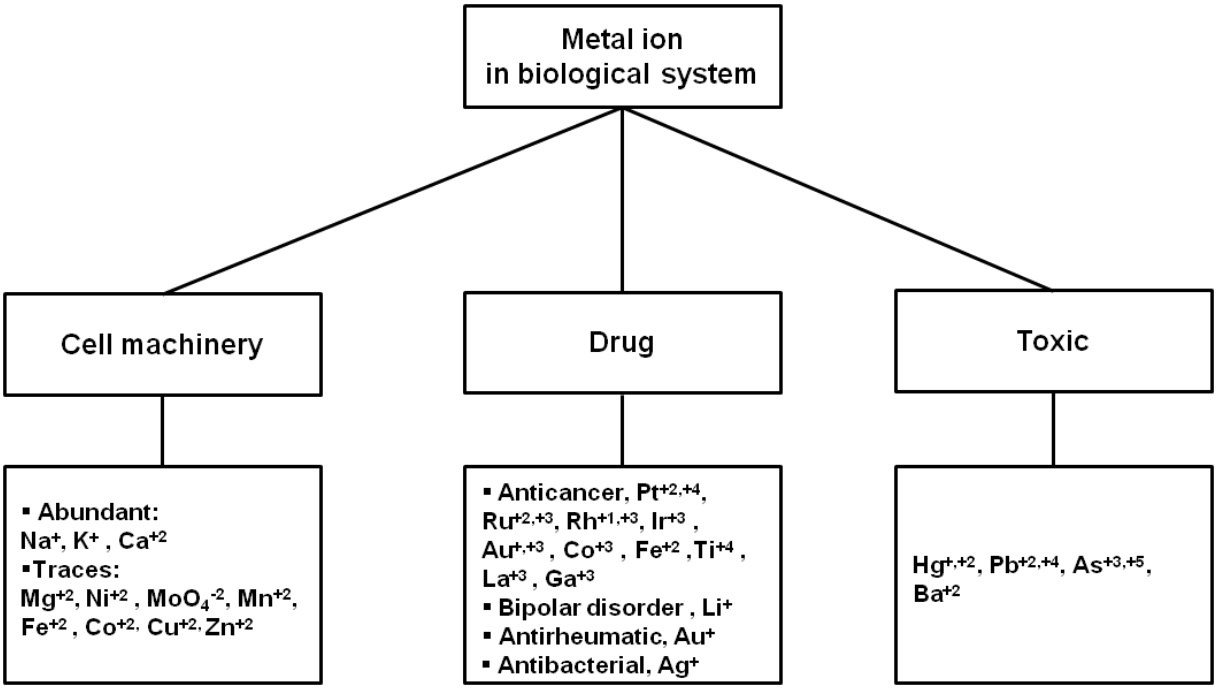

Figure 8: Functions of a wide variety of metal ions on the biological system.

1.3 Factors affecting protein-metal ion interaction

The characterization of the protein-metal ion interactions in the biological systems is quite complicated. Hence, relying on the properties of proteins and metal ions and the fundamental concepts of the complex formation could give preliminary insights into what might have happened. The selectivity of each protein for specific metal ions is of particular interest. The protein properties such as net charge, dipole moment, donating and accepting charge and the number of potential ligands for metal ions inside a binding site are the major factors affecting the interaction with metal ions [47]. Hence, the protein structure is the key to select the right metal ions. Amino acid side chains such as that of aspartic acid, glutamic acid and cysteine can be deprotonated in physiological pH and form negatively charged residues which favour ion-ion interaction with a given cation such as a metal ion [47, 48]. The dipole moments of the amide group of aspargine and glutamine residues and the imidazole group of histidine residue are strong and favor interaction with metal ions more strongly than those with serine, threonine and methionine [1, 47, 49]. Furthermore, the metal ions properties can contribute to the interaction selectivity of a target protein. The metal ion*'s* valency, atomic radius and charge accepting capacity contribute to the suitable metal binding sites [47, 48]. Increasing the number of valency enhance the ion-ion and ion-dipole interactions. Metal ions which are better electron acceptor (soft) such as Zn^{2+} can accept more charge from biological ligands and form more stable complexes than hard metal ions with the same ionic radius and charge such as Mg^{2+} [50, 51]. The selectivity of the soft metal ions to the nitrogen and sulfur containing groups is higher than oxygen, while hard metal ions have a tendency to bind oxygen containing groups [49, 50, 52]. Accordingly, the metal ions react preferentially with the target proteins of the similar overall hardness or softness [51, 53-56]. In general, the interaction selectivity can be estimated according to the hard and soft acid and base theory (HSAB). Table 1 shows the different possibilities for the protein-metal complexes formation and additional coordination with the surrounding anions.

Table 1. Prediction of the metal ions selectivity to various donor ligands using HSAB concept

	Hard*	Borderline*	Soft*
Acids	- Class A cations e.g. Li^{+}, Na^{+}, Mg^{2+}, Ca^{2+} , Ba^{2+}, Al^{3+} , Ga^{3+} - High oxidation state of class B cations e.g. V^{3+}, Cr^{3+}, Co^{3+}, Fe^{3+} - Lanthanide and actinide cations	- Medium oxidation state of Class B cations (almost divalent) e.g. Mn^{2+}, Fe^{2+}, Co^{2+}, Ni^{2+}, Cu^{2+}, Zn^{2+}, Pd^{2+}	- Low oxidation state of Class B cations (monovalent, heaviest) e.g. Cu^{+}, Ag^{+}, Cd^{2+}, Au^{+}, Hg^{+}
Base	Carboxylates (Glutamate and Aspartate), Hydroxyl group (Serine, Theronine, Tyrosine), Guanidinium (Arginine), Carbonyl, Alcohols, Amines, Ether, Water, Nitrate, Sulphate, Phosphate, Carbonate, etc.	Imidazole (Histidine), Amides (Asparagine, Glutamine), Nitrogen of the peptide bond, Indole (Tryptophan), Pyrrole (Porphyrin), Nitrite, Azides, Nitrogen gas. Pyridine, Aniline, Chloride, etc.	Thiols (Cysteine), Thioethers (Methionine), Phenyl (Phenylalanine), Ethylene, Cyanide etc.
* Acids with the same charge become softer (less hard) as the radius increases. Acids become harder (less soft) on going from left to right of the same period, as charge (oxidation state) increases.			

The metal ion binding sites of calmodulin, carboxypeptidase and multicopper oxidase are good examples for binding with different lewis acids; Ca^{2+} (hard), Zn^{2+} (borderline) and Ag^{+} (soft), respectively [57-59]. As shown in Figure 9, the binding site of Ca^{2+} consists of only carboxylates, while the imidazole and thioether groups at the binding site are important to selectively bind Zn^{2+} and Ag^{+}, respectively.

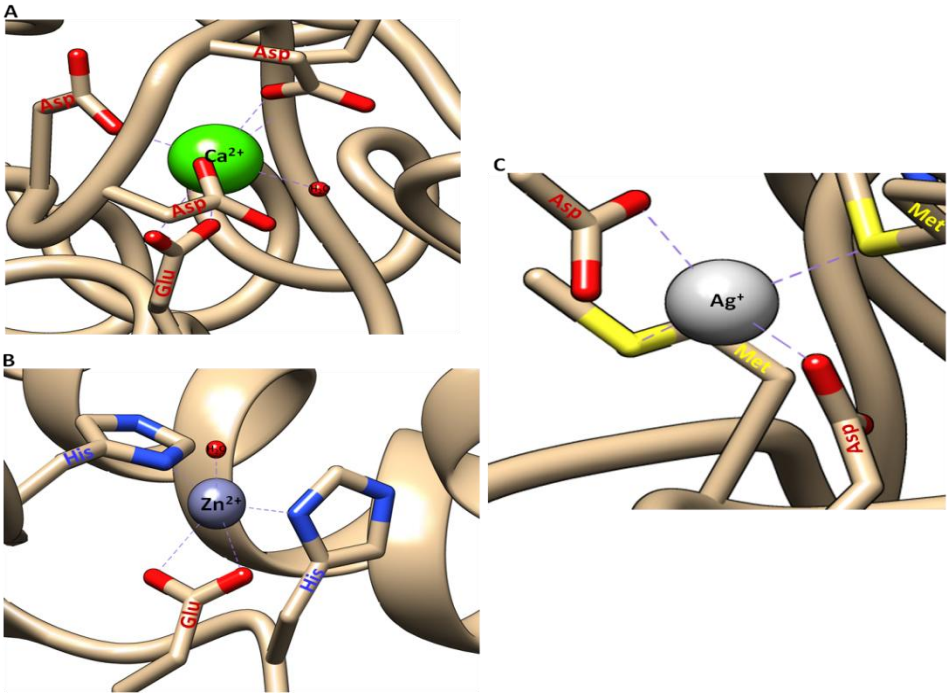

Figure 9. Binding site selectivity of different proteins to metal ions. Calmodulin-Ca^{2+} (A, PDB ID: 3CLN), carboxypeptidase-Zn^{2+} (B, PDB ID: 1YME) and multicopper oxidase-Ag^{+} (C, PDB ID: 3NSD).

The gas phase free energy for a metal ion ligand bond for functional groups containing oxygen such as carboxylates, alcohols, phenolates ligands decrease with increasing the ionic radii of metal group IA and IIA but not for IB or IIB due to the high ability of group B to accept charge [48]. The distances between functional groups of a binding site and a metal ion as central ion play an important role in the structural characterization and for the reactivity of the protein-metal ion complex [60]. Knowledge concerning a metal ion*'s* coordination numbers (CN) and their geometries could give an initial insight into the possible interactions with proteins [56, 61]. In general, the CN of a given metal ion is lower when it is bound to strong charge-donor atoms, while the interaction with weak charge-donor atoms increases the CN [61]. Furthermore, CNs are directly proportional to the ionic radii [61, 62].

1.4 Analytical techniques for studying protein-metal interactions

Several techniques can be used for this purpose. When comparing different techniques for investigating protein metal ion interactions, some factors should be taken into account. The analytical parameters of each technique such as sensitivity, precision, accuracy, time scale of analysis, ability to perform under physiological

condition and method complexity should be considered. Furthermore, the suitable sample complexity and concentration vary from one technique to another. Additionally, the instrument design, its cost and commercial availability with guaranteed maintenance are certainly of interest to researchers. In general, 20 techniques have been reported for investigating protein-ligand complexes [63]. Herein, the techniques which are specially used for protein-metal ion interaction were briefly discussed and compared. The complexity of sample and their special preparation are the most challenging part for each technique. Most of the techniques require pure sample for analysis such as x-ray crystallography, nuclear magnetic resonance (NMR), fourier transform infra-red spectroscopy (FTIR), circular dichroism (CD) spectroscopy, surface plasmon resonance (SPR) and atomic force microscopy (AFM) [63-65]. NMR technique performs with highly concentrated samples, and is restricted for small and soluble protein (<40kDa) due to often observed spectral overlaps for large proteins [66]. Therefore, large proteins must be isotopic labeled to solve this problem to a certain extent which increases the complexity of the method. A period of more than 4 weeks might be required to prepare proper and enough crystals of biological samples for x-ray crystallography [63, 66]. However, crystal formation is predominately difficult and in some cases impossible [63]. In contrast, NMR and x-ray crystallography are most suitable techniques for structural elucidation and can complement and confirm results of other techniques [63, 66-68]. The light scattering technique is mainly used to investigate the effect of metal ions on the aggregation behavior of various proteins [69]. Enzyme-linked immunosorbent assay (ELISA) and related techniques can be useful to investigate the reactivity of metal ion-treated antibodies or antigens, but they cannot characterize the metal ion interaction with both components [69, 70]. Since most of the biological samples are impure, it makes sense to discuss and compare the two most powerful techniques with high separation efficiency for this purpose, namely affinity chromatography [71, 72] and affinity capillary electrophoresis (ACE) [73-75]. The affinity chromatography and their sub-techniques suffer from the disadvantages that a large amount of sample and materials are needed in addition to the high cost of the affinity columns [71, 72]. Recently, ACE was successfully used to investigate the interaction of ovalbumin isoforms and other proteins with different metal ions [73-75]. The ability of this technique to investigate each isoform and separate a complex sample

components makes it more attractive than other techniques. Mass spectrometer can detect the known and unknown components present in a complex biological sample. It also provides binding information through m/z of target biomolecule before and after binding with ligand [76, 77]. Nonetheless, direct infusion mass spectrometry (DIMS) could provide unreliable interaction information due to four main problems, (1) different electrospray ionization efficiency of each compound presents in a biological mixture, (2) lack of separation increase the competition between components to bind with a ligand, (3) low stability of some protein-metal complexes in the gas phase, (4) irrelevant binding properties in the gas phase [76, 78, 79]. Therefore, MS might sometimes show different binding behavior compared to other techniques. However, the combination of ACE-UV and ACE-MS can provide similar and reliable affinity measurements [78]. Therefore, ACE-UV can be considered as the first choice to investigate the protein-metal interactions also due to its moderate costs for reagents and instrumentation. Furthermore, this techniques offers reliable binding information since it has been shown to give similar binding results of other interested techniques such as high-performance affinity chromatography (HPAC) and related methods [80-82].

Finally, ACE became more useful compared to other techniques due to its easy performance, rapid analysis, small sample injected volume (nano-level), high separation efficiency, direct injection of impure samples and even biological fluids, the ability to perform under physiological conditions such as pH 7.4 and body temperature 37 °C. In addition, high concentration of salts, additives or ligands up to 100 mmol/ L could be used [73-75, 83-86]. Furthermore, the sensitivity of ACE can be enhanced by using a high-sensitivity cell [25].

1.5 Capillary electrophoresis

It makes sense to give some information about the capillary electrophoresis (CE) prior to ACE. CE is an electrophoretical separation technique; it is based on the differential migration of charged analytes in a capillary filled with a semicondutive medium under the influence of an electric filed [87, 88].

1.5.1 Classification of CE modes

As shown in Figure 10, different modes of this technique are classified into three main groups, moving boundary CE, steady state CE and zone CE. (see Figure 10) [87, 88].

1.5.1.1 Moving boundary CE

In this group, the sample fills the first compartment at the injection position. The second compartment is filled with a highly mobile electrolyte. A capillary filled with the highly mobile electrolyte is used to connect both compartments. Under the electric field, the separation starts when the fastest compounds leave the sample bulk and followed by the slower compounds. This method offered very poor separation, thus now it is outdated [87].

1.5.1.2 Steady state CE

There are two modes under this group, isotachophoresis (ITP) and isoelectric focusing (IEF). In both modes, performance under generated gradients (electrolyte gradient for ITP and pH gradient for IEF) is important to obtain separation between different analytes. Furthermore, the occurrence of the electroosmotic flow (EOF) should be prevented for better separation. They are useful to separate ionic analytes such as various drugs and biomolecules.

1.5.1.3 Zone CE

In the zone CE, the sample components migrate in zones along the capillary filled with material that can be a gel such as in the capillary gel electrophoresis (CGE) or a solution containing electrolytes as in free solution capillary electrophoresis (free solution-CE) or a solution containing very small particles (less than 3 µm) as in capillary electrochromatography (CEC).

Here, free solution capillary electrophoresis and related methods were explained. They are the most widely used methods for the separation and binding studies due to their simplicity of operation and their versatility. Free solution capillary electrophoresis is divided into four modes based on the type of an additive in a running buffer. Capillary zone electrophoresis (CZE) is the simplest form because the capillary is filled with a running buffer without any further additive. In this mode, the separation is based only on the charge of analytes. The use of some additives in a running buffer could improve the separation for some analytes which are not separated by the simple CZE. For example, using of surfactants in micellar electrokinetic capillary chromatography (MEKC) for hydrophobic solutes and chiral selectors in chiral capillary electrophoresis (CCE) for chiral analytes. The separation feature of CE can be utilized in specific and non-specific affinity interactions; in this case the mode is

called affinity capillary electrophoresis (ACE). The ligand is added to a running buffer to investigate the interaction with an analyte (sample). Herein, ACE was selected to investigate the protein-metal ion interaction based on many features. Therefore, it is discussed in details in section 1.5.3.

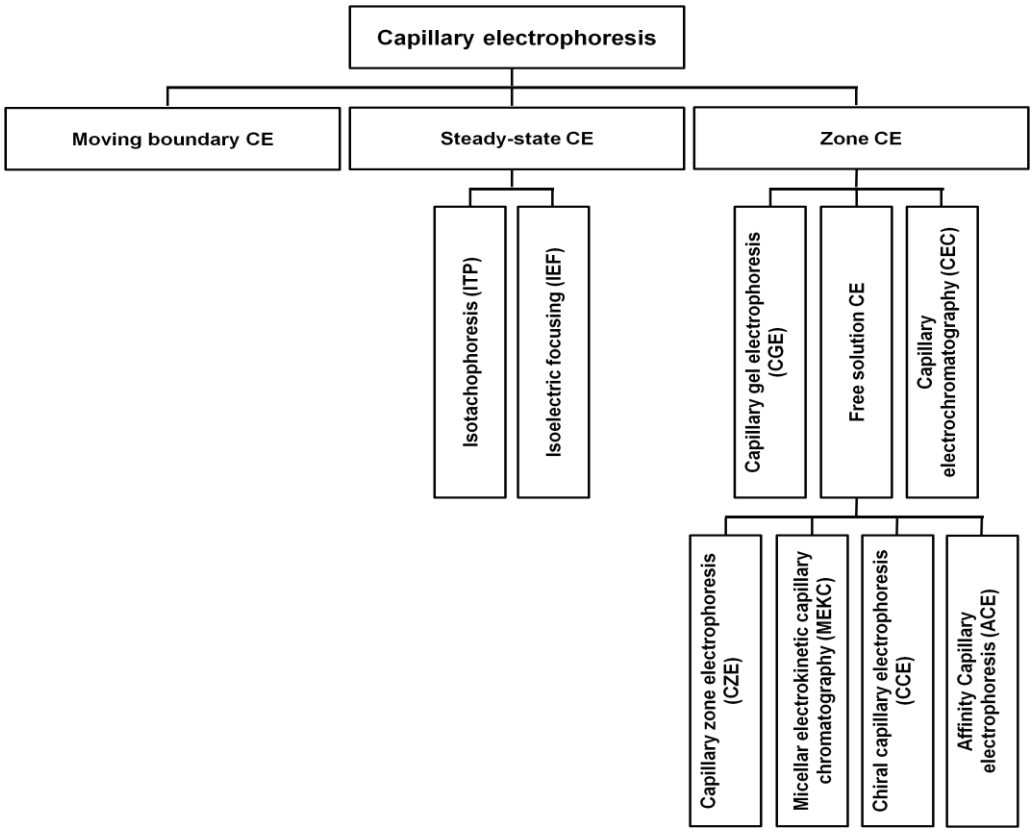

Figure 10. The CE methods and their modes.

1.5.2 Basic CE system

As shown in Figure 11, the instrument consists of two vials containing electrolyte (running buffer) which are connected by the capillary [88]. Electrodes are immersed in the running buffer and connected to a high voltage power supply. Thus, the electric field is created in the capillary and allows the charged analyts to start the migration along the capillary. The migrated analytes are detected on-column (inside the capillary before leaving out) by the optical detectors such as UV, UV-Vis and Fluorescence detectors, the place of the detector is before the outlet end of the capillary and usually is connected to the computer system for data acquisition. In order to obtain more information about the structure of the analyte, the CE can be coupled with a mass spectrometer (MS) by introducing the capillary outlet into a suitable ion source interface (e.g. electrospray ionization, ESI). Nowadays, the

commercial CE instrument contains some important facilities such as capillary cooling system, sample plate with numerous vial positions and additional buffer reservoirs to compensate the loss in buffer or other solutions during the routine work. Furthermore, most of the recent CE instruments contain a sample cooling system.

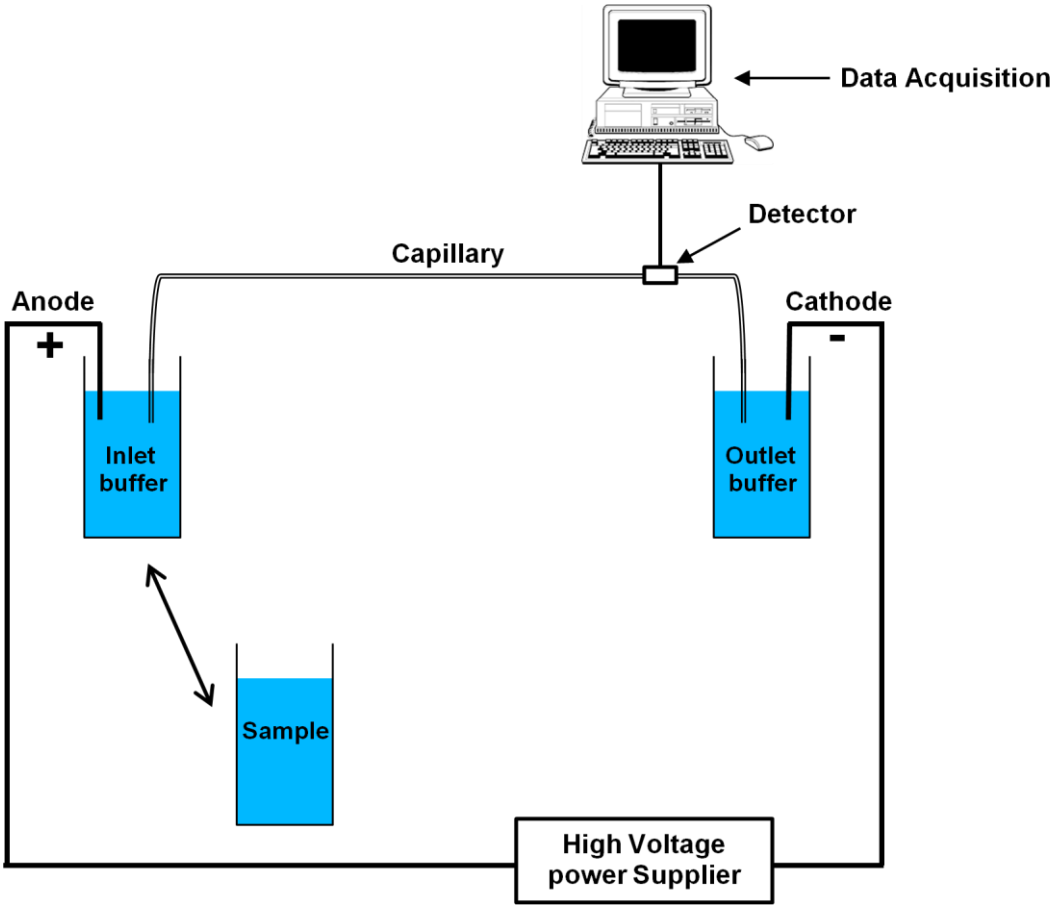

Figure 11. Simple representation of a CE system.

1.5.2.1 Capillary

1.5.2.1.1 Capillary types

Various types of capillaries can be used in CE, coated and uncoated capillaries. The uncoated capillary is usually made of silica glass (bare fused silica). It is commonly used for all CE modes. In brief, different coated capillaries have been used for some CE applications. Two types of coated capillary can be obtained, permanent and dynamic [89-93]. In permanent coating, the coated material is bound covalently to the silica glass such as coatings with polyacrylamide [89]. In dynamic coating, charged

materials can be used to coat the inner wall of the capillary by different interactions such as ionic- ionic interactions [90-91].

The bare fused silica capillary has been successfully used for metal ion binding studies in ACE mode [73-75]. It is coated from outside by polyimide to be less fragile. This coat can be removed easily at the place of the detection window to be suitable for on-column optical detection (such as UV, UV-Vis). The capillary is commercially available with different internal diameters (I.D.), 25-150 µm. The capillary internal diameter of 50 µm has been considered as the optimum for bimolecules since the joule heating is still small while its acceptable diameter offers good detection sensitivity [93]. Therefore, the bare fused silica capillary with the internal diameter of 50 µm has been selected for this study.

1.5.2.1.2 Conditioning the internal capillary wall

The inner surface of the capillary should be conditioned before the first use by a strong alkaline solution to activate the internal capillary wall through the ionization of the silanol groups (see section 1.5.2.4). After activating the internal wall, the capillary should be rinsed with water to remove the remaining amount of the alkaline solution. In a subsequent step, an equilibration of the surface can be achieved by flushing the capillary with sufficient running buffer within the rinsing protocol.

1.5.2.2 Injection modes

Samples and other solutions can be introduced into the capillary by two main injection modes, electrokinetic and pressure (hydrodynamic) [87, 94].

1.5.2.2.1 Electrokinetic injection mode

In the electrokinetic mode, the sample is injected into the capillary by applying voltage. The sample vial replaces the inlet vial buffer, and then voltage is applied. The amount of the injected sample is variable since it depends on the mobility of the analyte (s) in the sample. Therefore, this mode is not suitable for quantitative applications due to the poor reproducibility of the injected amount. The injected amount is given by Equation No. 1:

$$q = \frac{\left(\mu_a + \mu_{eof}\right) \cdot U \cdot \pi r^2 \cdot c \cdot t}{L} \quad \text{(Eq. 1)}$$

q is the injected amount, μ_a and μ_{eof} are the mobilities of the analyte and the EOF, respectively. U is the applied voltage, r is the inner radius of the capillary, c is the sample concentration, t is injected time, L is the total length of the capillary.

1.5.2.2.2 Hydrodynamic injection mode

In the hydrodynamic mode, the sample is introduced into the capillary by using pressure. This mode is widely used especially when non- or low viscous buffers are used for the experiments. The injected amount of the sample can be calculated by equation No. 2.

$$q = \frac{\Delta P \cdot r^4 \cdot \pi \cdot c \cdot t}{8 \cdot \eta \cdot L} \quad \text{(Eq. 2)}$$

q is the injected amount, ΔP is applied pressure, r is the inner radius of the capillary, c is the sample concentration, t is injected time. η is the viscosity of the sample solution, L is the total length of the capillary.

1.5.2.3 Electrophoretic mobility

The electrophoretic seperation is due to the difference velocities of the migrated charged analytes under the influence of the generated electric field [87, 88, 94]. Inside a capillary filled with running buffer, the charged analyte is subjected to the influence of the electric force (F_{el}) and the friction force (F_s) according to the Stokes law for spherical particles. At the steady state the equation for these two forces can be written as following (Equations No. 3, 4 and 5):

$F_{el} = F_s$ (Eq. 3)

$F_{el} = q_i \cdot E$ (Eq. 4)

$F_s = 6\pi \cdot \eta \cdot r_i \cdot v_{eff}$ (Eq. 5)

The equation 3 can be further expressed as shown in Equation No. 6.

$q_i \cdot E = 6\pi \cdot \eta \cdot r_i \cdot v_{eff}$ (Eq. 6)

q_i is the overall charge of the analyte, E is the electric filed strength for given capillary length and applied voltage, η is the viscosity of the separation medium, r_i is the hydrodynamic radius of the charged analyte, v_{eff} is the effective electrophoretic velocity of the analyte.

The effective mobility of the analyte is expressed as shown in Equation No. 7.

$$\mu_{eff} = \frac{v_{eff}}{E} \quad \text{(Eq. 7)}$$

Therefore, the equation 6 can be changed to:

$$\mu_{eff} = \frac{q_i}{6\pi \cdot \eta \cdot r_i} \quad \text{(Eq. 8)}$$

The electric filed strength is expressed as shown in Equation No. 9.

$$E = \frac{U}{L}$$ (Eq. 9)

Since the velocity is equal to the distance divided by the time, the effective electrophoretic velocity can be expressed as shown in Equation No. 10.

$$v_{eff} = \frac{l}{t_{eff}}$$ (Eq. 10)

where l is the effective length (the length of the capillary from the beginning of the inlet to the detection window) and t_{eff} is the effective migration time of the charged analyte.

Form equation 7, 9 and 10, t_{eff} can be expressed simply as shown in Equation No. 11.

$$t_{eff} = \frac{l \cdot L}{\mu_{eff} \cdot U}$$ (Eq. 11)

1.5.2.4 Electroosmotic flow

The electroosmotic flow (EOF) plays an important role during the electrophoretic separation [95]. As shown in Figure 12, the EOF is the bulk movement of the running buffer inside the capillary due to the generated zeta potential at the inner capillary wall. It usually helps to allow detection of positive, neutral and even negative analytes in one single run. Indeed, the zeta potential is depending on the density of the charge at the inner capillary wall, which is certainly depends on the ionization of the silanol groups of the inner capillary wall. It has been reported that the silanol groups start to ionize at pH ≥ 2.5 (Figure 12) [95].

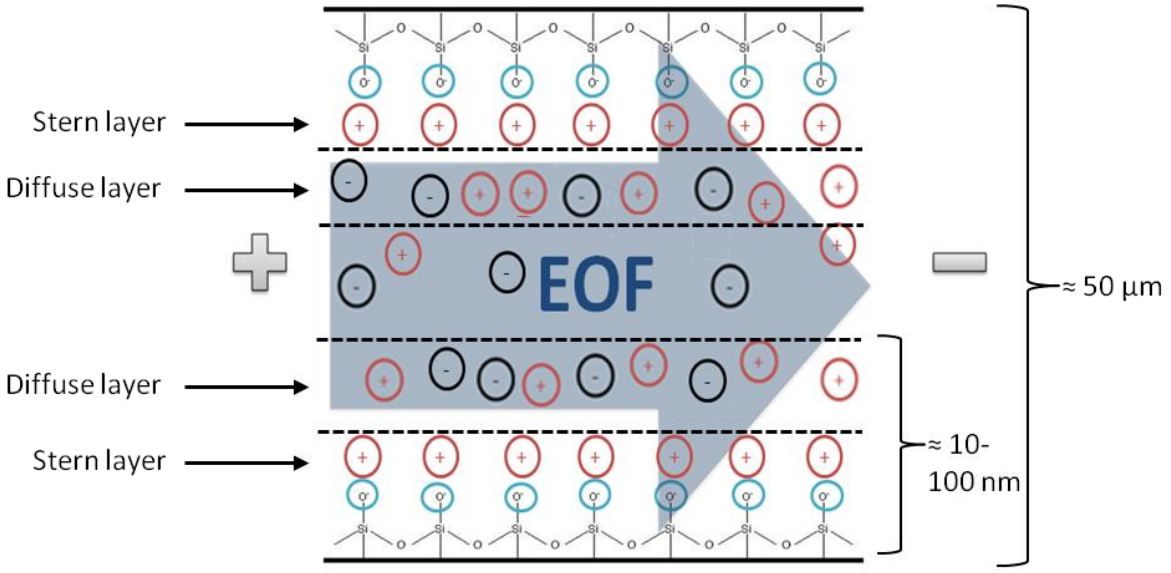

Figure 12. Generation of the EOF by the double electric layers; stern and diffuse layers, between the internal wall of the capillary and a running buffer.

Therefore, the electroosmotic mobility (μ_{eof}) should be considered when calculating the apparent mobility of the analyte (see section 1.5.2.5). μ_{eof} is expressed by the equation No. 12:

$$\mu_{eof} = \frac{\varepsilon \cdot \zeta}{4\pi \cdot \eta} \quad \text{(Eq. 12)}$$

ε is the dielectric constant of the running buffer, ζ is zeta potential at the surface of the inner capillary wall.

1.5.2.5 Electophoretic migration and separation

The apparent mobility of a given analyte in CE is the combination of two mobilities (Figure 13), the effective mobility of the analyte and the EOF mobility (Equation 13). The observed migration time of a given analyte can be expressed as shown in Equation No. 13:

$$t = \frac{l}{v_{app}} = \frac{l \cdot L}{(\mu_{eff} + \mu_{eof}) \cdot U} \quad \text{(Eq. 13)}$$

In normal mode (the anode at the inlet of the capillary and the cathode at the outlet of the capillary) and when using bare fused silica capillary, the direction of the EOF is usually toward the cathode. Thus, the apparent migration time of the analyte is depending on its charge, positive effect for the positive charged compound and negative effect for the negative charged compound. Furthermore, there is no effective mobility for the neutral compound thus it migrates with the EOF. Therefore, different analytes in a sample can be separated electrophoretically based on their charges, masses and sizes (Figure 14).

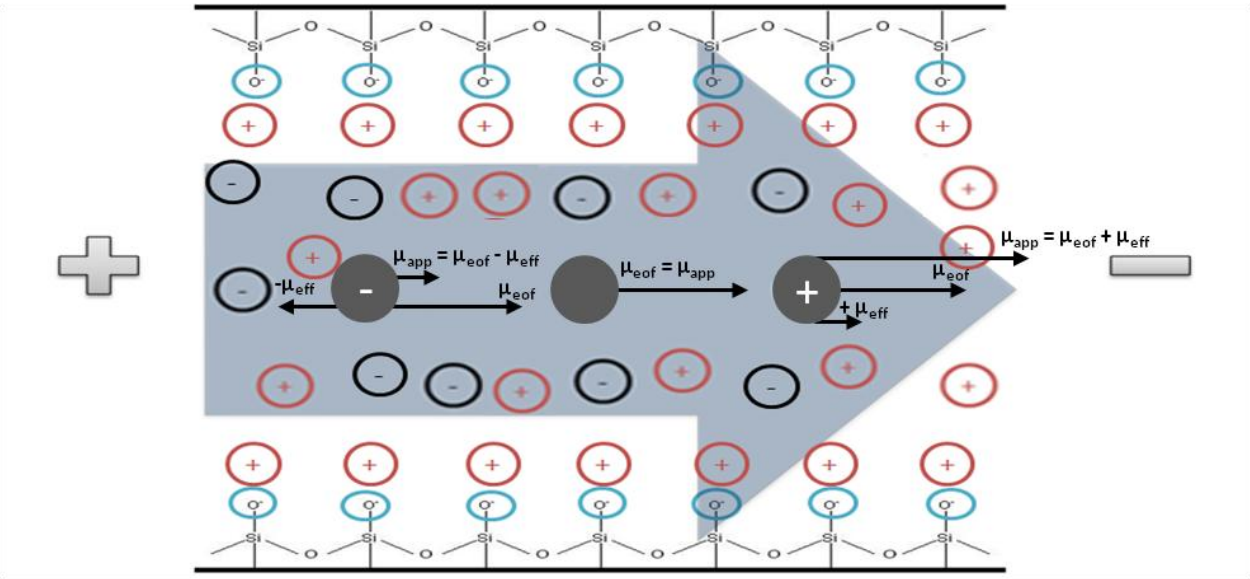

Figure 13. Illustration of possible apparent mobilities for positively charged, negatively charged and uncharged analytes.

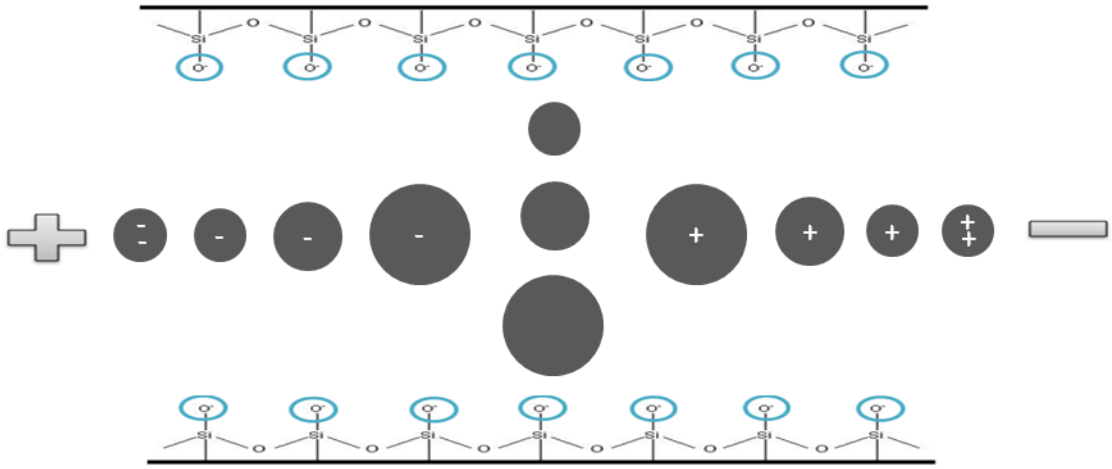

Figure 14. Typical separation order of differently charged and uncharged compounds.

1.5.2.6 Electophoretic separation conditions

During optimization of a CE method, a relatively large number of parameters should be taken into account. Polarization of the electrodes, applied voltage, temperature, capillary and buffer (composition, concentration and pH) are the most important parameter for developing a CE method.

1.5.2.6.1 Polarization of electrodes

The normal polarization mode (positive mode, cathode at the outlet end of the capillary) is the standard set, while the reversed mode (negative mode, anode at the outlet end of the capillary) can be used when the anions have higher mobilities than EOF mobility, or if the EOF direction is changed toward the anode by some cation additives.

1.5.2.6.2 Applied voltage

The high voltage power supply of the commercial CE instrument is designed to produce very stable (± 0.1) kV of ± 0-30 to maintain a high reproducibility of the migration time of the analyte. Increasing the voltage will accelerate the migration time of the analyte by increasing the EOF. The main disadvantage of increasing the voltage is the production of the joule heat, which has unfavourable effects on the peak shape (peak broadening) and the stability of the analyte.

1.5.2.6.3 Temperature

Temperature is one of the main parameters which should be controlled, especially for analysing an unstable analyte and for binding investigation. The joule heat is generated inside the capillary filled with the running buffer based on the produced power per unit volt [94]. The joule heat has indirect influence on the EOF by altering the viscosity of the running buffer. It could also change the conformation of some analytes such as proteins. Therefore, all recent CE instruments contain a capillary cooling system to minimize the unfavourable influence of the generated joule heat on the analyte and its peak shape (such as broadening).

1.5.2.6.4 Capillary internal diameter and length

The use of small internal diameter of the capillary offers a high surface to volume ratio leading to an increase in heat dissipation and thus minimizing the effect of joule heat [87]. At a constant applied voltage, increasing the capillary length will increase the migration time of the analyte, decrease the electric field strength and hence decrease the generated joule heat. In most cases, the length of the capillary has no significant influence on the electrophoretic separation.

1.5.2.6.5 pH

The pH of the running buffer has a significant influence of the electrophoretic seperation by influences the ionization of the analytes and the silanol groups of the

internal capillary wall. Therefore, the electrophoretic seperation could be improved by a proper selection of a running buffer and its additives.

1.5.2.6.5 Ionic strength

Increasing ionic strength of the running buffer has various influences on the separation. It increases the migration time by decreasing the EOF and hence the resolution could be improved [87]. One should however be careful when dealing with a buffer of high conductivity. In this case, increasing the ionic strength will lead to increase the current, and subsequently the joule heat will increase. This influence is minimized by applying the capillary cooling system of the modern CE instrument. On the other hand, when increasing the ionic strength the binding of the analyte to the internal capillary wall will be reduced.

1.5.3 Affinity capillary electrophoresis

ACE is one of the free solution CE methods. In this method the change in electrophoretic migration time or peak (area or height) for one of the reactants (an analyte or a ligand) before and after binding are used to investigate the interaction [93, 96]. ACE has gained increasing popularity in the last few years in pharmaceutical and biological research [76, 84, 96-104]. There are different ACE modes for studying the binding. Each mode has been developed based on the kinetic on- and off-rate of the interaction.

1.5.3.1 ACE Modes

ACE can be classified into three main modes, dynamic equilibrium, pre-equilibrated and kinetic method [105]. In dynamic equilibrium mode, the relaxation time of the equilibrium is short with respect to the separation time. In pre-equilibrated mode, solute and ligand mixed outside the capillary to allow the equilibrium and then introduced for separation. This mode is only suitable if the separation time is shorter than the relaxation time of the equilibrium. In between these two modes is the kinetic method [105], the separation time is similar to the relaxation time of the equilibrium. Therefore, it has been used for complex dissociation study.

1.5.3.1.1 Dynamic equilibrium

It is well known that most of metal ions bind quickly to proteins and the relaxation time of the equilibrium is usually very short (fast on-off kinetic) with suspect to the electrophoretic separation time [93, 105]. Therefore, the dynamic equilibrium mode was selected for this work. Several methods were developed based on this concept

[105, 106]. Mobility shift-ACE, Hummel-Dreyer (HD), vacancy-ACE (VACE) and vacancy-peak (VP) are dynamic equilibrium related methods (Table 2). Furthermore, they can be classified according to the used electrophoretical parameter for binding investigation as following: 1) change in the electrophoretic mobility for mobility shift-ACE and VACE, 2) change in the peak area or height for HD and VP.

Table 2. The experimental and application details of the four dynamic equilibrium methods.

Method	Sample	Running buffer	Parameter for investigation	Application
Mobility shift-ACE	Analyte	Running buffer+ ligand	Migration time	Investigation of reactions with fast on-off kinetics
HD	Analyte alone, or + ligand	Running buffer+ ligand	Peak height or area	
VACE	Blank running buffer	Running buffer + analyte and ligand	Migration time	
VP	Blank running buffer	Running buffer + analyte and ligand	Peak height or area	

1.5.3.1.1.1 Mobility shift-ACE

In mobility shift-ACE, the sample for injection contains an analyte and an EOF marker while the running buffer contains a ligand in varying concentration. Under the electric field, two positive peaks will be detected which are corresponding to the EOF marker and the analyte. The migration time of the analyte peak can be changed after binding to a ligand. Therefore, this parameter is used for binding calculation. The use of an EOF marker is important to avoid calculation errors due to the possible change of the EOF during experiments (Figure 15).

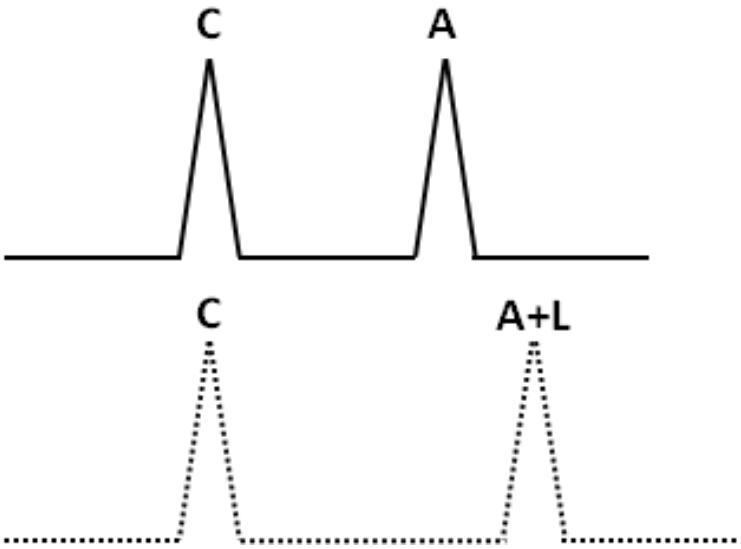

Figure 15. Mobility shift-ACE. Solid line shows two positive peaks. C is a control, in this case the EOF marker. A is the analyte without adding a ligand in the running buffer. Dotted line shows the mobility shifts of an analyte after binding with a ligand which is added in the running buffer.

1.5.3.1.1.2 Vacancy-ACE

In VACE, the capillary is filled with the running buffer containing an analyte and ligand in varying concentration. This will lead to a high response of a detector to the background. Therefore, under the influence of the electric field and injecting a small amount of a pure running buffer, two negative (vacancy) peaks will appear which correspond to an analyte and a ligand. The binding of a ligand to an analyte can be easily calculated based on the change in the mobility of the analyte negative peak, as shown in Figure 16.

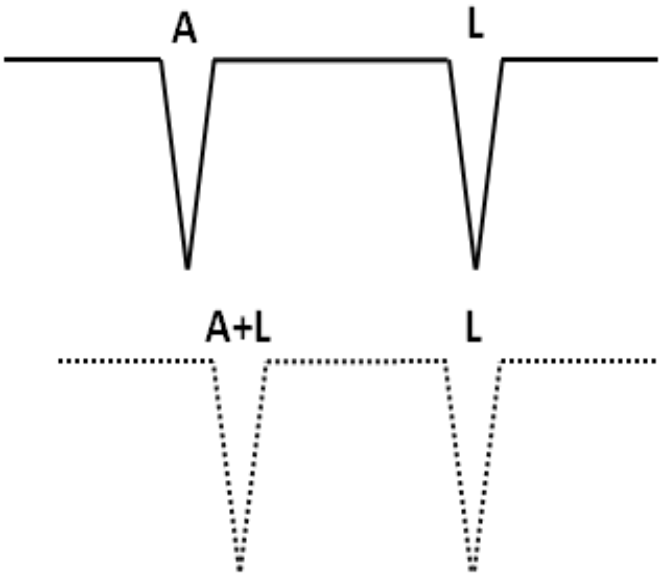

Figure 16. Vacancy-ACE. Solid line shows two negative peaks, A is an analyte, L is a ligand. Dotted line shows the the mobility shifts of an analyte after binding with a ligand.

1.5.3.1.1.3 Vacancy-Peak

In VP (Figure 17), similar to VACE but in this case the peak area or height are used. In this method, both free analyte and analyte bound with a ligand are considered to have similar mobility. Therefore, the negative peak of a ligand can be used for binding calculation since it is directly proportional to the quantity of the formed complex.

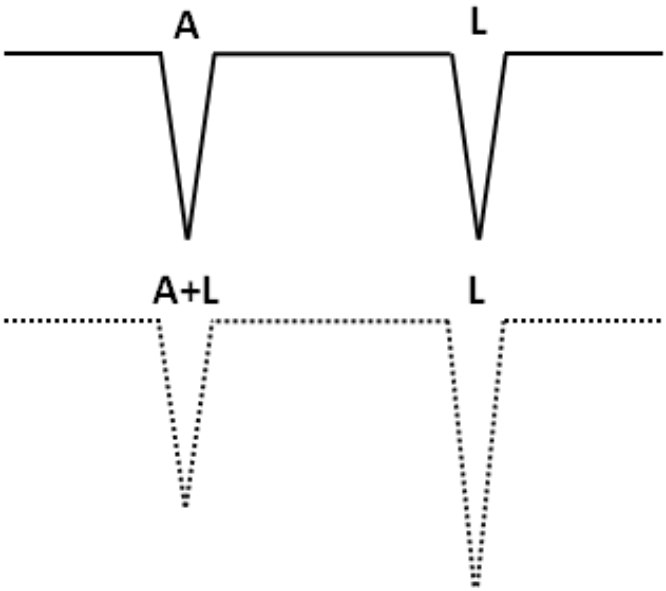

Figure 17. Vacancy-peak method. Solid line shows two negative peaks, A is an analyte, L is a ligand. Dotted line shows the possible change in a ligand negative peak area or height after binding with an analyte.

1.5.3.1.1.4 Hummel-Dreyer

In HD, the peak area is used. A capillary is filled with a ligand, which has ability to absorb UV-light and then small amount of an analyte is injected. As shown in Figure 18, two peaks could be observed, positive and negative. The positive peak corresponds to analyte-ligand complex and free analyte, in this case both have similar mobility. The negative peak is due to the local deficiency of a ligand in the running buffer. Therefore, the change in the peak area of the negative peak is used to calculate the amount of an analyte bound to a ligand.

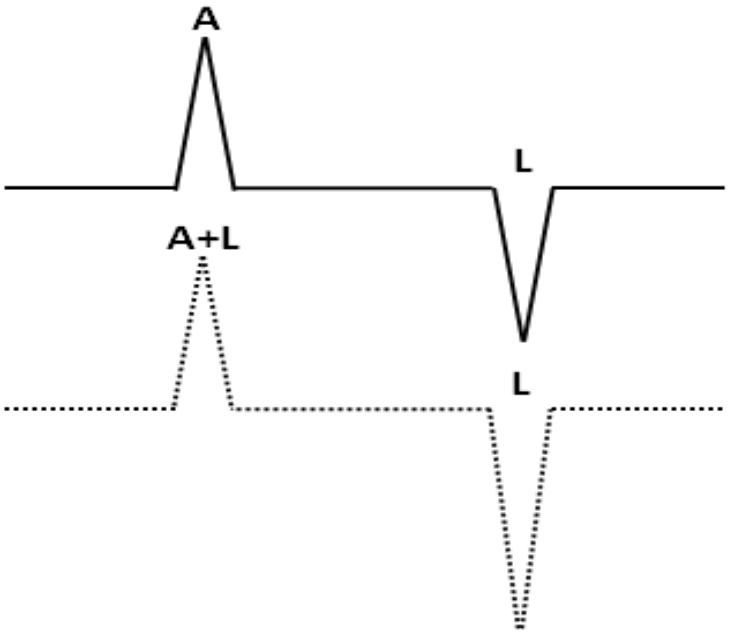

Figure 18. Hummel-Dreyer. Solid line shows two peaks, positive and negative. A is an analyte, L is a ligand. Dotted line shows the possible change in a ligand negative peak area or height after binding with an analyte.

1.5.3.2 Why mobility shift-ACE

The mobility shift-ACE was selected in this work due to many advantages. It is very sensitive method since a very weak interaction can be detected by the migration time change of 0.1 s [73-75]. Furthermore, the small change in the migration time is more obvious when the overall charge of a protein is changed by a metal ion and other

surrounding anions (Figure 19). It allows to work with very small amount of an analyte, e.g. at the level of limit of detection (LOD) since the binding investigation is based only on the migration time. On the other hand, ligands with no UV absorption can be used. It has the ability for simultaneous investigation of metal ion interactions with a number of analytes in one sample (mixture or even impure sample) due to the high separation power of this method. Recently, this method has been successfully used for interaction screening of an analyte (protein) with a ligand (metal ion) [73]. The screening was based on using of a high concentration of a ligand to achieve the saturation [73-75].

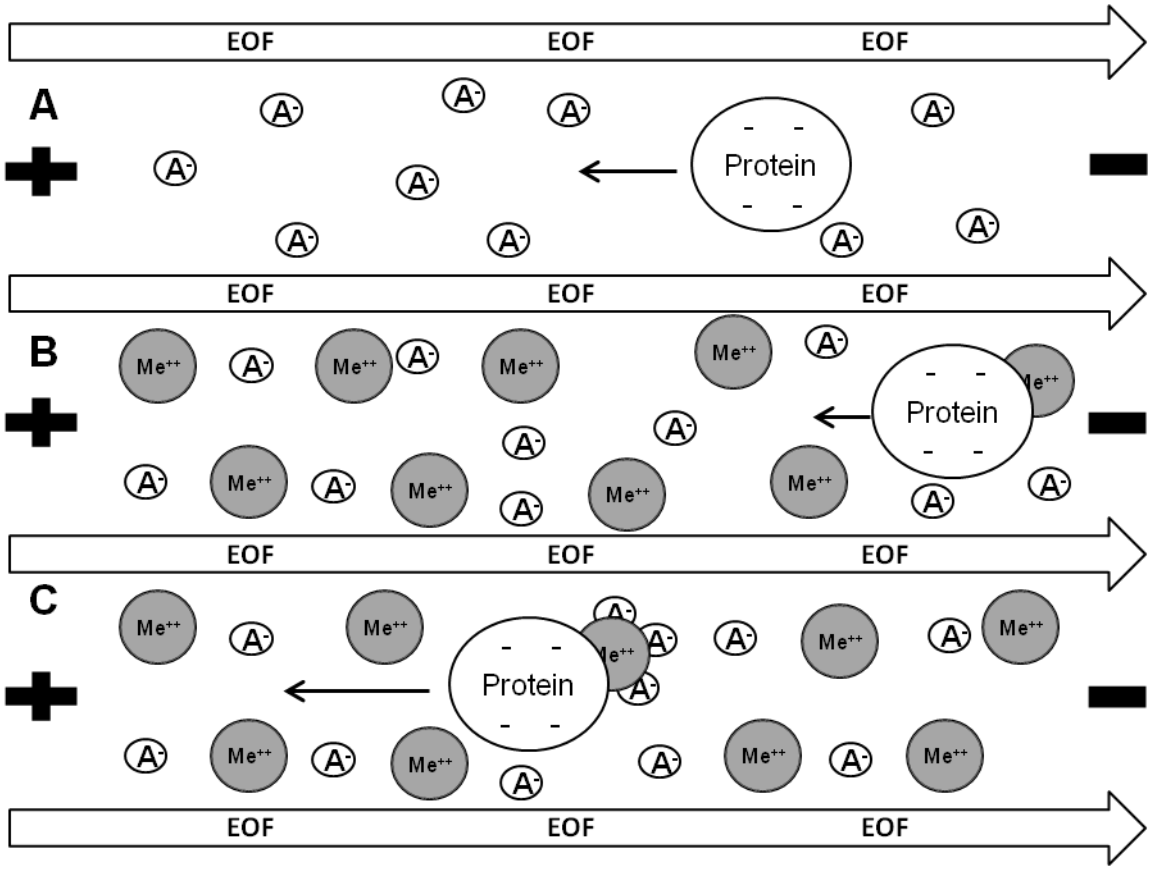

Figure 19. Illustration of shifted protein mobility under the influence of a metal ion (Me) and a coordinatively bound anion (A^-). Mobility of protein without (A) and with (B and C) metal ion. EOF: Electroosmotic flow.

1.5.3.2.1 Calculation and interpretation

1.5.3.2.1.1 EOF marker

Many factors are contributing to the change in migration times. Some substances such as positively charged ligands [107-111] and proteins [112, 113] adsorb to the

capillary wall leading to changes in the electroosmotic flow (EOF), resulting in a mobility shift which is not related to the interaction between two substances. Furthermore, a change in the temperature during the electrophoretic separation has significant influence on the EOF. Hence, EOF markers are often necessary to correct this effect [85, 110].

1.5.3.2.1.2 Mobility ratio

The use of the mobility ratio for the interaction screening is important to obtain precise results. The mobility ratio can be expressed as shown in Equation No. 14 [114].

$$R = \mu_{prot}/\mu_{eof} \quad \text{(Eq. 14)}$$

Since mobility μ is already defined as $l{\cdot}L/U{\cdot}t$. All these parameters apart from the migration time t are the same for the protein and the EOF and hence can be cancelled and the mobility ratio can then be calculated easily by using the observed migration time as shown in Equation No. 15:

$$R = t_{eof}/t_{prot} \quad \text{(Eq. 15)}$$

Where t_{eof} is the migration time of an EOF marker such as acetanilide and t_{prot} is the migration time of a protein.

1.5.3.2.1.3 Normalized mobility ratio and its confidence intervals

The fast interaction screening is based on the electrophoretic mobility ratio (with respect to EOF marker) of an analyte (protein) with and without a ligand (metal ion) in the running buffer, R_i and R_f, respectively.

Changes in charge, mass and size of a protein after interaction with a metal ion can be determined by using the normalized difference of mobility ratios ($\Delta R/R_f$), where $\Delta R = R_i - R_f$ (Eq. 16) [73-75].

A confidence interval (*cnf*) of $\Delta R/R_f$ can be calculated as following:

$$cnf(\Delta R/R_f) = (\Delta R/R_f) \pm \left(t_{\alpha/2,n_1+n_2-2} \cdot \hat{\sigma}_{total} \cdot \sqrt{\frac{2}{n_1+n_2}} \right) / R_f \quad \text{(eq. 17)}$$

$t_{\alpha/2}$ is the t-value of the probability 0.975 ($\alpha/2$ = 0.025) for a given degree of freedom. The n_1 and n_2 are the two data numbers of the series to estimate R_i and R_f. The value n_1+n_2-2 is the degree of freedom. The total standard deviation of the two series data of R_i and R_f is shown in Equation No. 18.

$$\hat{\sigma}_{total} = \sqrt{\frac{2 \cdot \left(f_1 \cdot \hat{\sigma}_1^2 + f_2 \cdot \hat{\sigma}_2^2 \right)}{\left(f_1 + f_2 \right)}} \quad \text{(Eq. 18)}$$

where f_1 and thef_2 are the numbers of freedom (*n-1*) while $\hat{\sigma}_1$ and $\hat{\sigma}_2$ are the standard deviations of the two series data for R_i and R_f, respectively.

A $\Delta R/R_f$ absolute value ≥ 0.01 is typically sufficient to indicate significant interactions [73-75]. Furthermore, the *cnf* of $\Delta R/R_f$ should not intersect the zero line for a significant interaction. Additionally, $\Delta R/R_f$ values can be positive or negative depending on the formed complex. Normally, the overall charge of a protein could get less negative after binding with a metal ion and thus can easily be detected by positive $\Delta R/R_f$ value. In another case, the bound metal ion on a protein could further bind coordinatively with the surrounding anions of the buffer leading to a more negative overall charge of the protein. This can then be detected by negative $\Delta R/R_f$ values.

1.5.3.2.1.4 Binding constant

The binding constant can be calculated by four mathematical plotted equations; x-reciprocal, y-reciprocal, double-reciprocal and nonlinear regression [85, 105, 115]. Those equations are summarized in Table 3 with their references. As known, most of biomolecules including proteins exhibit multiple target sites for ligand binding. Therefore, the 1:1 binding stoichiometry is not common. Hence, a nonlinear regression equation found to be more accurate and precise for estimating the binding constants in ACE compared to other equations [85]. Furthermore, the calculation of both association and dissociation constant in ACE was less sensitive to random error using nonlinear regression plotting method.

Table 3. The calculation of binding constant by different mathematical equations

Plot method	Mathematical equations	Fitting method	K
Nonlinear regression Eq. (19)	$K \cdot c(L) = \frac{R_f - R_i}{R_i - R_c}$	$\frac{R_f - R_i}{R_i - R_c}$ VS. $c(L)$	Slope
x-reciprocal Eq. (20)	$\frac{1}{R_i - R_f} = \frac{1}{(R_c - R_f) \cdot K} \cdot \frac{1}{c(L)} + \frac{1}{R_c - R_f}$	$\frac{R_i - R_f}{c(L)}$ VS. $R_i - R_f$	-Slope
y-reciprocal Eq. (21)	$\frac{c(L)}{R_i - R_f} = \frac{1}{R_c - R_f} \cdot c(L) + \frac{1}{(R_c - R_f) \cdot K}$	$\frac{c(L)}{R_i - R_f}$ VS. $c(L)$	Slope/intercept
double-reciprocal Eq. (22)	$\frac{R_i - R_f}{c(L)} = -K \cdot (R_i - R_f) + K \cdot (R_c - R_f)$	$\frac{1}{R_i - R_f}$ VS. $\frac{1}{c(L)}$	Intercept/ Slope

- K is binding constant
- $c(L)$ is the concentration of receptor.
- R_i and R_f are the migration time ratio of the substrate ($t_{eof}/t_{analyte}$) in background electrolyte with and without ligand respectively.
- R_c is the migration time ratios of an analyte ($t_{eof}/t_{analyte}$) at saturated concentration of ligand.

1.5.3.3 ACE method transfer

Analytical method transfer includes intra and inter-company as well as intra and inter-instrument transfer. Intra and inter-company method transfer challenges can be minimized by good working practice, using the same parameters and the same quality reagents and working materials, whenever possible [87]. This process can be facilitated by excellent contact between the analytical transfer teams (ATM) of different companies [116] or between the analysts if there is no ATM. Exchanging an instrumental parameter (e.g. the capillary length) between ACE methods on the same

instrument can be defined as intra-instrument transfer. The inter-instrument method transfer involves transferring a method to different instruments. So far, all reproducible ACE methods in the literature are defined only for one instrument. Hence, transferring an ACE method could be challenging because of different instrument designs especially in cooling system. A good inter-instrument transfer strategy will later facilitate inter and intra company or working group transfers.

1.5.3.3.1 Influence of capillary cooling system design

It is well known that the affinity interaction measurement is strongly temperature dependant [117, 118]. For example, Bohlin et al. faced difficulties (peak disappearance and unstable current) when performing ACE at 37 °C, but these difficulties were diminished at 22 °C [119]. Therefore, the temperature is the most important factor for transferring a CE method due to its variation along the capillary [119]. The overall temperature of the capillary is significantly different from CE instrument to another due to different capillary cooling system designs [120]. The capillary cooling systems of the commercially available CE instruments cover mainly the middle part of the capillary (efficiently cooled part). The inlet and outlet (inefficiently cooled parts) of the capillary are out of the cooling system. The temperature was determined in different parts across the whole capillary length and found to be up to 15 degrees higher in inlet region (inefficiently cooled) than in the efficiently cooled part, depending on power per unit volt [117, 121-124]. It is well known that, lengths of the inefficiently cooled parts are different from CE instrument to another, thus the overall capillary temperature of each instrument could vary. This may cause different interaction results on different instruments. For example, the protruded inlet and outlet parts (inefficiently cooled) in the Prince model C760 instrument are twice longer than in the Agilent model G1600A instrument (Figure 20).

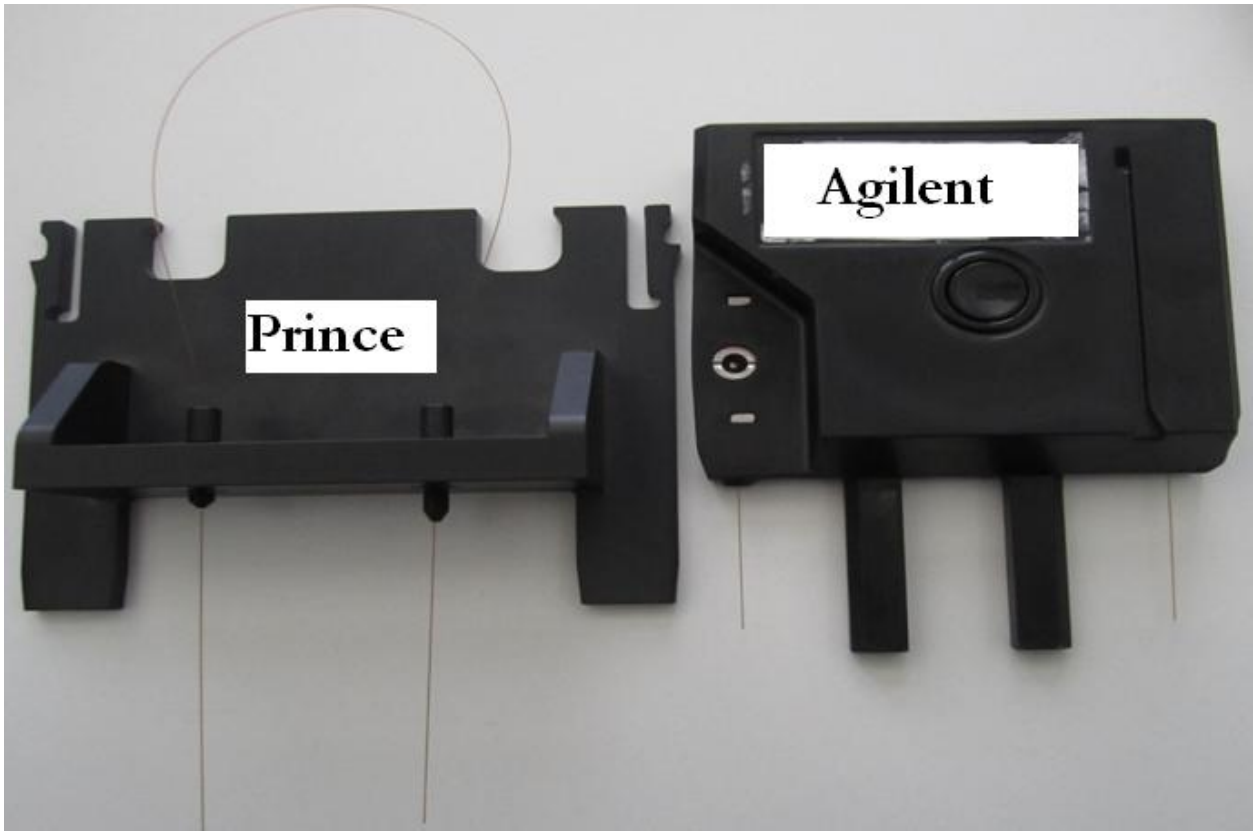

Figure 20. Different cartilage models of different manufacturers, Prince: PrinCE-C760 system (Prince Technologies, Netherland), Agilent: Agilent CE system model G1600A (Agilent Technologies, Germany).

1.6 Aim of the work

As mentioned in section 1.4, ACE is becoming more important and is growing up steadily to investigate different analyte-ligand interactions for different research fields. Up-to-date, there is only one published mobility shift-ACE method to characterize a protein-metal ion interaction [73]. This method is still not optimized since it offers approximately a total run time of 30 min including the rinsing protocol and extra flushing protocol of 30 min after each 30 subsequence runs [73, 85]. The throughput of this method is only moderate which makes it not optimally suitable for routine screening work. Therefore, developing and accelerating a new a mobility shift-ACE method was considered as one of the major goals in our work. A literature search reveals that there is no study regarding ACE method transfer. In the same time, there are different CE instruments with different cooling systems which probably lead to variation in interaction results. Therefore, investigating the ACE method transfer among different instruments was considered as the second goal. It is well known that

most of the metal ions can strongly bind to the internal capillary wall, which lead to change in EOF, and hence the interaction results. Therefore, enhancing the precision of the results especially by improving a rinsing protocol is considered as the third goal. The fourth goal of this work was to investigate and characterize the influence of different metal ion groups on the various globular proteins using the accelerated mobility shift-ACE method and providing reference values as well as a comprehensive, generic platform to characterize metal ion interactions in general.

2 Materials and Methods

2.1 Chemicals and reagents

Bovine serum albumin (BSA, 99%), human serum albumin (HSA, 97%), ovalbumin (OVA, 98%), β-lactoglobulin (β-LG, 85% bovine milk) and myoglobin (MB, 90%), also chromium (III) chloride hexahydrate ($CrCl_3 \cdot 6H_2O$), cobalt (II) chloride hexahydrate ($CoCl_2 \cdot 6H_2O$), copper (I) chloride (CuCl), gallium (III) chloride ($GaCl_3$), gold (I) chloride (AuCl), gold (III) chloride ($AuCl_3$), iridium (III) chloride ($IrCl_3$), lithium chloride (LiCl), nickel chloride hexahydrate ($NiCl_2 \cdot 6H_2O$), osmium (III) chloride hydrate ($OsCl_3$), palladium (II) nitrate dehydrate ($Pd(NO_3)_2 \cdot 2H_2O$), platinum (IV) chloride ($PtCl_4$), rhodium (III) nitrate hydrate ($Rh(NO_3)_3$), ruthenium (III) chloride hydrate ($RuCl_3$), sodium molybdate (Na_2MoO_4), vanadium (III) chloride (VCl_3), Selenium (IV) chloride **(**$SeCl_4$) and tris powder were purchased from Sigma-Aldrich (Steinheim, Germany). Silver (I) nitrate ($AgNO_3$) was obtained from Grüssing (Filsum, Germany). Ethylenediaminetetraacetic acid disodium salt dihydrate (EDTA-$Na_2 \cdot 2H_2O$) and sodium chloride (NaCl) were purchased from ROTH (Karlsruhe, Germany). Malonic acid was from Riedel de Häen (Hannover, Germany). Acetanilide and barium chloride ($BaCl_2$) were obtained from Fluka (Steinheim, Germany). Conc. hydrochloric acid (HCl) and copper (II) chloride ($CuCl_2$) were purchased from Merck (Darmstadt, Germany). Bidistilled water was produced in our institute.

2.2 Apparatus and instrumentation

Developing a mobility-shift ACE method (acceleration and improving the precision of binding results) for the investigation of protein-metal ion interaction were performed on Agilent CE system model G1600A (Agilent Technologies, Germany) consisting of an automatic sampler, a capillary cooling system and a diode array detector (operating at 214 nm), the high pressure was applied by using the normal air plug at laboratory. Bare fused silica capillaries of 50 µm I.D. with a total length of 31 cm (short capillary) and an effective length of 22 cm were obtained from Polymicro Technologies (Phoenix, AZ, USA). Rotilabos-syringe filters were obtained from Carl Roth (CME, 0.22 mm, Karlsruhe, Germany). The pH of the used buffer solutions was adjusted on a Mettler Toledo FE20/EL20 pH-meter (Carl Roth, Karlsruhe, Germany).

For the investigation of ACE method transfer, total capillary lengths of 62 cm with 50 µm I.D. (long capillary) were used to fit on the three CE instruments from different manufacturers: (1) Agilent CE system model G1600A (Agilent Technologies,

Germany) containing a capillary cooling system covering 86% of the capillary length (effective length 53 cm), (2) PrinCE-C760 system (Prince Technologies, Netherland) containing a capillary cooling system covering 71% of the capillary length (effective length 53.5 cm), (3) UniCAM Crystal 310 CE System (UniCAM Ltd., Cambridge, UK) containing a capillary cooling system covering 15% of the capillary length (effective length 48 cm).

The collected data were integrated by the installed software of each instrument. Agilent ChemStation software for Agilent data and DAx 3D software for PrinCE-C 700 data. In case of UniCAM Crystal system, the electropherograms were monitored with a Crystal CE program V.1.3 and then integrated by a homemade integration program CISS [39]. Finally, the mobility ratios, $\Delta R/R_f$ (and its confidence interval) and the statistical analysis were performed by Microsoft EXCEL™ (Microsoft Corporation, version 2007).

2.3 Rinsing protocol

New capillaries were conditioned at 1 bar with 1 N sodium hydroxide (20 min for short capillary and 40 min for long capillary) followed with 10 min water. Furthermore, extra flushing at 2.5 bar with 0.1 N sodium hydroxide for 20 min and water for 10 min for long capillaries was applied at the beginning and at the end of each working day, while the same procedure with half times was used for short capillaries. At the beginning of each analysis, capillaries were rinsed at 2.5 bar for an enough time with 0.1 N sodium hydroxide, water, and running buffer.

2.4 Separation conditions

Electrophoretic separations were carried out at a temperature of 23°C and voltages of 10 and 20 kV using the normal mode (anode at inlet and cathode at outlet). Samples were injected hydrodynamically at 50 mbar. Sample pushing was applied in short capillaries; the injected sample was followed by injecting the running buffer at 50 mbar for 2.5 s. For each protein-metal ion interaction screening, twelve runs were conducted, six for protein without metal and six for protein with metal.

2.5 Preparation of solutions

Two sets of tris buffer (20 mmol/ L) at pH 7.4 were prepared. For each set, an amount of 2.42 g of tris was weighted and dissolved in 200 ml bidistilled water. The pH of the first set was adjusted to 7.4 by using hydrochloric acid and then filled up to 1000 mL with water. The pH of the second set was adjusted to 7.4 by using acetic

acid instead of hydrochloric acid to be suitable for dissolving the metal salts of Pd^{2+}, Rh^{3+} and Ag^{+} which are precipitated by Cl^{-}. Acetanilide has pKa value of 0.5 due to the delocalization of the non-bonded electrons of nitrogen via resonance effect of the conjugation system. Therefore, it has been used as EOF marker since it is neutral at pH 7.4 [73-75, 85]. A stock solution of acetanilide (750 µg/ mL) was prepared by dissolving 37.5 mg acetanilide in 50 ml tris buffer and then sonicated until complete dissolving. The protein and metal ion solutions were prepared freshly in the same tris buffer every working day. Proteins OVA (50 µmol/L), BSA (20 µmol/L), HSA (20 µmol/L), β-LG (50 µmol/L) and MB (60 µmol/L) were prepared separately. An amount of 53.5 mg of OVA, 33 mg of BSA, 33.18 of HSA, 23 mg of β-LG and 25.8mg of MB were weighed in separate 25 mL volumetric flasks. Then 5 mL of the acetanilide stock solution were added and filled up by tris buffer. These protein solutions were diluted three-fold before starting the experiments to avoid band broadening and to minimize protein adsorption. Each metal ion solution was prepared using tris buffer (20 mmol/ L, pH 7.4) to give concentrations of 25, 100 and 250 µmol/L. In case of iron ions, they tend to precipitate with both tris buffer sets. Therefore, stock solutions of ferric and ferrous ions (5 mmol/L) were prepared by dissolving an appropriate amount of iron salt (ferric or ferrous chloride) in a solution consisting of unadjusted-pH tris (20 mmol/L) and malonic acid (15 mmol/L). Malonic acid was used to improve the solubility of iron salts by weakly chelating iron ions and forming complexes which can exchange ligands with protein residues [51]. Further required concentrations for ACE experiments were prepared by diluting the stock solutions with the first set tris buffer.

CuCl was precipitated by both tris buffer sets as well. However, Cu^{+} can dissolve in ammonia solution by forming complex with ammonia which is easily exchangeable with the most soft protein residues [125]. Hence, the stock solution of CuCl (5 mmol/L) was prepared by dissolving 12.37 mg first in 1 ml ammonia solution (25 %) to improve its solubility and then completing to 25 ml using first set tris buffer. The pH of the CuCl stock solution was adjusted to 7.4 using hydrochloric acid just before complete filling with the tris buffer, and then the required concentrations for mobility shift-ACE experiments were prepared by diluting the stock solutions with the first set tris buffer. All solutions were filtered with 0.22 µm filter before introducing into the capillary.

3 Results and discussion

3.1 Developing a mobility shift-ACE method

3.1.1 Acceleration

3.1.1.1 Using short capillary

BSA and the EOF marker (acetanilide) were used as test system for the acceleration study of the mobility shift-ACE method. The migration time of a given analyte is directly proportional to the square of the capillary length [88]. Therefore, the capillary was prepared as short as possible to speed up the method. The shortest possible capillary length to fit in the capillary cartridge of all modern CE instruments was found to be 31 cm; this length can be used without scaring of breaks. A voltage of 20 kV has been applied for good acceleration and run stability. As shown in Figure 21, the use of the short capillary decreases the migration time of BSA to approximately 3 min instead of 9 min when using long capillaries as in a previously published mobility shift-ACE method (long method) [73]. Since the peak area is not important for mobility shift-ACE performance, further acceleration has been achieved by diluting the protein sample (three-fold) and reducing the injected volume (50 %) due to decrease in the peak band broadening (Figure 21).

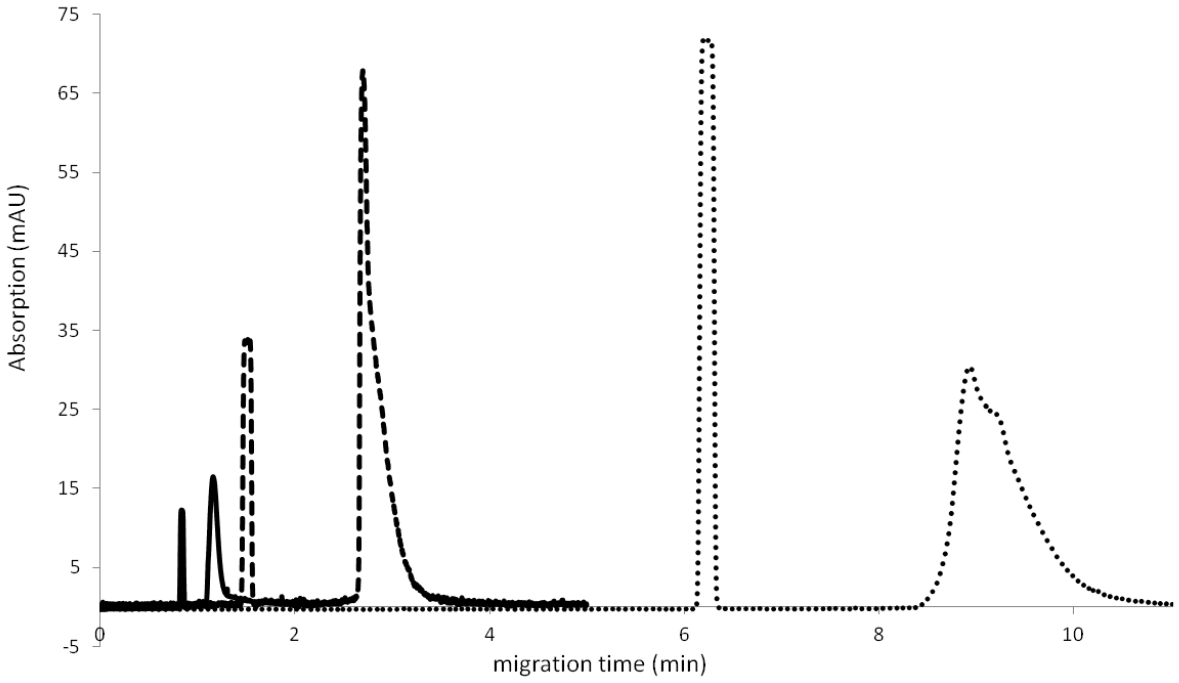

Figure 21. Different electropherograms of EOF marker and BSA using the same applied voltage of 20 kV, a capillary cartridge temperature 23°C and UV detection of 214 nm, but different capillary lengths, sample concentration and

injected volume. Dotted line (····) shows electropherogram using the long method [73], capillary length of 62 cm and 50 µm I.D, BSA concentration of 20 µmol/L and injected at 50 mbar for 18 s. Dashed line (----) shows electropherogram using the short capillary length of 31 cm and 50 µm I.D, BSA concentration of 20 µmol/L and injected at 50 mbar for 9 s. Solid line shows electropherogram peaks using the short capillary length of 31 cm and 50 µm I.D, BSA concentration of 6.66 µmol/L injected at 50 mbar for 4.5 s.

3.1.1.2 Short rinsing protocol

The smaller wall area of the short capillary of 31 cm length requires a shorter rinsing protocol compared to the previously used long rinsing protocol (total 12.5 min) for the long capillary of 62 cm length [73, 85]. Furthermore, the use of low protein concentration and small injection volume decreases the adsorbed amount of protein on the capillary wall over long-term runs, and hence further reduction in the rinsing time was possible. Different sets of rinsing protocols were tested and evaluated depending on the calculated relative standard deviation percentage (RSD%) for long-term mobility ratios measurements (Table 4).

Table 4. Summary of the used rinsing protocols and the obtained RSD % values

Protocol	Number of runs (n)	Rinsing pressure and time	Sample injection	RSD%
1	20	At 2.5 bar with 1 min 0.1 N NaOH, 1 min water, 1.5 min tris buffer	50 mbar for 4.5 s	**1.173**
2	20	At 2.5 bar with 1 min 0.1 N NaOH, 1 min water, 1 min tris buffer	50 mbar for 4.5 s	2.05
3	20	At 2.5 bar with 0.75 min 0.1 N NaOH, 0.75 min water, 1 min tris buffer	50 mbar for 4.5 s	2.49

As shown in Figure 22, scattering of mobility ratios has been increased after slightly decreasing the rinsing time by only 0.5 min. Hence, the short rinsing protocol (protocol 1, see table 4) at 2.5 bar of 0.1 N sodium hydroxide for 1 min, water for 1

min, and running buffer for 1.5 min was found to be the best for the accelerated method since the long-term mobility ratio measurements (n= 20) already showed good precision with RSD% of 1.17%.

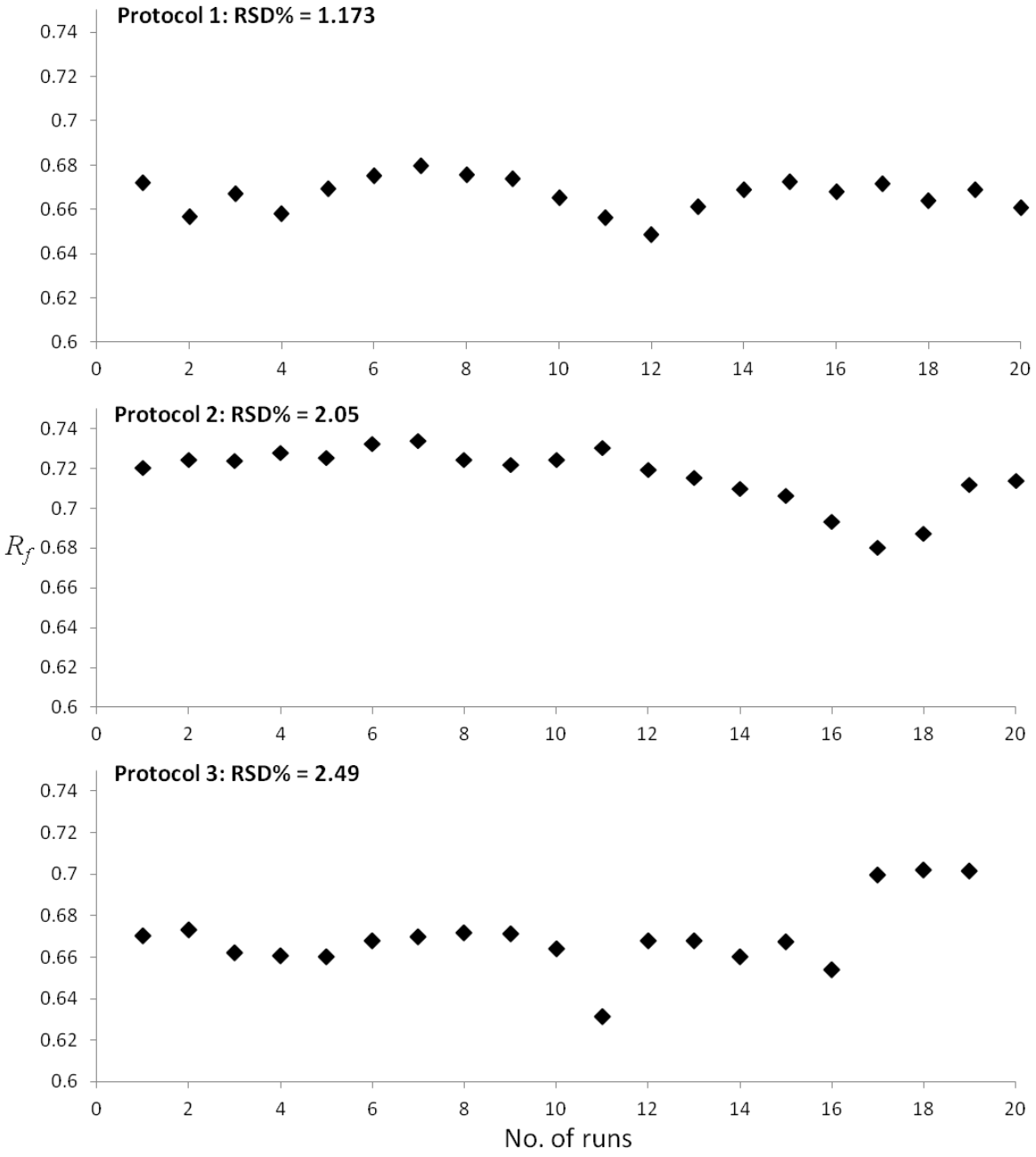

Figure 22. R_f values of BSA using different rinsing protocols. All rinsing protocols were implemented with the same solutions at 2.5 bar but with different rinsing times. Protocol 1: 1 min 0.1 N NaOH, 1 min water, 1.5 min tris buffer. Protocol 2: 1 min 0.1 N NaOH, 1 min water, 1 min tris buffer. Protocol 3: 0.75 min 0.1 N NaOH, 0.75 min water, 1 min tris buffer. Separation condition: capillary 50 µm I.D. with 31 cm total length and 22 cm effective length, buffer 20

mmol/L tris (pH 7.4), injection (50 mbar, 4.5 s), voltage 20 kV, UV 214 nm, capillary cartridge temperature 23°C.

3.1.2 Separation optimization

In order to evaluate the separation efficiency of the accelerated mobility shift-ACE method (accelerated method) and compare to the long method, OVA and acetanilide were used as model. As mentioned in the introduction, see section 1.1.3.4, the electropherogram should in principle show three isoforms for OVA, which are attributed to different degree of phosphorylation. Please note that the amount of each isoform could be different within different batches [103-104]. The accelerated method operated with 20 kV did not however offer separation for OVA isoforms (Figure 23).

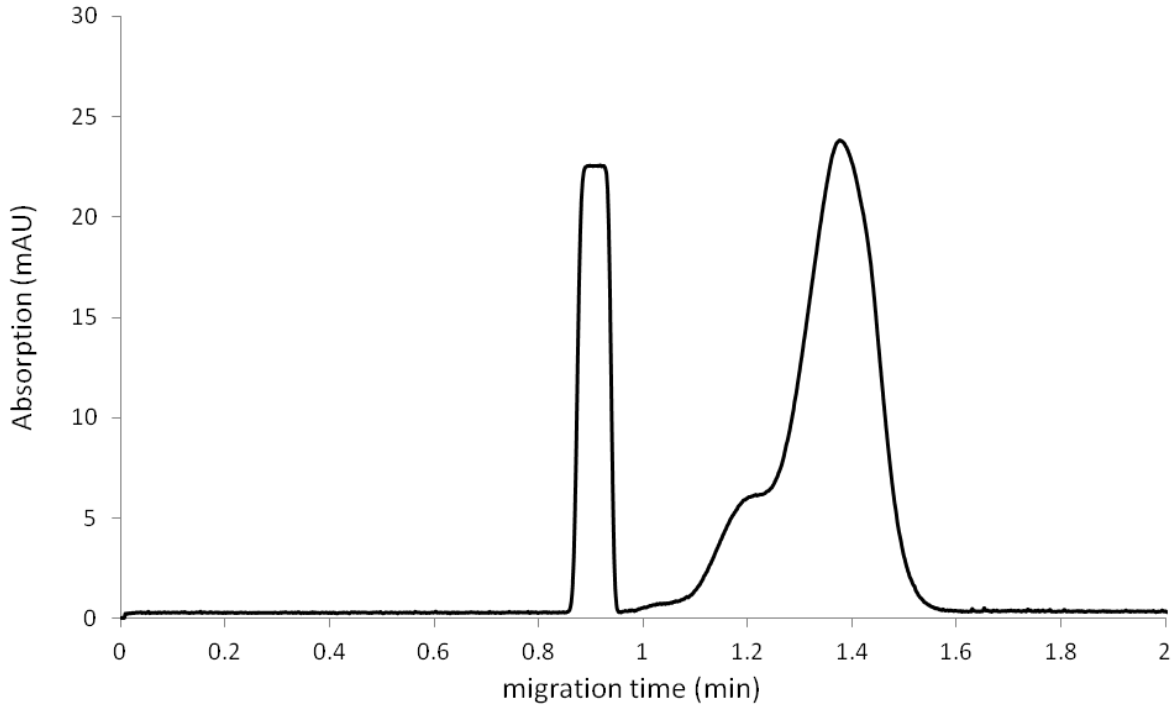

Figure 23. Electropherograms of acetanilide (EOF marker) and ovalbumin, respectively. Separation condition: capillary with 50 µm I.D., 31 cm total length and 22 cm effective length, tris buffer 20 mmol/L (pH 7.4), injection (50 mbar, 4.5 s), applied voltage 20 kV, detection wavelength at 214 nm, capillary cartridge temperature 23°C, rinsing protocol: at 2.5 bar 0.1 N sodium hydroxide for 1 min then water for 1 min after that tris buffer for 1.5 min.

Therefore, we considered the optimization of the applied voltage to allow the separation between the OVA isoforms. As shown in Figure 24, the separation between OVA isoforms was successfully achieved using the same electric field of the long method $32.25 \cdot 10^3$ V m^{-1}; in this case the optimum applied voltage was set to 10 kV for the accelerated method.

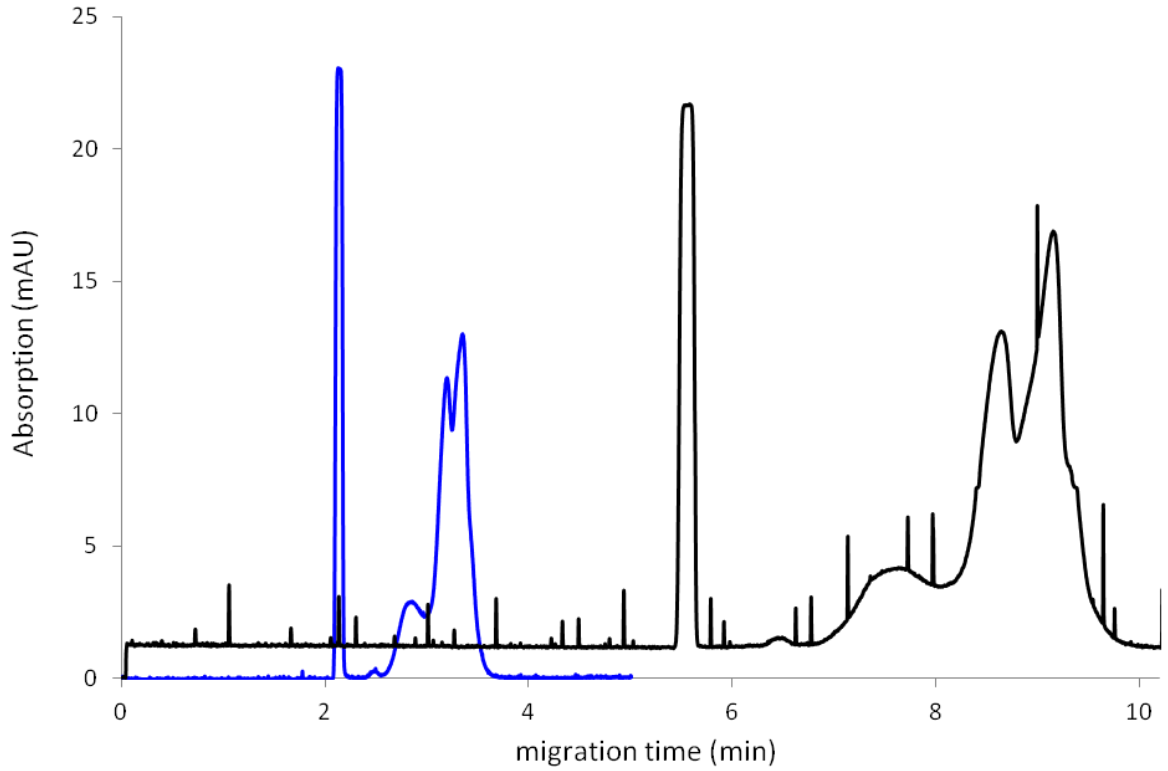

Figure 24. Electropherograms of the same batches of acetanilide (EOF marker) and ovalbumin using accelerated and long methods. The black line exhibits the long method on the UniCAM CE instrument: capillary with 50 µm I.D., 62 cm total length and 48 cm effective length, tris buffer 20 mmol/L (pH 7.4), injection (50 mbar, 18 s), applied voltage 20 kV, detection wavelength at 214 nm, capillary cartridge temperature 23°C, rinsing protocol: at 2.5 bar 0.1 N sodium hydroxide for 3.5 min, water for 3.5 min and tris buffer for 5.5 min (reprinted with permission from reference No. 73). The blue line exhibits the accelerated method on the Agilent CE instrument: capillary with 50 µm I.D., 31 cm total length and 22 cm effective length, tris buffer 20 mmol/L (pH 7.4), injection (50 mbar, 4.5 s), applied voltage 10 kV, detection wavelength at 214 nm, capillary cartridge temperature 23°C, rinsing protocol: at 2.5 bar 0.1 N sodium hydroxide for 1 min then water for 1 min after that tris buffer for 1.5 min.

Table 5 compares the mobility shift-ACE operating conditions between the accelerated method and the long method [73]. Using the accelerated method it is possible to perform the electropherotic separation with maximum run time of 4 min without a ligand in the running buffer depending on the protein overall charge, mass and size.

Table 5. Mobility shift-ACE separation conditions for two different capillary lengths

Method	Capillary	Rinsing protocol	Sample inject. & conc.	kV, run time	Maximum total time
Long (Ref. 73)	50 µm ID, 62 cm L, 54 cm l.	3.5 min 0.1 N NaOH, 3.5 min water, 5.5 min tris buffer.	100 mbar for 9 s. 20 µmol/L for BSA & HAS, 50 µmol/L for OVA & β-LG .	20 kV, 9-16 min	28.5 min
Accelerated	50 µm ID, 31 cm L, 22 cm l.	1 min 0.1 N NaOH, 1 min water, 1.5 min tris buffer.	50 mbar for 4.5 s. 6.66 µmol/L for BSA & HAS, 16.66 µmol/L for OVA & β-LG .	10 kV, 4-6 min	9.5 min

3.1.3 ACE method transfer

3.1.3.1 Intra-instrument

The performance of the accelerated method was evaluated and compared to the long method [73]. BSA and OVA and the metal ions Ba^{2+} and Ni^{2+} were selected as interaction models to investigate the intra-instrument ACE method transfer from the long method to the accelerated method on the same CE instrument (Agilent CE instrument model G1600A). Both methods (see Table 5) were developed to compare the binding of metal ions to biomolecules such as proteins. As known, the 1:1 binding stoichiometry is not common here since most of the biomolecules including proteins exhibit multiple target sites for ligand binding [73, 85]. Therefore, a high concentration of the metal ion ligand should be used to ensure that the interaction equilibrium is achieved. In the long method [73], the used concentrations of metal ion ligands were at least 5 folds higher than the concentration of the proteins. As shown in Figure 25, the accelerated method using the three folds diluted protein and metal ion concentrations compared to the long method (with the aim to speed up the analysis) gives different $\Delta R/R_f$ results. Similar $\Delta R/R_f$ results were only obtained when keeping the same metal ion concentration of 250 µmol/L as for the long method.

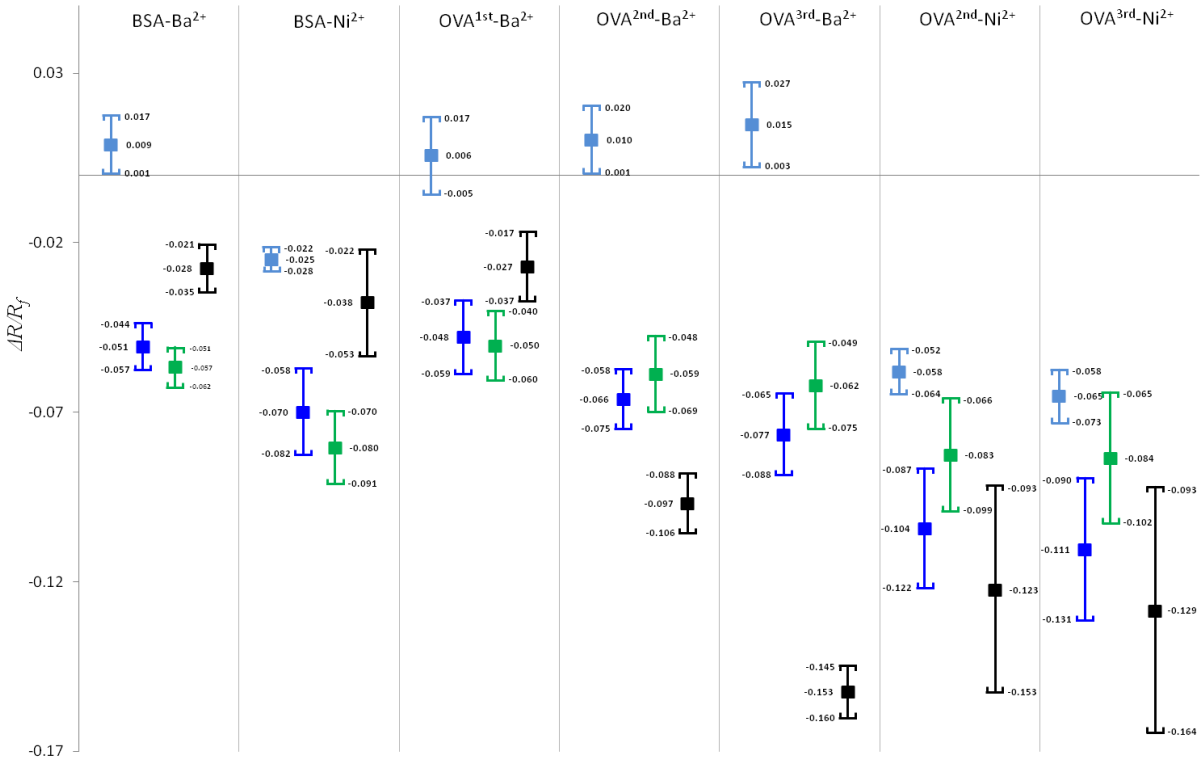

Figure 25. $\Delta R/R_f$ values of different model protein-metal ion pairs using the accelerated method (blue) and the long method (green) on the Agilent instrument, and only the long method on the UniCAM (black, reprinted with permission from reference No. 73). Metal ion (Ba^{2+} and Ni^{2+}) concentrations of 250 µmol/L were used for BSA and OVA and 100 µmol/L for β-LG. The three-fold diluted metal ion concentrations were also used on the accelerated method, 83.33 µmol/L for BSA and OVA and 33.33 µmol/L for β-LG, degree of darkness of the blue color corresponds proportionally to the concentrations of the metal ions, dark blue for the high metal concentration and light blue for the diluted metal ion concentration.

The observed different $\Delta R/R_f$ values between accelerated and long method by using three folds diluted metal ion concentration in the accelerated method could not probably be attributed to the capillary temperature. The influence of the capillary temperature is negligible since the same electric field has been applied and the cooling system of the used CE instrument (Agilent) covers more than 70% of the capillary length. Thus it ensures low temperature variation along the capillary. However, it is well known that each protein molecule is influenced by a ligand

concentration at its interface. Thus using three folds diluted metal ions (83.33 µmol/L) offered insignificant interaction using the accelerated method, this probably due to the low amount of metal ions at the protein interface. Therefore, the use of metal ion concentration of 250 µmol/L of the long method for accelerated method experiments offered similar interaction results.

Meanwhile, the binding curves of BSA with Ba^{2+} for calculating the binding constant were created using both methods (Figure 26). The binding constants were calculated as well, based on the non-linear regression model [85]. The binding curves show that both methods find very similar affinities of Ba^{2+} to BSA. Furthermore, there was no significant difference between the calculated binding constants (K_b) of both methods, 15 $mmol^{-1}$·L and 14 $mmol^{-1}$·L for the accelerated and the long method, respectively.

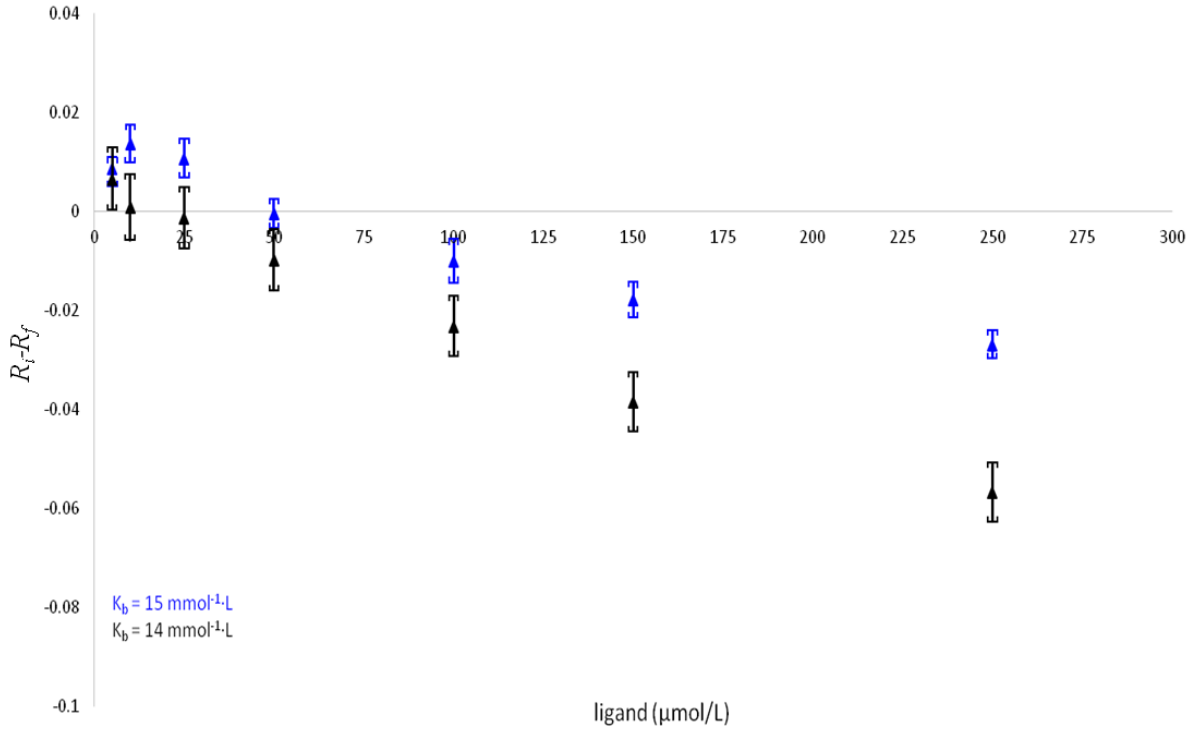

Figure 26. Binding curves of BSA-Ba^{2+} model which were conducted on the Agilent CE instrument using the accelerated method (blue) and the long method (black, reference No. 73).

The obtained $\Delta R/R_f$ values and their confidence intervals from the accelerated method were compared to the results of the long method using a different instrument (UniCAM). As shown again in Figure 25, the interaction results of the pairs BSA-Ba^{2+}, BSA-Ni^{2+} and OVA-Ba^{2+} were slightly different on both instruments. This could be

attributed to the different capillary cooling system designs of both instruments. Therefore, transferring ACE method between different instruments was considered in the next section.

3.1.3.2 Inter-instrument

In order to investigate the ACE method transfer among different instruments and the influence of their capillary cooling systems on binding measurements, other parameters such as voltage, rinsing procedure, injection volume and detection wavelength were kept constant on all of the used CE instruments. The values are shown in the legend of Figure 27. The two proteins (OVA and BSA) and the two metal ions (Ba^{2+} and Ni^{2+}) were used as interaction models for this study. As shown in Figure 27, the $\Delta R/R_f$ values of OVA-Ba^{2+} and OVA-Ni^{2+} are similar on Agilent and Prince instruments while slightly lower on UniCAM instrument. This could be attributed to the short cooled capillary part of the UniCAM instrument since only 15 % of the capillary length is inside the cooling system compared to 86 % and 71 % on Agilent and Prince instruments, respectively.

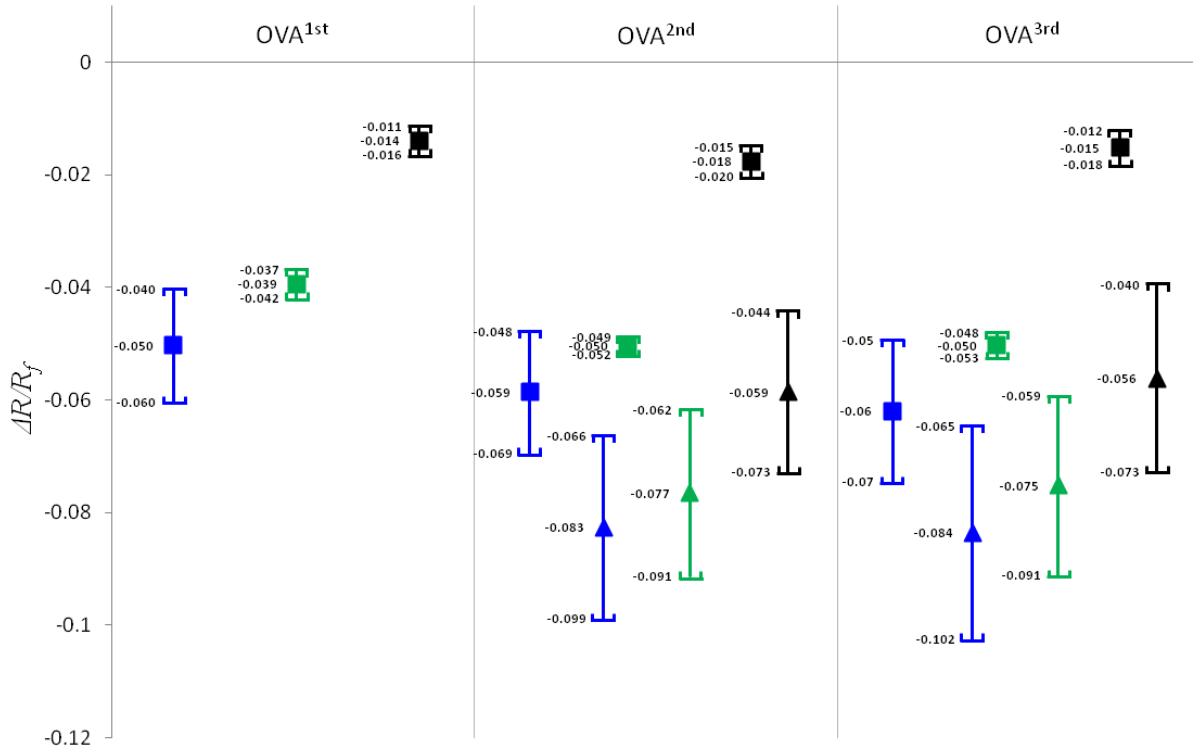

Figure 27. $\Delta R/R_f$ values of OVA isoforms interaction with Ba^{2+} (■) and Ni^{2+} (▲), the blue, black and green colors represent the results on Agilent, UniCAM and Prince instruments, respectively. Separation condition: capillary 50 µm I.D., 62

cm total length, effective length (53 cm Agilent, 48 cm UniCAM and 53.5 cm Prince),buffer 20 mmol/L tris (pH 7.4), injection (50 mbar, 18 s), voltage 20 kV, UV 214 nm, capillary cartridge temperature 23°C. Rinsing protocol at 2.5 bar with 0.1 N sodium hydroxide for 3.5 min, water for 3.5 min and tris buffer for 5.5 min. The capillaries were extra flushed after each screening at 2.5 bar with 0.1 N sodium hydroxide for 20 min and water for 10 min.

In case of the BSA-Ni^{2+} interaction, $\Delta R/R_f$ values were highly influenced by the small variation in the capillary cooling system of Agilent (efficiently cooled part 86 %) and Prince (efficiently cooled part 71 %) instruments. The obtained results from the Prince instrument show no significant BSA-Ni^{2+} interaction compared to significant interaction results on the Agilent instrument (Figure 28). However, the interaction of the BSA-Ni^{2+} on the Prince instrument became significant and similar to the results on the Agilent instrument after reducing the capillary cooling system temperature setting gradually from 23°C to 18 °C (Figure 28).

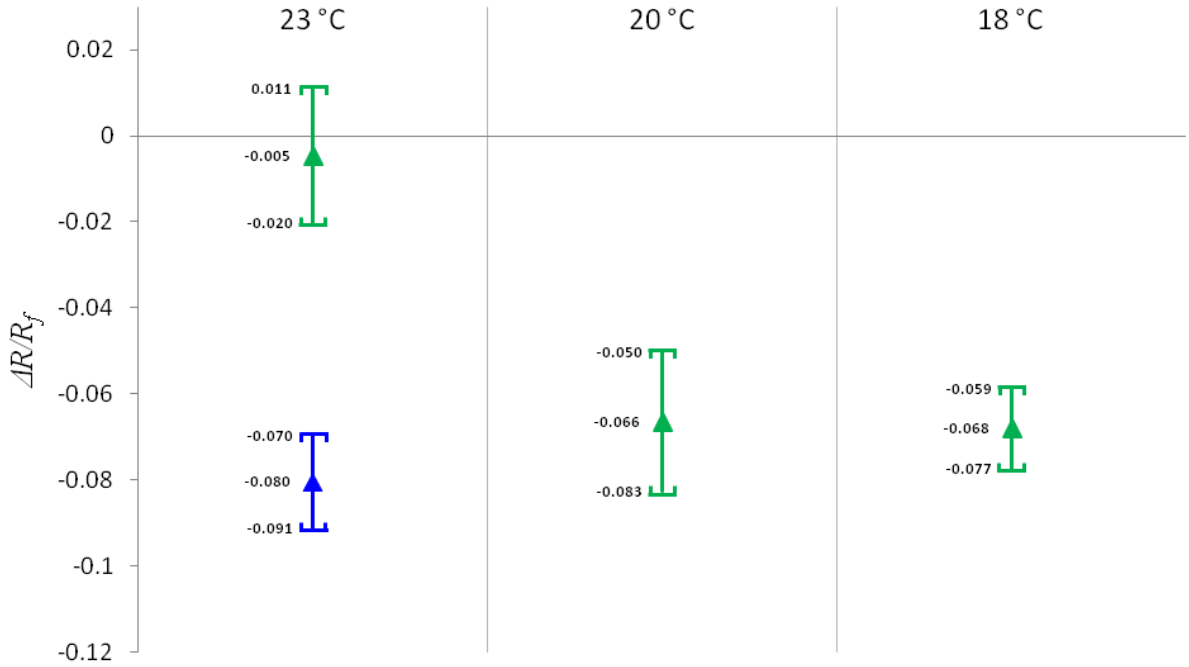

Figure 28. Influence of the overall capillary temperature on BSA-Ni^{2+} interaction. Similar results were achieved through adjustment of Prince temperature setting. The blue and green colors represent the results on Agilent and Prince instruments, respectively. Separation condition, rinsing protocol and extra flushing procedure are as mentioned in Figure 26.

As shown in Figure 29, this influence (23°C at Prince instrument) was incessant during further 5 repeated screenings. Therefore, adjustment of the capillary cooling setting can easily optimize the method and hence successful method transfers between different instrument types can be achieved.

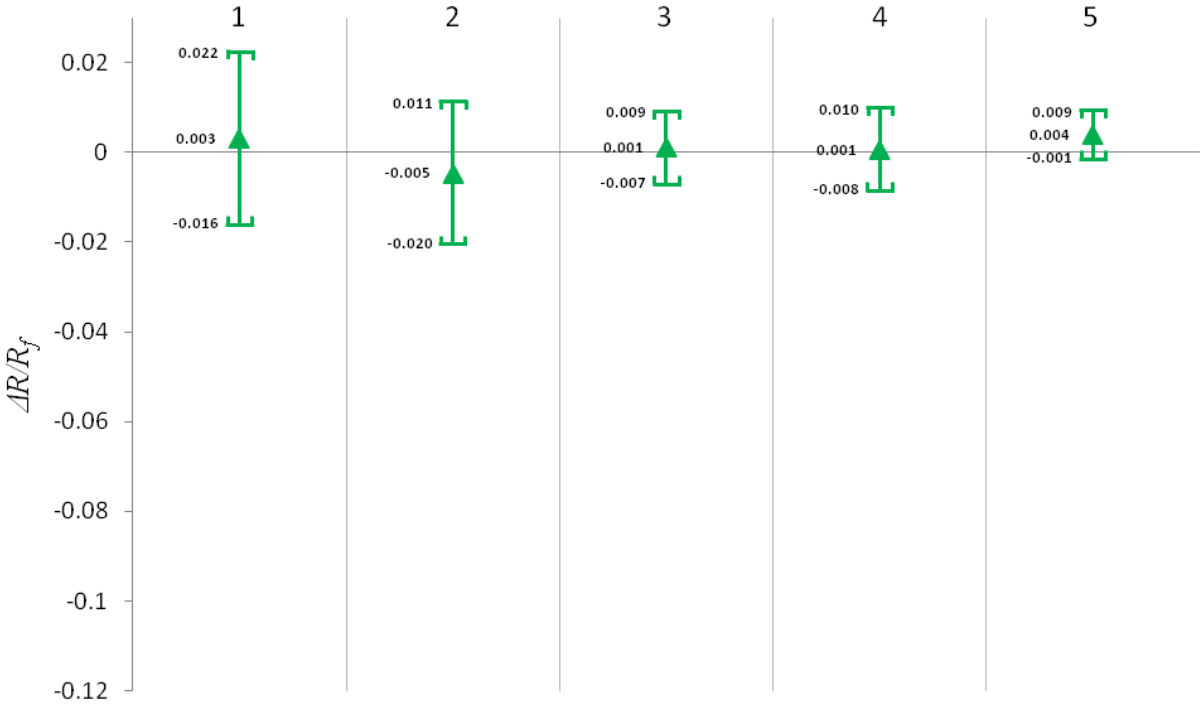

Figure 29. Repeated $\Delta R/R_f$ values and their confidence intervals of BSA with Ni^{2+} on Prince instrument. Separation condition: capillary 50 µm I.D., total length of 62 cm, effective length of 53.5 cm, buffer 20 mmol/L tris (pH 7.4), injection (50 mbar, 18 s), voltage 20 kV, UV 214 nm, capillary cartridge temperature 23°C. Rinsing protocol at 2.5 bar with 0.1 N sodium hydroxide for 3.5 min, water for 3.5 min and tris buffer for 5.5 min. the capillaries were extra flushed after each screening at 2.5 bar with 0.1 N sodium hydroxide for 20 min and water for 10 min.

3.1.3.3 Influence of room temperature

The influence of the changes in room temperature on the interaction results was investigated (Figure 30). The $\Delta R/R_f$ values of OVA-Ni^{2+} pair were slightly increased at low room temperature 15°C (by switching off the room heating system). This is probably due to the effect on the inefficiently cooled parts of the capillary (capillary

inlet and outlet) which could be further cooled by the surrounding air. The influence of the room temperature should be taken into account especially when the interaction rate of a given protein-ligand pair is highly temperature dependent. Alternatively, for fast comparison interaction studies, ACE experiments should be performed with only small temperature changes over time.

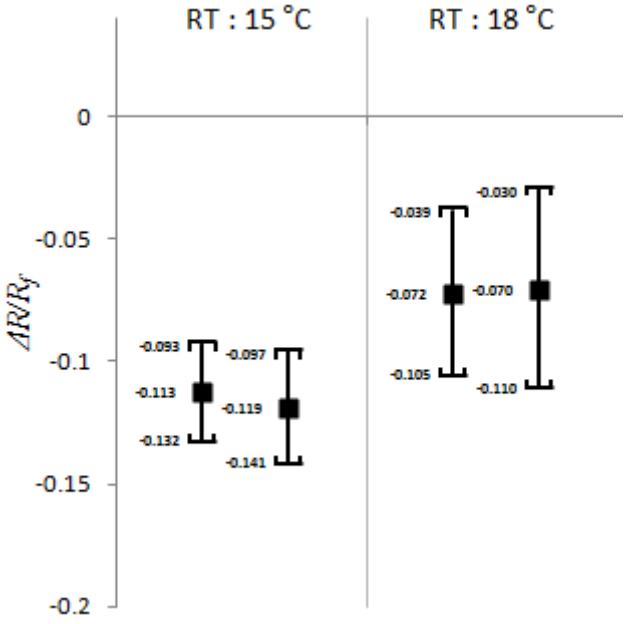

Figure 30. The influence of the room temperature on the measured interaction strength. (RT: Room temperature) Separation condition: capillary 50 µm I.D. with 62 cm total length and 53 cm effective length, buffer 20 mmol/L tris (pH 7.4), injection (50 mbar, 18 s), voltage 20 kV, UV 214 nm, capillary cartridge temperature 23°C. Rinsing protocol at the beginning of each run: 2.5 bar with 0.1 N sodium hydroxide for 3.5 min, water for 3.5 min and tris buffer for 5.5 min. the capillaries were extra flushed after each screening at 2.5 bar with 0.1 N sodium hydroxide for 20 min and water for 10 min.

3.1.3.4 Influence of rinsing solution

The concentration of the sodium hydroxide in the rinsing solutions can influence the interaction results (Figure 31). Two sets of rinsing solutions at 2.5 bar were investigated: (i) 0.1 N sodium hydroxide for 10 min and water for 5 min (procedure 1) and (ii) 1 N sodium hydroxide for 10 min and water 5 min (procedure 2). The obtained $\Delta R/R_f$ values of the OVA-Ni^{2+} pair show significant interaction when applying rinsing procedure 1 while no interaction was observed when applying rinsing procedure 2.

Furthermore, similar results of procedure 1 were observed when not applying extra flushing procedure before running the method (see Figure 31, procedure 3).

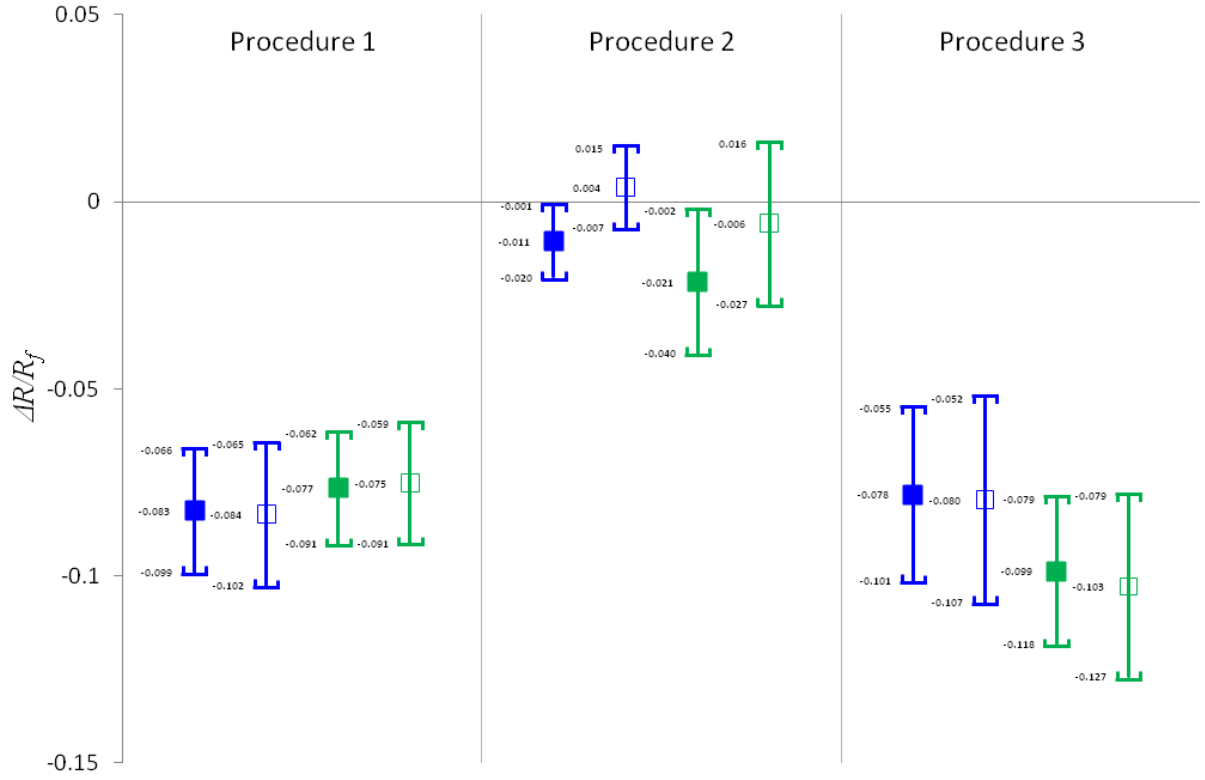

Figure 31. OVA 2nd (■) and 3rd(□) isoforms-Ni^{2+} interactions on Agilent (blue) and Prince (green) CE instruments. Three extra flushing procedures before each screening were examined: Flushing procedure1: 0.1 N sodium hydroxide and water. Flushing procedure 2: 1 N sodium hydroxide and water. Flushing procedure 3: No extra flushing was used before running the method. Separation condition: capillary 50 µm I.D. with total length of 62 cm and effective length of 53 and 53.5 cm on Agilent and Prince CE instruments, respectively, buffer 20 mmol/L tris (pH 7.4), injection (50 mbar, 18 s), voltage 20 kV, UV 214 nm, capillary cartridge temperature 23°C. Rinsing protocol at the beginning of each run: 2.5 bar with 0.1 N sodium hydroxide for 3.5 min, water for 3.5 min and tris buffer for 5.5 min.

The influence of 1 N sodium hydroxide was diminished gradually after 4 repeated runs and capillary equilibrium achieved at the fourth run (Figure 32). Hence, for a successful method transfer, the first 4 runs after conditioning the capillary with 1 N

sodium hydroxide should be excluded from the data, and a high concentration of sodium hydroxide should be avoided in the rinsing protocol prior to each run and between long-term runs for better routine interaction screening.

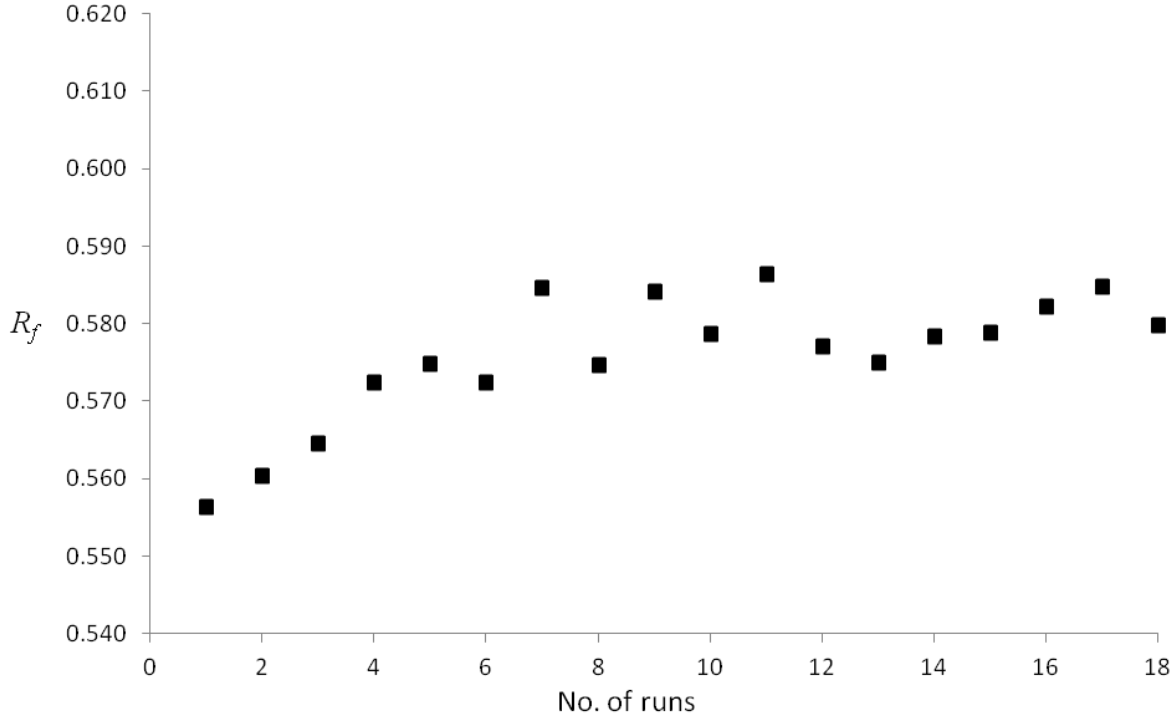

Figure 32. R_f values of of one OVA isoforms after flushing the capillary according to procedure 2 (rinsing at 2.5 bar with1 N sodium hydroxide for 10 min and water 5) using of Prince CE instrument. Separation condition: capillary 50 µm I.D. with 62 cm total length and 53.5 cm effective length, buffer 20 mmol/L tris (pH 7.4), injection (50 mbar, 18 s), voltage 20 kV, UV 214 nm, capillary cartridge temperature 23°C. Rinsing protocol at the beginning of each run: 2.5 bar with 0.1 N sodium hydroxide for 3.5 min, water for 3.5 min and tris buffer for 5.5 min.

3.1.4 Precision

At the beginning of this study, the mobility ratio (R) of proteins such as BSA was used as a parameter to study the precision of the accelerated method. Table 6 was added as one example for calculating the precision of long-term mobility ratio measurements.

Table 6. Mobility ratios of BSA during long-term runs.

	EOF MARKER (t_m in min)	BSA (t_m in min)	R_f
1	1.189	1.770	0.672
2	1.245	1.896	0.657
3	1.227	1.839	0.667
4	1.227	1.865	0.658
5	1.201	1.794	0.669
6	1.189	1.761	0.675
7	1.193	1.756	0.679
8	1.199	1.775	0.675
9	1.209	1.795	0.674
10	1.209	1.817	0.665
11	1.240	1.890	0.656
12	1.259	1.942	0.648
13	1.236	1.869	0.661
14	1.212	1.812	0.669
15	1.210	1.800	0.672
16	1.214	1.818	0.668
17	1.232	1.835	0.671
18	1.243	1.873	0.664
19	1.237	1.849	0.669
20	1.255	1.900	0.661
	Mean ($\bar{x}$)		0.667
	Standard deviation (σ)		0.008
	RSD %		1.173

In addition to the developed rinsing protocol (described in section 3.1.1.2) which gave good precision of RSD% = 1.17%, n = 20, further improvement of the precision has been achieved by employing sample pushing, extra flushing procedures after several subsequent runs, scheduled refreshing inlet and outlet buffer solutions and adding EDTA to the rinsing protocol.

3.1.4.1 Sample pushing

Pushing the sample plug at 50 mbar for 2.5 s, just above the beginning of the capillary inlet dramatically further improved the precision of the mobility ratio measurements, the obtained RSD % was 0.2 % (n = 20) instead of the already well acceptable 1.17 % without sample pushing (Figure 33). Therefore, this step should be implemented after injecting the sample.

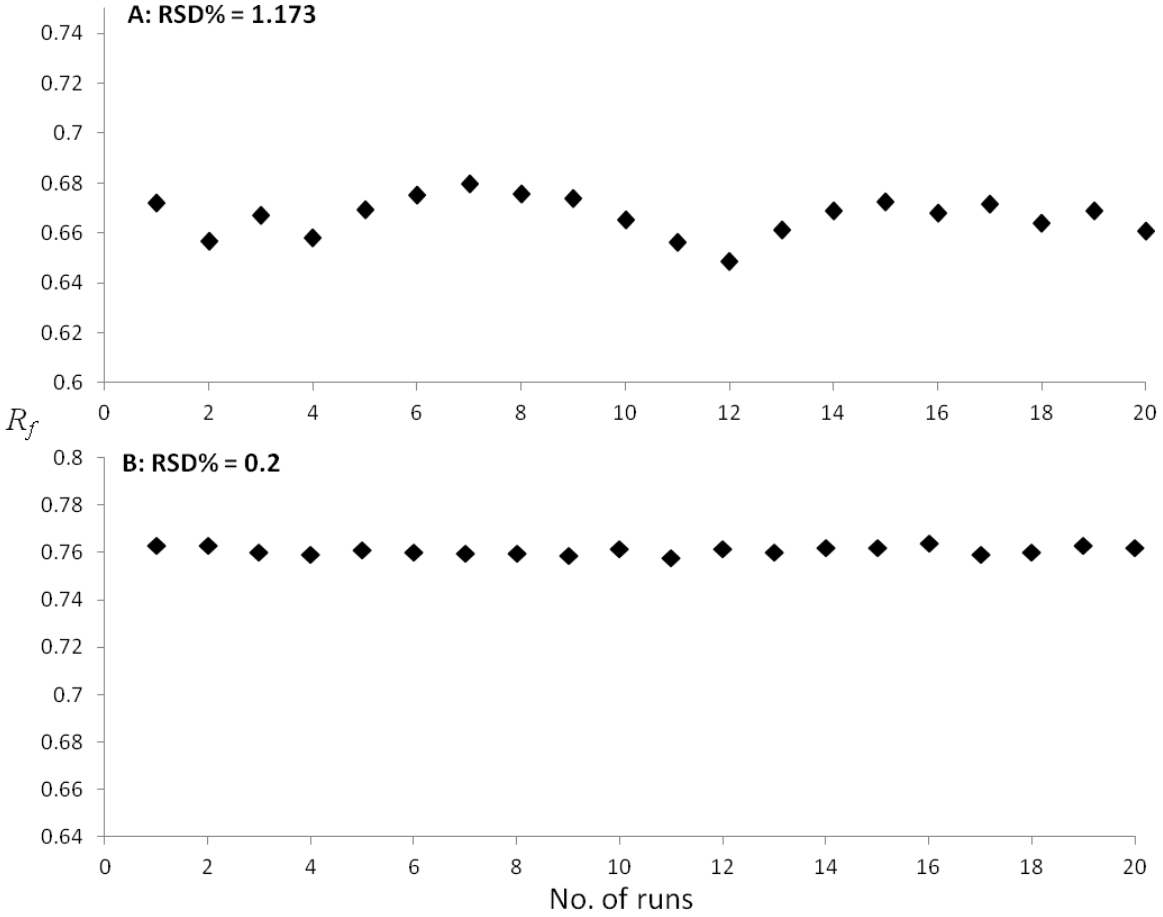

Figure 33. Improving the precision of Long-term R_f values of BSA, A) not employing the sample pushing, B) employing the sample pushing at 50 mbar for 2.5 s. Seperation conditions: capillary with 50 µm I.D., 31 cm total length and 22 cm effective length, tris buffer 20 mmol/L (pH 7.4), injection (50 mbar, 4.5 s), applied voltage 10 kV, UV at 214 nm, capillary cartridge temperature

23°C, rinsing protocol at 2.5 bar with 0.1 N sodium hydroxide for 1 min then water for 1 min after that tris buffer for 1.5 min.

3.1.4.2 Extra flushing and refreshing the buffer

As shown in Figure 34, long series of 112 runs using the optimum rinsing protocol and employing the sample pushing step were performed to evaluate the precision over long-term runs.

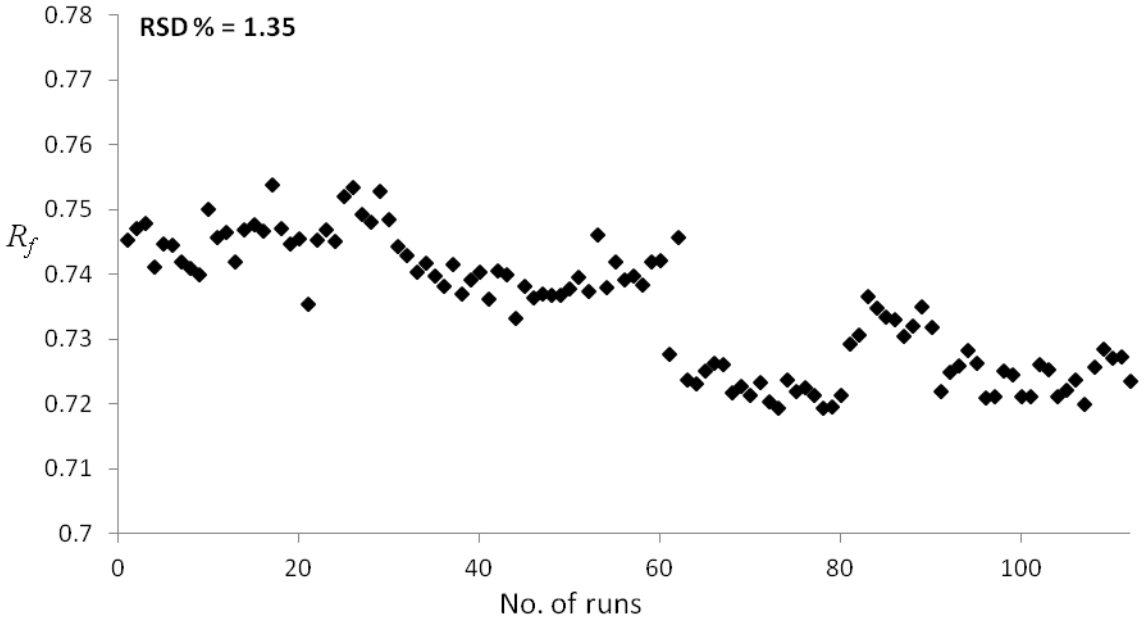

Figure 34. Long-term mobility ratio measurements (112 runs). Separation condition: capillary 50 µm I.D. with 31 cm total length and 22 effective length, buffer 20 mmol/L tris (pH 7.4), sample injection (50 mbar for 4.5 s followed by buffer for 2.5 s), voltage 10 kV, UV 214 nm, capillary cartridge temperature 23°C. Rinsing protocol at 2.5 bar with 0.1 N sodium hydroxide for 1 min, water for 1 min and tris buffer for 1.5 min.

The measured mobility ratios showed RSD % of 1.35% for 112 runs instead of the previously obtained RSD % of 0.2 % for 20 runs; this was probably due to gradual accumulation of the protein on the capillary wall surface over long series of runs. Therefore, an extra flushing step at 2.5 bar with 0.1 N sodium hydroxide for 10 min and water for 5 min was used after each 60 subsequent runs to prevent the gradual accumulation of trace amounts of protein. For further improvement of the long series precision, refreshment of inlet and outlet buffer solutions have been considered. As

can be seen in Figure 35, using the same inlet and outlet vials for more than 30 subsequent runs leads to a continual increase in the mobility ratios probably due to the influence of ions depletion over runs. Please note, that this increase only becomes clearly visible through the choice of using the expanded scale in Figure 35. The continual increase in mobility ratios is damped by refreshing the buffer solution of inlet and outlet vials after each 30 subsequent runs.

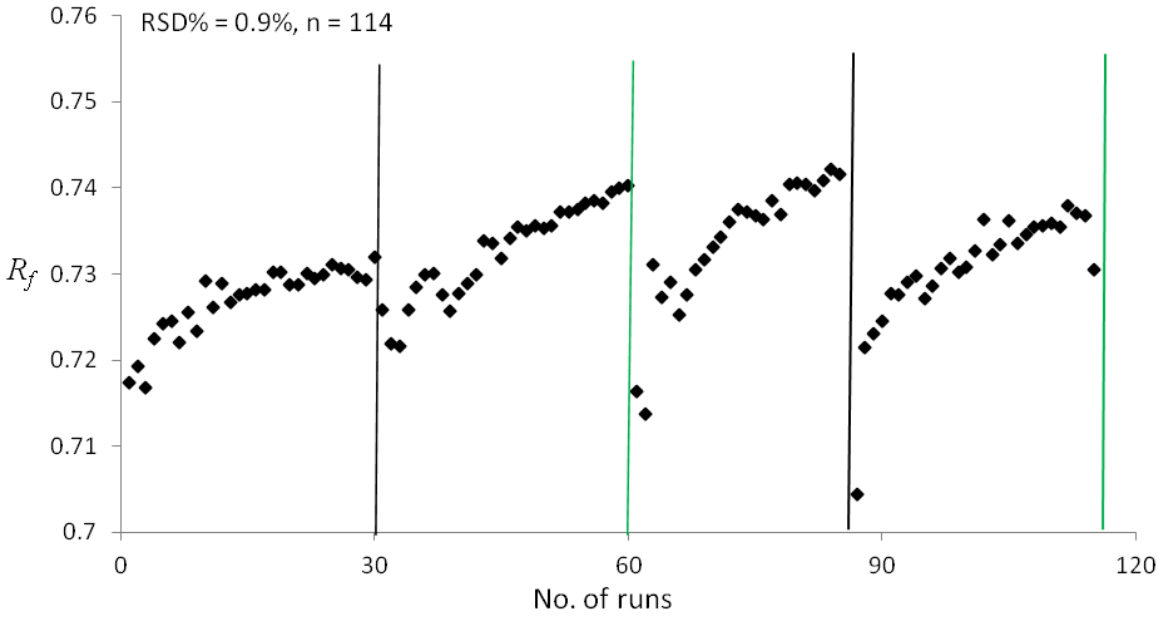

Figure 35. Preventing the continual increase in mobility ratios (R_f) by refreshing the inlet vial solution. The buffer solutions of inlet and outlet vials were refreshed every ≈ 30 runs. Separation condition: capillary 50 µm I.D. with 31 cm total length and 22 effective length, buffer 20 mmol/L tris (pH 7.4), sample injection (50 mbar for 4.5 s followed by buffer for 2.5 s), voltage 10 kV, UV 214 nm, capillary cartridge temperature 23°C. Rinsing protocol at 2.5 bar with 0.1 N sodium hydroxide for 1 min, water for 1 min and tris buffer for 1.5 min. Extra flushing every ≈ 60 runs under 2.5 bar with 0.1 N sodium hydroxide for 10 min and water for 5 min (green line). Please note that the y-axis was expanded to exhibit the change in the mobility ratio over runs.

As shown in Figure 36, excellent precision result (RSD% = 0.86%) for long-term mobility ratio measurements of 251 runs was obtained by considering the sample pushing, extra flushing protocol and refreshing the inlet and outlet vials.

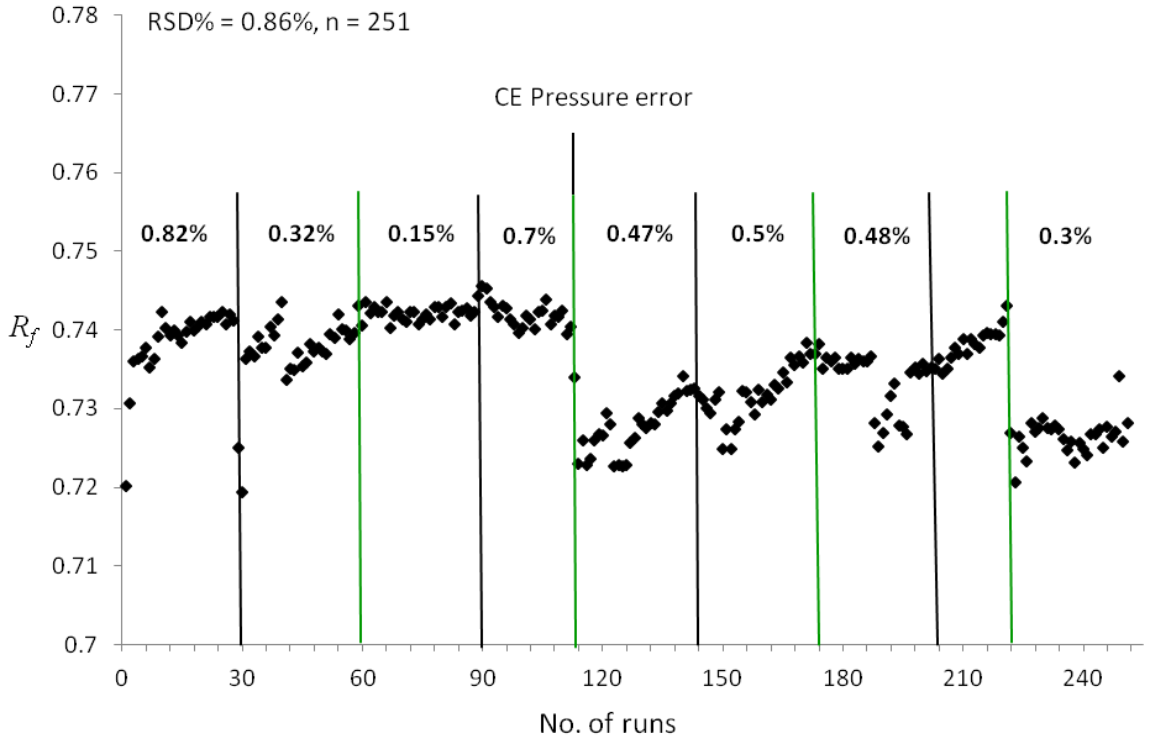

Figure 36. Long-term mobility ratio measurements (251 runs) using the optimum rinsing protocol (at 2.5 bar with 0.1 N sodium hydroxide for 1 min, water for 1 min and tris buffer for 1.5 min) and employing sample pushing (at 50 mbar for 4.5 s followed by buffer for 2.5 s), extra flushing protocol after each 60 subsequence runs (at 2.5 bar with 0.1 N sodium hydroxide for 10 min and water for 5 min, see green line) and refreshing the inlet and outlet buffer vials after each 30 subsequence runs. Please note that the y-axis was expanded to exhibit the change in the mobility ratio over runs.

The pressure system of the CE instrument should be carefully considered. The stability of pressure system of the CE instrument is very important for the reproducibility of the results. A small leakage in the pressure system tubes could not be detected usually by the CE instrument software since the fluctuation could prevent the CE to give a message error when the pressure starts to drop. Figure 37 is a good example for this problem. The pressure leakage was started at the beginning of the series. The measured mobility ratios were fluctuated with poor precision (RSD % = 3.5 for the first 30 subsequence runs). The pressure leakage decreases the volume of the injected rinsing solutions. This will lead to increase in the amount of the

adsorbed proteins and change in the EOF over runs. Surprisingly, in the beginning the CE instrument did not show any message error regarding a pressure leakage since the leakage insignificant. Only after the pressure leakage was became strong, a pressure error message was shown, and then the CE instrument has been stopped automatically. Hence, the pressure system and its tubes should be continuously inspected even if there is no a message error for a pressure value.

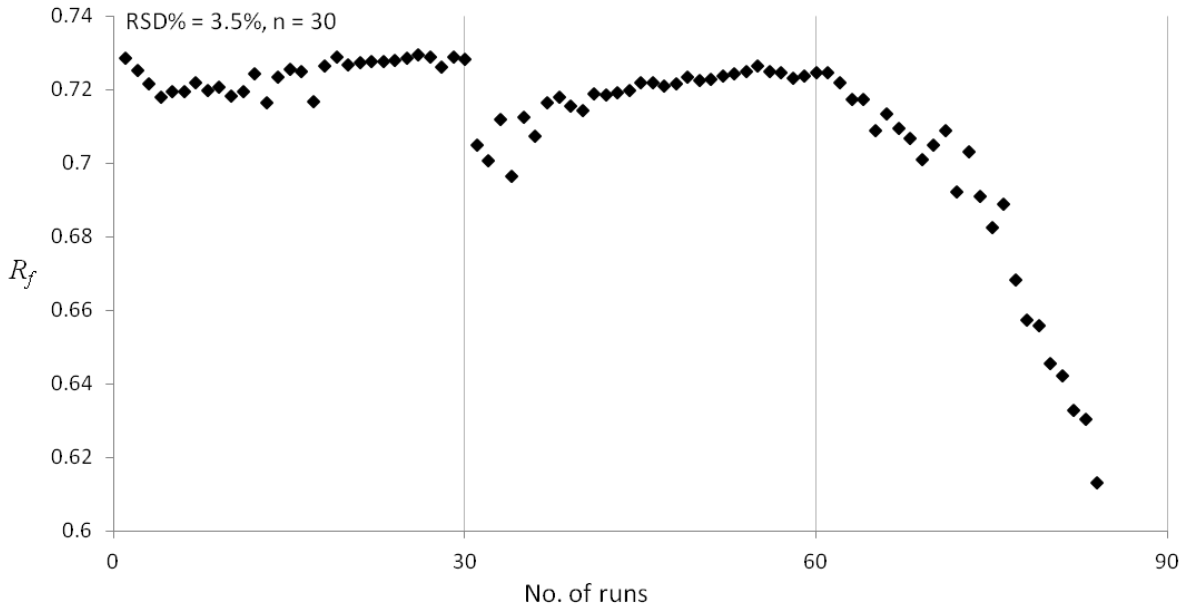

Figure 37. The effect of unstable pressure (air leakage from tube system) on reproducibility of mobility ratios

3.1.4.3 Using EDTA

The confidence intervals of the $\Delta R/R_f$ values for some of the different models of protein-metal ion pair are wide (see Figure 25). Furthermore, the influence of Cu^{2+} on the EOF is highly pronounced which leads to wider confidence intervals of the $\Delta R/R_f$ values over different tested metal ions [73, 74]. Moreover, the influence of Ni^{2+} (250 µmol/L) on the EOF was investigated depending on R_i of OVA isoforms. As shown in Figure 38A, the R_i decreased dramatically after each run using the initial rinsing protocol without EDTA over 13 runs. This could due to two anticipated reasons, the suppression of the EOF over each run due to metal ion capillary wall adsorption [111], and possibly to the binding of proteins to the adsorbed metal ions.

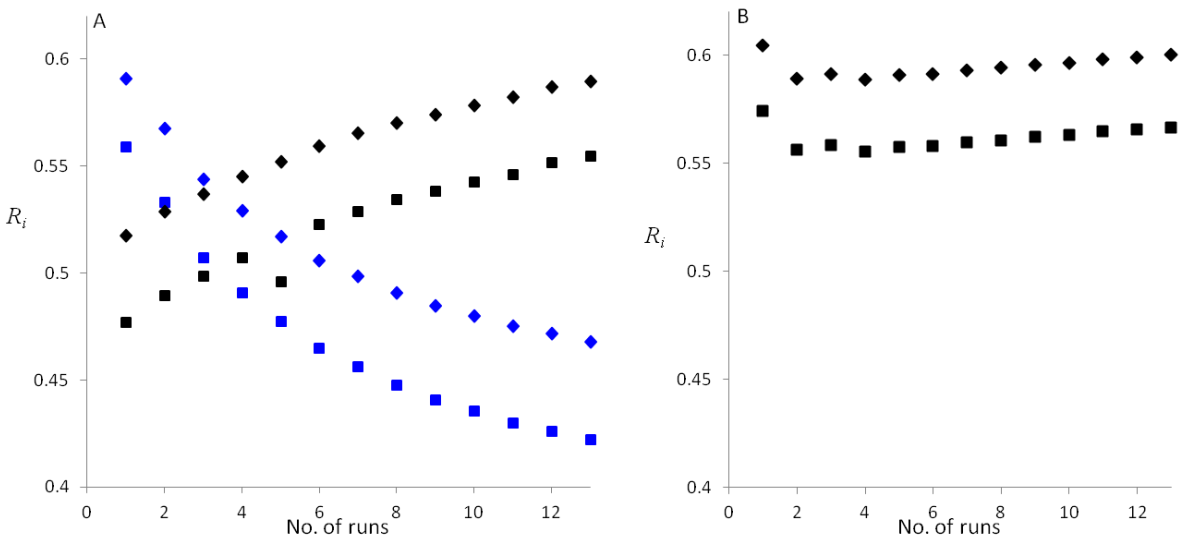

Figure 38. A: R_i values of long series runs of acetanilide and OVA isoforms using a buffer solution containing Ni^{2+} (250 µmol/L) as well as the rinsing protocol without EDTA (blue), and regeneration of the capillary wall after adding 0.1 M EDTA within the rinsing protocol (black). B: Stabilization of R_i values over 13 runs using 0.1 M EDTA within the rinsing protocol.

It is well known that EDTA strongly binds to most of the metal ions [45]. Therefore, an appropriate amount of EDTA has been added to the 0.1 N sodium hydroxide step of the developed rinsing protocol (at 2.5 bar for 1 min) to obtain a solution consisting of 0.1 M EDTA and 0.1 N sodium hydroxide (see the experimental part). As shown in Figure 38B, the capillary wall was successfully regenerated, and the obtained R_i values after long series are similar to that at the starting levels when using the EDTA in the rinsing protocol.

Figure 39 illustrates the role of EDTA in improving the precision of ACE result for an interested protein-metal ion interaction. The metal ions might first adsorb on the capillary wall forming a positively charged wall, the anions of the background buffer solution can then form a rigid and/or diffuse (mobile) layers which finally reverse the EOF direction. The rate of the capillary wall modification is anticipated to be influenced by the type of the metal ion.

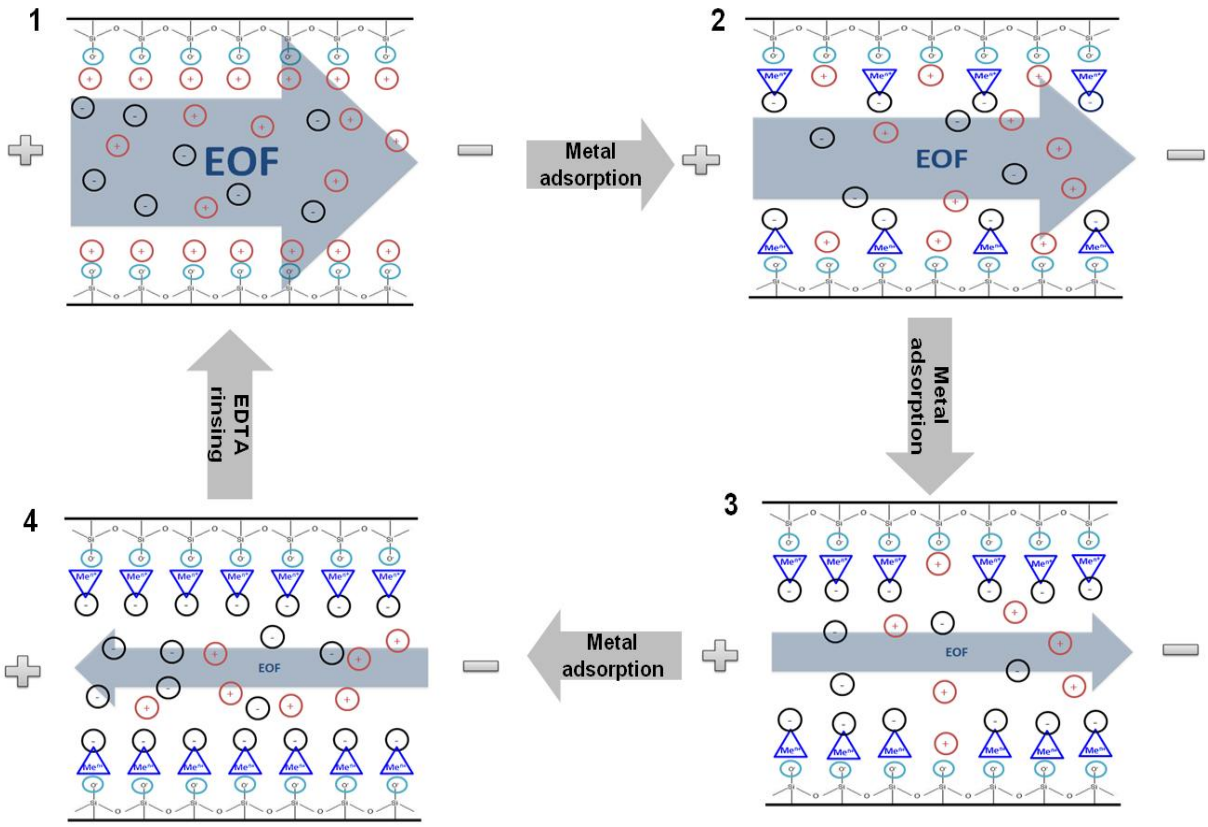

Figure 39. Inversion of the EOF by the metal ions: 1) Starting buffer cations form rigid and diffuse layers, 2) initiation of metal ion adsorption and formation of anions rigid and diffuse layers lead to decrease in the EOF, 3) a continual increase in the metal ion adsorption which further decrease the EOF, 4) equilibrium state of a capillary wall that is completely coated causing inversion of EOF to anode. Step 4 to 1 shows the possibility to regenerate the capillary wall by a strong chelating agent such as EDTA.

Increasing the rinsing time of the EDTA-sodium hydroxide rinsing step to 2.5 min further improved the precision so that stable long-term mobility ratios of OVA- Ni^{+2} model (R_i , n=30: 0,57% for OVA^{2nd}. 0,69% for OVA^{3rd}) were achieved (Table 7, protocol 1). Hence, different sets of rinsing protocols were studied depending on stabilizing the EOF (Table 7). The advantage of protocol 1 are that both solutions of 0.1 M EDTA and 0.1 N sodium hydroxide are combined which lead to saving at least 1 min of a total rinsing time and offers reproducible EOF. As shown in Table 7, there were no benefits from dividing the combined solution of protocol 1 as for protocol 3 and 4 since higher RSD % values were obtained.

Table 7: Tested rinsing protocols for OVA- Ni^{2+} interaction.

Protocol	Rinsing solutions and time	RSD % of R_i
1	2.5 min 0.1 M EDTA in 0.1 N NaOH, 1 min water and 1.5 min buffer	n=30: OVA^{2nd}: 0,57% OVA^{3rd}: 0,69%
2	3.5 min 0.1 M EDTA in 0.1 N NaOH, 1 min water and 1.5 min buffer	n=30: OVA^{2nd}: 2.18% OVA^{3rd}: 2.39%
3	1,5 min 0.1 M EDTA in 0.1 N NaOH, 1 min 0.1 N NaOH, 1 min water and 1 min buffer	n=30: OVA^{2nd}: 0.78% OVA^{3rd}: 1%
4	2,5 min 0.1 M EDTA in 0.1 N NaOH, 1 min 0.1 N NaOH, 1 min water, 1 min buffer	n=30: OVA^{2nd} (0.94%), OVA^{3rd} (1%)

Therefore, the rinsing protocol (protocol 1) at 2.5 bar with a solution consisting of 0.1 N sodium hydroxide and 0.1 M EDTA for 2.5 min, water for 1 min and running buffer for 1.5 min was evaluated, and applied to investigate the influence of Ba^{+2}, Ni^{+2} and Cu^{+2} on different globular proteins. As shown in Figure 40, narrower confidence intervals of the $\Delta R/R_f$ values were successfully achieved. Therefore, this rinsing protocol has been used to investigate behaviours of the various interesting metal ions on the selected proteins (see section 3.2).

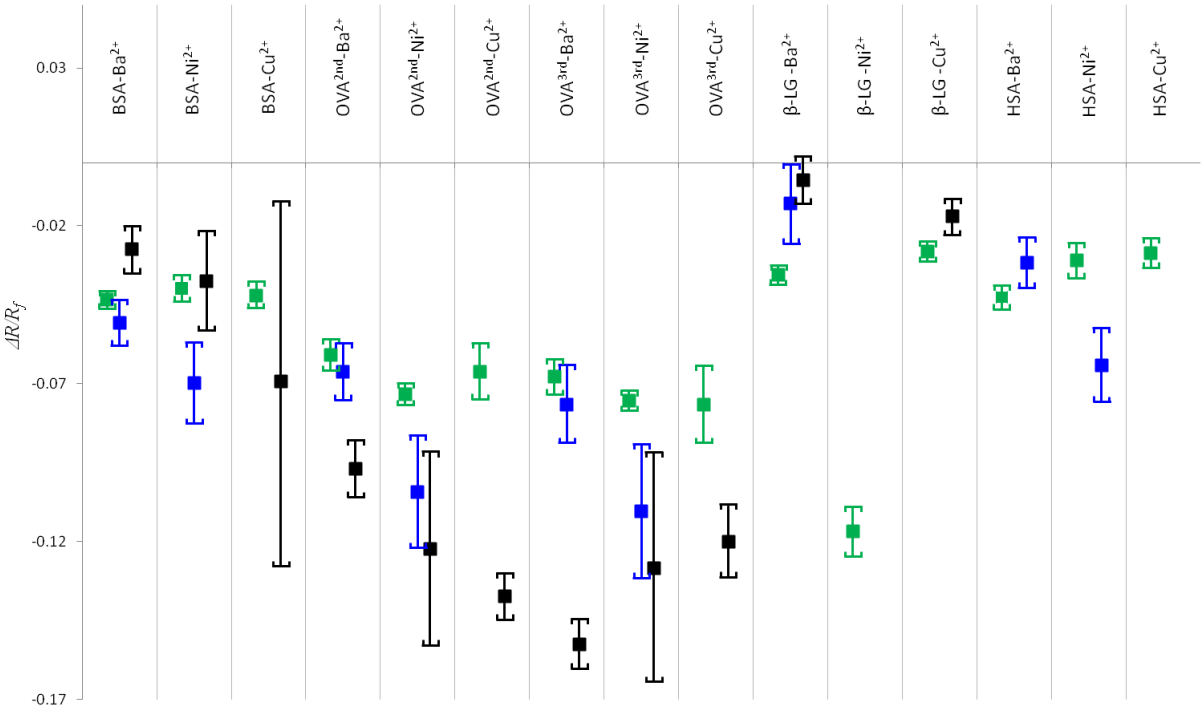

Figure 40. Using of EDTA to improve the $\Delta R/R_f$ measurements for different protein-metal ion interactions. Green: The accelerated method using 0.1 M EDTA within the developed rinsing protocol. Blue: The accelerated method using the developed rinsing protocol without 0.1 M EDTA. Black: the long method using its long rinsing protocol without 0.1 M EDTA (reprinted with permission from reference No. 73).

3.2 Applications

3.2.1 Influence of different metal ions on proteins

The interaction behavior of each metal group (Table 8) on the selected proteins, BSA, β-LG, HSA, MB and OVA was investigated under physiological pH 7.4. Five metal ions of the group A with different valences, all noble metal ions, other important heavy metals and two anion complexes containing metal and semimetal ions were examined (total 28 metal and semimetal ions. Figure 41 A shows that there is no enough separation between acetanilide (EOF marker) and MB since their peaks are overlapped. Therefore, the electrophoretic separation between acetanilide and MB was further improved by reducing the injection time to 1.5 s instead of 4.5 s (Figure 41 B).

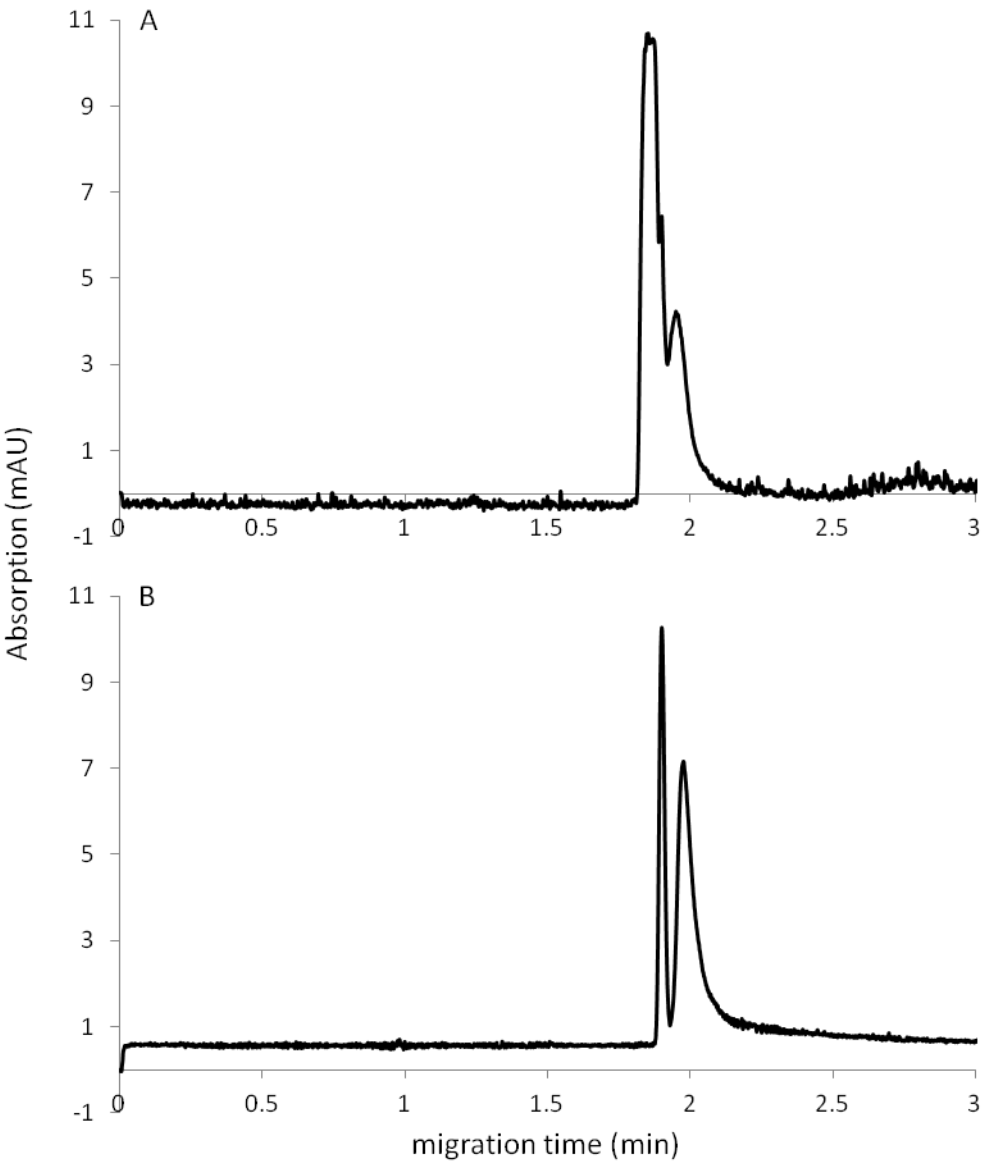

Figure 41. Two electropherograms each showing peaks for acetanilide (first) and myoglobin (second), respectively. A: sample injection at 50 mbar for 4.5 s followed by buffer for 2.5s. B: sample injection at 50 mbar for 1.5 s followed by buffer for 2.5s. Separation condition of both electropherograms: capillary 50 µm I.D. with 31 cm total length and 22 effective length, buffer 20 mmol/L tris (pH 7.4), voltage 10 kV, UV 214 nm, capillary cartridge temperature 23°C. Rinsing protocol at 2.5 bar with a solution consisting of 0.1 N sodium hydroxide and 0.1 M EDTA for 2.5 min, water for 1 min, and running buffer for 1.5 min.

As mentioned in the introduction (section 1.5.3.2.1.4), most of proteins exhibit multiple sites for various metal ions [16, 20]. Therefore, a high concentration of each

metal ion was used for fast interaction screening with a protein to achieve the saturation [73-75]. The metal ion concentration of up to 250 µmol/L was found to be suitable for the tested proteins except for β-LG and MB, because their peak shapes were intensively changed and could not be integrated when using metal ion concentrations above 100 µmol/L for β-LG [73-75] and above 25µmol/L for MB (Figure 42).

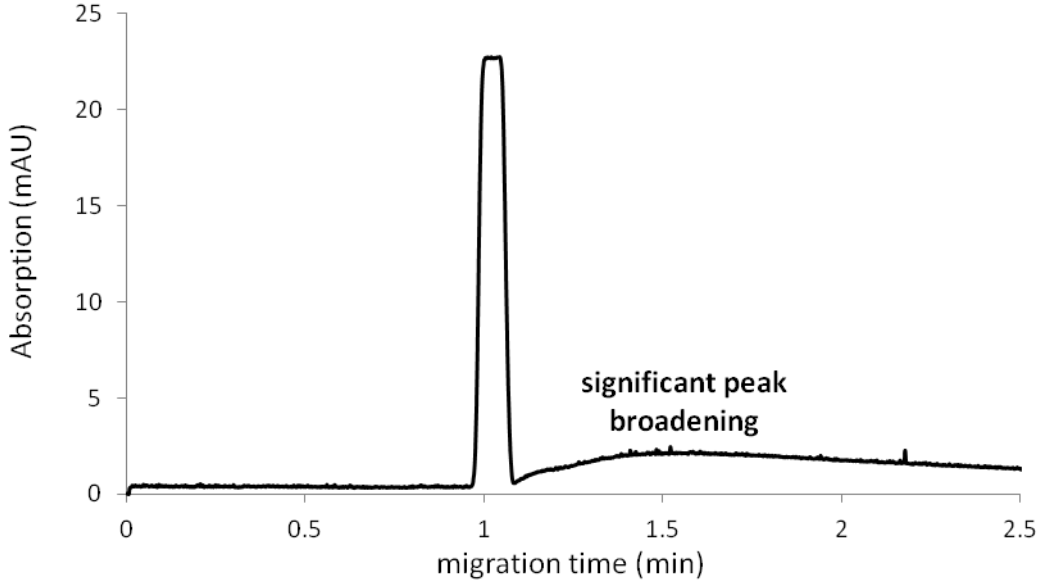

Figure 42. Electropherogram shows two peaks, acetanilide (first) and myoglobin (second), respectively, under the influence of Ni^{2+} (100 µmol/L Nickel chloride in the running buffer). The peak of MB is extremely broad and cannot be integrated.

Please note that for each interaction screening, two running solutions were prepared; without and with metal ion. Six repeated runs under each solution were performed and their data (see Figure 43 as example) were used for calculating the $\Delta R/R_f$ values and their confidence intervals to detect the strength of interaction using equations 15, 16 and 17 (see section 1.5.3.2.1). All obtained $\Delta R/R_f$ values and their cnfs are summarized in Table 8. Indeed, it is difficult to compare between metal ions by using this Table. Hence, $\Delta R/R_f$ chart (Figure 44) was successfully created to make comparisons easier. Furthermore, this chart is considered as comprehensive platform for investigating different protein-metal ion interactions.

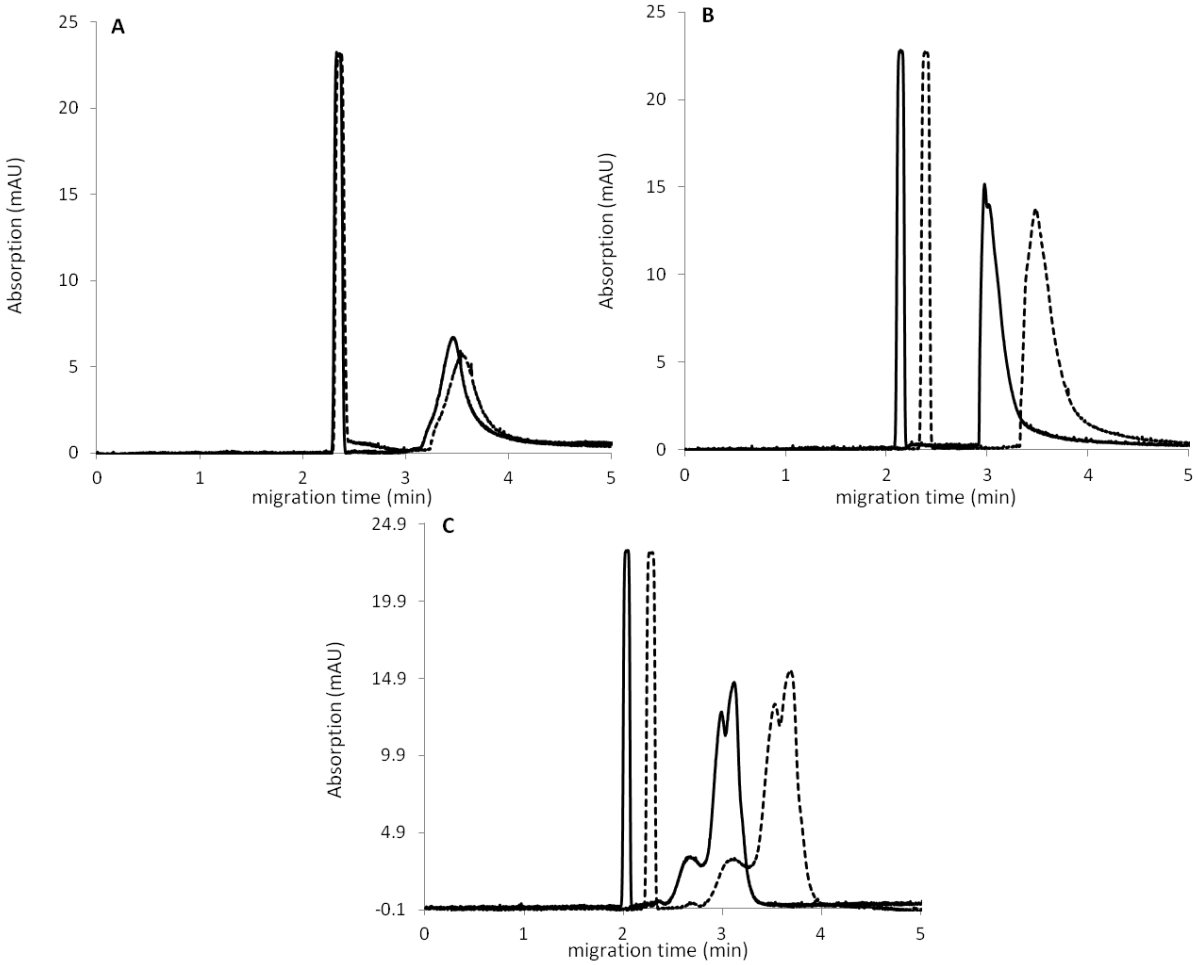

Figure 43. Three examples of typical electropherograms for calculating $\Delta R/R_f$ values and their confidence intervals of Ba^{2+} interaction with β-LG (A), BSA (B) and OVA (C). The dotted line and the solid line show migration times of EOF marker (acetanilide) and a protein with and without adding of 250 µmol/L $BaCl_2$ in the running buffer, respectively. Separation condition: capillary 50 µm I.D. with 31 cm total length and 22 effective length, buffer 20 mmol/L tris (pH 7.4), sample injection (50 mbar for 4.5 s followed by buffer for 2.5 s), voltage 10 kV, UV 214 nm, capillary cartridge temperature 23 °C. Rinsing protocol at 2.5 bar with a solution consisting of 0.1 N sodium hydroxide and 0.1 M EDTA for 2.5 min, water for 1 min, and running buffer for 1.5 min.

Table 8. $\Delta R/R_f$ values and their cnfs of all investigated protein-metal ion interactions.

Metal ion \ Protein		BSA	β-LG	HSA	MB	OVA[1st*]	OVA[2nd**]
Group Ia	Li^+	-0.0145 ± 0.0103	0.0029 ± 0.0088	-0.0061 ± 0.0086	0.0024 ± 0.0026	-0.0058 ± 0.0108	-0.0070 ± 0.0146
	Na^+	-0.0065 ± 0.0102	0.0029 ± 0.0078	-0.0021 ± 0.0065	0.0032 ± 0.0010	0.0040 ± 0.0114	0.0012 ± 0.0130
Group IIa	Mg^{2+}	-0.0036 ± 0.0092	-0.0006 ± 0.0049	-0.0076 ± 0.0054	-0.0044 ± 0.0013	0.0008 ± 0.0095	0.0023 ± 0.0102
	Ca^{2+}	-0.0402 ± 0.0115	-0.0209 ± 0.0153	-0.0244 ± 0.0132	-0.0053 ± 0.0024	-0.0199 ± 0.0206	-0.0324 ± 0.0219
	Ba^{2+}	-0.0434 ± 0.0025	-0.0355 ± 0.0027	-0.0426 ± 0.0034	-0.0015 ± 0.0013	-0.0608 ± 0.0046	-0.0678 ± 0.0052
Group IIIa	Al^{3+}	0.0484 ± 0.0087	0.0371 ± 0.0152	0.0584 ± 0.0110	0.0072 ± 0.0011	0.0293 ± 0.0053	0.0367 ± 0.0072
	Ga^{3+}	0.0670 ± 0.0064	0.0284 ± 0.0167	0.0511 ± 0.0194	0.0070 ± 0.0066	0.1320 ± 0.0099	0.1607 ± 0.0162
Group b (heavy metals)	noble	Ag^+	0.0053 ± 0.0056	-0.0017 ± 0.0093	0.0317 ± 0.0090	-0.2816 ± 0.0131	0.0770 ± 0.0071	0.0728 ± 0.0144
		Au^+	0.0005 ± 0.0088	0.0006 ± 0.0114	0.0088 ± 0.0046	0.0057 ± 0.0038	0.0079 ± 0.0170	0.0079 ± 0.0244
		Au^{3+}	0.0155 ± 0.0086	-0.0030 ± 0.0019	0.0064 ± 0.0064	-0.0004 ± 0.0009	0.0218 ± 0.0110	0.0228 ± 0.0131
		Os^{3+}	-0.0402 ± 0.0123	-0.0068 ± 0.0057	-0.0435 ± 0.0164	0.0011 ± 0.0008	0.0087 ± 0.0093	0.0053 ± 0.0109
		Pd^{2+}	0.0129 ± 0.0117	0.0050 ± 0.0052	-0.0147 ± 0.0103	-0.0154 ± 0.0047	-0.0427 ± 0.0119	-0.0458 ± 0.0154
		Pt^{4+}	-0.0335 ± 0.0105	-0.0117 ± 0.0100	-0.0519 ± 0.0073	0.0044 ± 0.0031	0.0018 ± 0.0086	0.0009 ± 0.0113
		Rh^{3+}	-0.0237 ± 0.0048	-0.0159 ± 0.0051	-0.0200 ± 0.0037	-0.0573 ± 0.0101	-0.0257 ± 0.0138	-0.0311 ± 0.0157
		Ru^{3+}	-0.0142 ± 0.0053	-0.0064 ± 0.0091	-0.0050 ± 0.0096	0.0024 ± 0.0005	-0.0138 ± 0.0113	-0.0194 ± 0.0101
		Ir^{3+}	-0.2511 ± 0.0132	-0.0110 ± 0.0094	-0.2837 ± 0.0071	-0.0001 ± 0.0017	-0.0018 ± 0.0102	-0.0001± 0.0131
	other	Co^{2+}	-0.0482 ± 0.0089	-0.0250 ± 0.0083	-0.0211 ± 0.0095	-0.0011 ± 0.00195	-0.0859 ± 0.0098	-0.0926 ± 0.0112
		Cu^{1+}	-0.0754 ± 0.0088	-0.0460 ± 0.0111	-0.0529 ± 0.0057	0.0068 ± 0.0016	-0.0291 ± 0.0090	-0.0482 ± 0.0110
		Cu^{2+}	-0.0420 ± 0.0038	-0.0281 ± 0.0028	-0.0286 ± 0.0043	0.0034 ± 0.0033	-0.0661 ± 0.0085	-0.0765 ± 0.0118
		Ni^{2+}	-0.0397 ± 0.0037	-0.1168 ± 0.0075	-0.0309 ± 0.0053	-0.0027 ± 0.0023	-0.0732 ± 0.0032	-0.0754 ± 0.0028
		Cr^{3+}	-0.1447 ± 0.0247	-0.1185 ± 0.0262	-0.1241 ± 0.0065	0.0236 ± 0.0091	-0.1372 ± 0.0226	-0.1641 ± 0.0263
		Fe^{3+}	-0.1384 ± 0.0136	No peak	-0.0308 ± 0.0068	0.0025 ± 0.0011	-0.1580 ± 0.0157	-0.1221 ± 0.0173
		Fe^{2+}	-0.1290 ± 0.0100	-0.1173 ± 0.0140	-0.1415 ± 0.0134	0.0027 ± 0.0011	-0.3102 ± 0.0245	-0.2881 ± 0.0263
		La^{3+}	-0.0079 ± 0.0148	0.0035 ± 0.0067	0.0050 ± 0.0027	-0.0038 ± 0.0070	0.0180 ± 0.0098	0.0218 ± 0.0107
		V^{3+}	0.0250 ± 0.0050	-0.0040 ± 0.0089	0.0309 ± 0.0035	-0.0008 ± 0.0016	0.0458 ± 0.0069	0.0525 ± 0.0099
Complex of metal ions		MoO_4^{2-}	-0.0263 ± 0.0064	-0.0004 ± 0.0082	-0.0111 ± 0.0082	0.0012 ± 0.0012	0.0040 ± 0.0087	0.0024 ± 0.0087
		SeO_3^{2-}	0.0091 ± 0.0054	0.0110 ± 0.0067	0.0211 ± 0.0066	-0.0026 ± 0.0021	-0.0141 ± 0.0104	-0.0237 ± 0.0116

*** First peak of OVA**
**** Second peak of OVA**

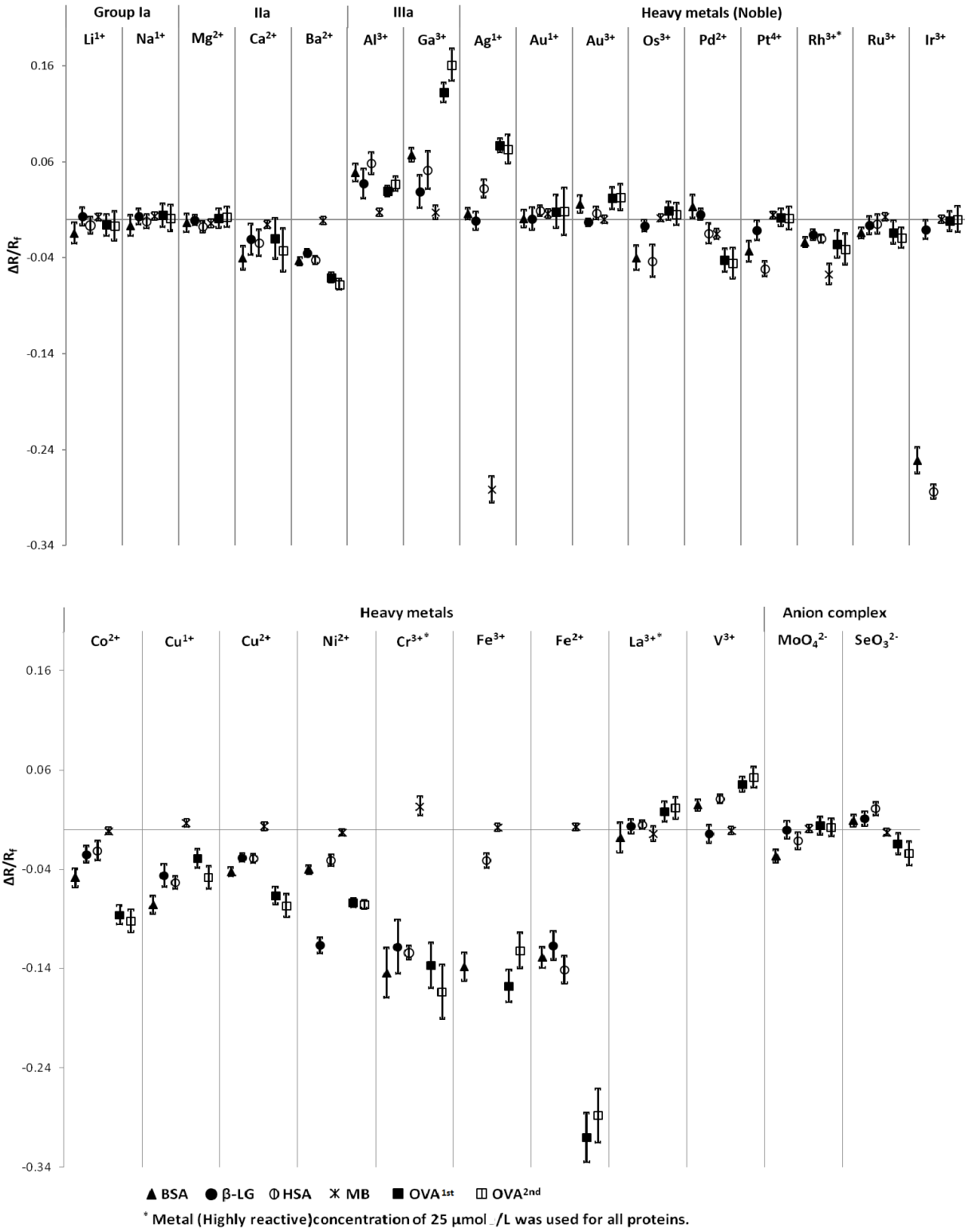

Figure 44. Comprehensive interaction screening platform of all tested metal ions to the given set of proteins. The typically used metal concentrations were 250 µmol/L for BSA, HSA and OVA, 100 µmol/L for β-LG and 25 µmol/L for MB.

However, 25 µmol/L of the highly reactive metal ions Cr^{3+}, Rh^{3+} and La^{3+} was used for all proteins without exception. For each screening result, twelve runs for protein were performed (six without metal ion and six with metal ion). Separation condition: capillary 50 µm I.D. with 31 cm total length and 22 effective length, buffer 20 mmol/L tris (pH 7.4), sample injection at 50 mbar for 4.5 s (1.5 s for MB) followed by buffer for 2.5s, voltage 10 kV, UV 214 nm, capillary cartridge temperature 23°C. Rinsing protocol at 2.5 bar with a solution consisting of 0.1 N sodium hydroxide and 0.1 M EDTA for 2.5 min, water for 1 min, and running buffer for 1.5 min. Extra flushing after each screening at 2.5 bar with 0.1 N sodium hydroxide for 20 min and water for 10 min.

The sign (negative or positive) of $\Delta R/R_f$ is highly important for the preliminary characterization of protein-metal ion interactions. It could give insight into the coordination of bound metal ion with the protein residues. For example, the estimated initial charge at pH 7.4 of BSA is -18 (http://www.scripps.edu/~cdputnam/protcalc.html) without adding metal ion ligand in the running buffer. While, when adding a metal ion ligand in the running buffer, the charge of BSA would normally decrease ≤ -18 (less negative) leading to increase in electrophoretic mobility and hence positive $\Delta R/R_f$ value will be obtained (as in case of BSA- Al^{3+}, see Figure 44). On the other hand, the bound metal ion on BSA could undergo further coordination with the surrounding anions causing increase in charge of BSA ≥ -18 (more negative), in this case a decrease in electrophoretic mobility can be observed and a negative $\Delta R/R_f$ value will be obtained (as in case of BSA- Ba^{2+}, see Figure 44).

Since the metal ions are interesting for different research fields, the results were discussed in view of metal and semimetal group's behaviour in details.

3.2.1.1 Group A metal ion

At the beginning of the screenings, different metal ions such as alkali metals (Li^+, Na^+), alkaline earth metal (Ba^{2+}), group IIIa (Al^{3+}, Ga^{3+}) were selected for comprehensive interaction investigations including the influence of valency (mono, bi, and tri), the ionic radii and coordination geometry. Figure 44 shows that the interactions of Li^+ and Na^+ with all investigated proteins were not significant since their *cnf* ($\Delta R/R_f$) values intersect the zero line, except that for Li^+ with BSA which might

indicate a weak interaction ($\Delta R/R_f$ = - 0.0145 ± 0.0103). The $\Delta R/R_f$ values and their confidence intervals of the di-valent metal ions Ca^{2+} and Ba^{2+} show significant interactions comparing to Mg^{2+} and the mono-valent metal ions. Mg^{2+} has a smaller ionic radius (more hardness) than Ca^{2+} and Ba^{2+}, and this property makes Mg^{2+} behave similar to Li^{+} and Na^{+}. The metal ion Ca^{2+} behaves in level between Mg^{2+} (harder) and Ba^{2+} (softer), and these results confirm the influence of the ionic radii and generally the HSAB concept. Additionally, Ba^{2+} not only binds to hard bases, but also has the ability to bind coordinately to borderline bases such as imidazole (His), amide (Asn and Gln) and chloride [51, 126]. Ba^{2+} has coordination numbers (CNs) in the range from six to nine [51]. Therefore, it could provide higher CNs than the possible numbers of ligands at the binding site, allowing for further coordination to anions such as chloride. Hence, the overall charge balance after protein interactions to Ba^{2+} ions is often more negative, and the $\Delta R/R_f$ values and their confidence intervals can mostly be observed in the negative range.

The metal ions Al^{3+} and Ga^{3+} have similar properties regarding their valency. Their valency (tri) makes them hard with CNs of 4 to 6. Ga^{3+} has a larger ionic radius than Al^{3+}, and is relatively softer [51, 62]. The positive $\Delta R/R_f$ values of the interactions between these metals and proteins might be explained by two cases: (1) a complete coordination of the metal ions (Al^{3+} and Ga^{3+}) with the functional groups of the binding site, in this case no spare coordination sites are available to bind anions, (2) spare coordination sites after binding with the functional groups of a binding site are available but bind preferably to water rather than to anions [51]. The strength of the interactions of Al^{3+} and Ga^{3+} are similar, except for the interactions with OVA. In this case, Ga^{3+} shows a stronger binding behavior. This is possibly due to the different coordination geometry of both metals; Al^{3+} complexes are typically octahedral and Ga^{3+} are tetrahedral, or probably that Ga^{3+} (less hard) has a tendency to bind further with other functional groups containing nitrogen such as imidazole of histidine.

3.2.1.2 Group B metal ion

3.2.1.2.1 Noble metal ions

Most of the metallodrugs are based on noble metal ions which make them very interesting to study as well. Noble metal ions from the platinum group (Os^{3+}, Pd^{2+}, Pt^{4+}, Rh^{3+}, $Ru^{3+}$and Ir^{3+}) as well as Ag^{+}, Au^{+} and Au^{3+} were selected for this study. As known these nobel metal ions are a subgroup of the transition metals which are all

rather soft acids. Their softness is relatively more or less depending on the oxidation state and ionic radius (see Table 1). Figure 44 shows the interaction results of this group. Os^{3+} and Pt^{4+} interact similarly with the given proteins, the interactions with BSA and HSA are significant while they have weak interactions with β-LG. No other significant interactions with the investigated proteins were observed. Different weak interactions of BSA ($\Delta R/R_f$ = + 0.0129) and HSA ($\Delta R/R_f$ = - 0.0147) with Pd^{2+} were obtained; this could refer to different binding sites at both proteins. In case of Rh^{3+}, a ten-fold lower concentration of 25 µmol/L was employed due to the strong decrease of the EOF and significant baseline drifting at 250 µmol/L (Figure 45). Furthermore, no EOF and protein peaks had appeared at this concentration (250 µmol/L).

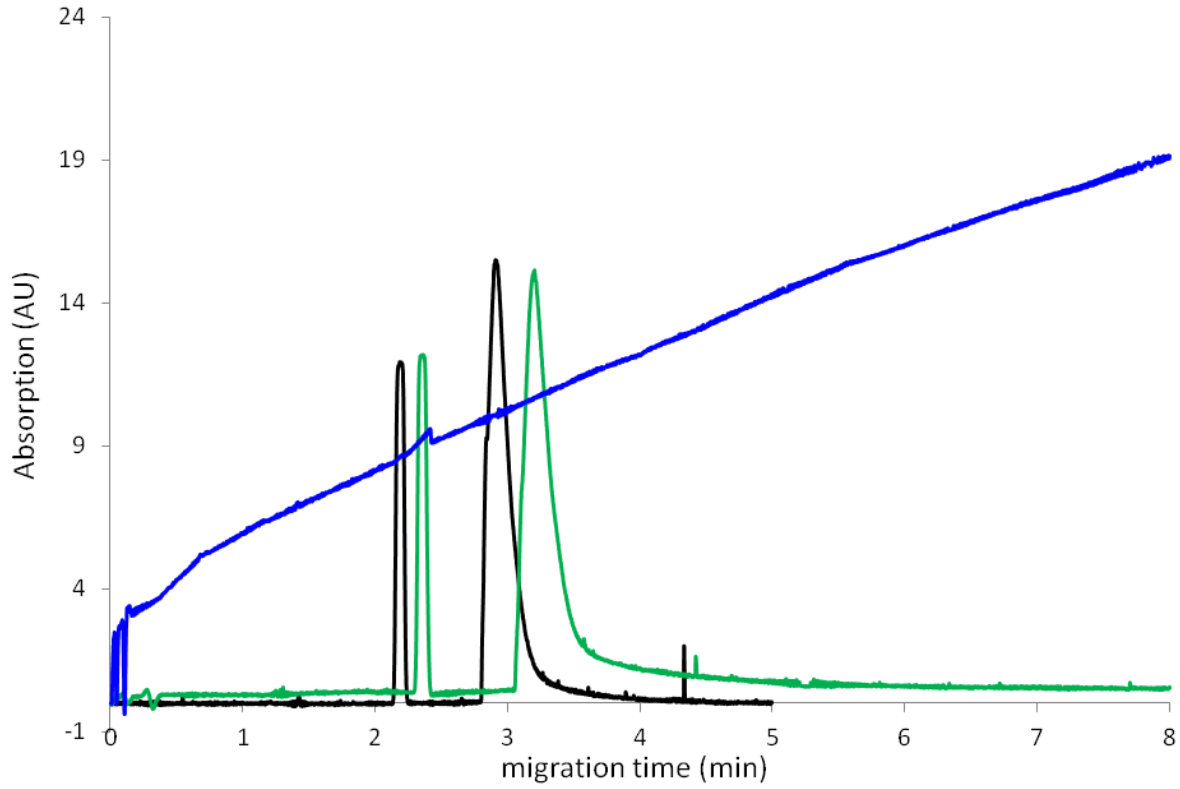

Figure 45. Three electropherograms of acetanilide (first migrated peak) and BSA (second migrated peak). Black: without Rh^{3+} in the running buffer. Blue: with 250 µmol/L of Rh^{3+} in the running buffer. Green: with 25 µmol/L of Rh^{3+} in the running buffer.

Surprisingly, the $\Delta R/R_f$ values of the Rh^{3+} interactions exhibit strong affinity to all proteins at low concentration of 25 µmol/L, especially to MB. On first glance it seems the metal ion Ru^{3+} has similar chemical properties and geometry to Os^{3+}, but indeed it

behaves differently. It did not interact significantly with HSA, β-LG and MB, but weak affinity to BSA and OVA isoforms were observed. The metal ion Ir^{3+} shows very high affinities to BSA and HSA while a weak one with β-LG and not significant ones with MB and OVA isoforms. Hence, several selective binding sites present at BSA and HSA should be taken into account when considering new Ir^{3+} based drugs. Additionally, the influence of the metal ion on protein electropherograms is highly pronounced in case of BSA and HSA after binding with Ir^{3+} since an unresolved new peak appeared before the main peak, see Figure 46. The new peak was more obvious with HSA (Figure 46 A). This might probably indicate significant conformational changes in both proteins after interaction with Ir^{3+}.

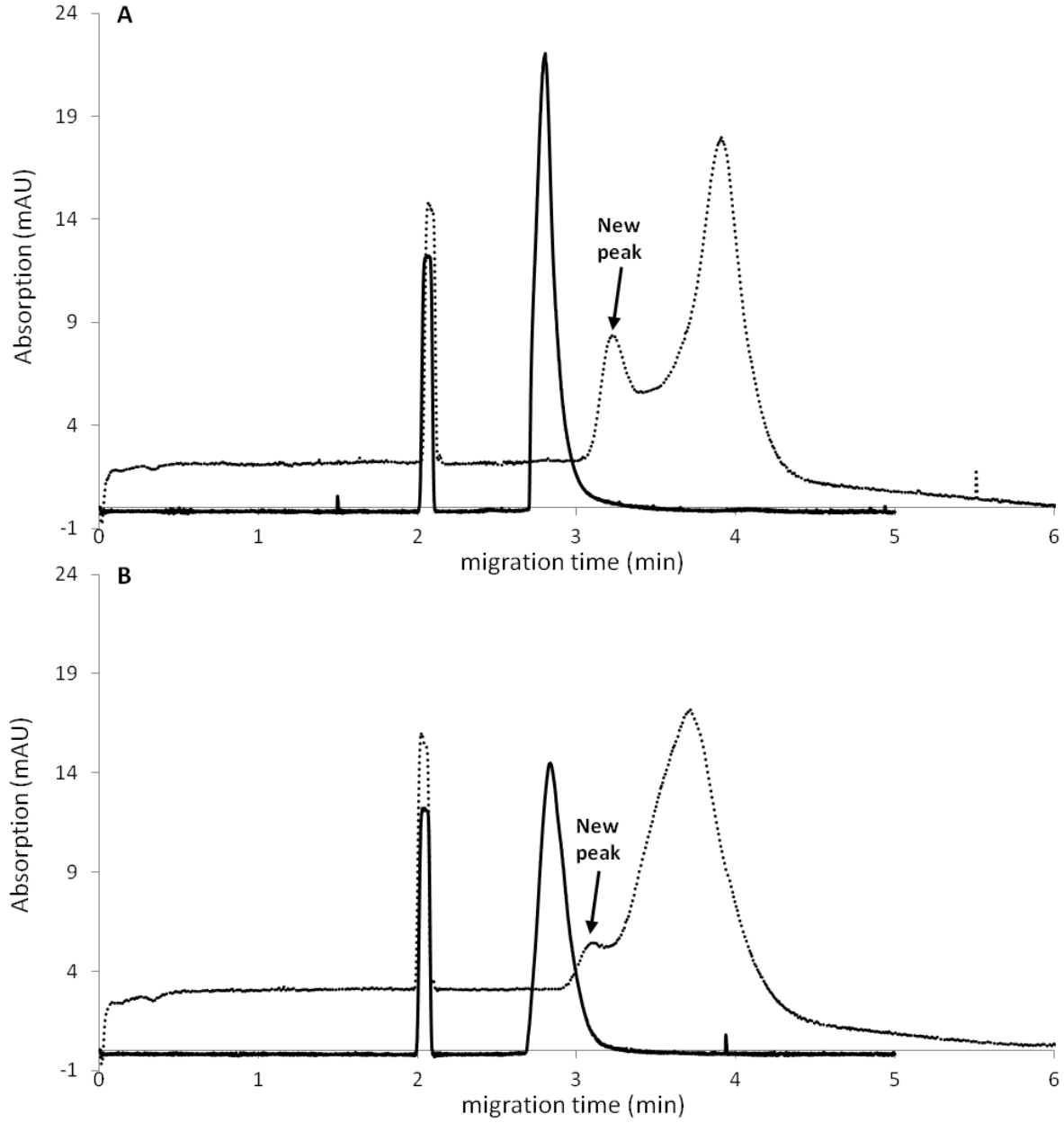

Figure 46. A: electropherograms of acetanilide (first migrated peak) and HSA (second migrated peak). B: electropherograms of acetanilide (first migrated peak) and BSA (second migrated peak). In both A and B, the solid lines show the electrophoretic separation without Ir^{3+} in the running buffer while dotted lines show the electrophoretic separation with Ir^{3+} in the running buffer.

Au^{3+} has various CNs with different geometries (square planar, trigonal bipyramidal, square pyramidal and octahedral) depending on the type of the ligands [51]. Hence, the positive $\Delta R/R_f$ values of the interaction between Au^{3+} and the proteins BSA, HSA and OVA isoforms could be related to these versatile complex geometries of this metal and their fitting, and coordinating mostly with the present functional groups at the binding site. The interactions of Au^{+} with all proteins (except HSA, weak) were not significant. However, this could be due to the formation of gold nanoparticles since the Au^{+} solution became blue immediately during sonication. Probably the effective Au^{+} concentration was decreased. Ag^{+} favors to display CNs of 2, but in some cases further CNs up to 4 might be observed depending on the type of base ligands [51, 59, 127]. Ag^{+} is very soft due to the lower oxidation state. Thus, it favorably interacts with sulfur containing functional groups such as thiol of cysteine and thioether of methionine. The results show significant interactions between Ag^{+} and HSA, MB and OVA isoforms while insignificant interactions were observed with BSA and β-LG. The interaction with MB is highly pronounced, but with negative values of the $\Delta R/R_f$. In general, these results might be helpful to provide insight into the selectivity of each protein to different noble metal ions and preliminary characterization of their binding. A further possible benefit of these results is to provide better information about the possibility to transport noble metal ions to their target binding sites via interactions with transporter proteins such as HSA.

3.2.1.2.2 Other heavy metal ion

In a further screening, the interaction of the given proteins with the biologically essential trace metal ions (Co^{2+}, Cu^{1+}, Cu^{2+}, Ni^{2+}, Fe^{2+}, Fe^{3+}) as well as other interesting metal ions (Cr^{3+}, La^{3+}, V^{3+}) were studied (Figure 44). The metal ions Co^{2+}, Cu^{1+}, Cu^{2+} and Ni^{2+} have similar affinities on the examined proteins, except Ni^{2+} shows stronger binding behavior toward β-LG. No interaction was observed for Co^{2+} on MB. As can be seen in Figure 47, Cr^{3+} showed an unexpected effect since the

EOF has been reversed during the electrophoretic separations with the high concentration of Cr^{3+} (250 µmol/L) . Cr^{3+} can bind strongly to the capillary wall during the run, thereby inducing a positive charge. This can in turn reverse the electroosmotic flow [111]. Therefore, a reduced concentration of 25 µmol/L became necessary for further experiments with this metal ion. Interestingly, Cr^{3+} has strong influence on all proteins even at low concentration. The adduct $CrCl_6^{3-}$ can be formed quickly [51], probably it might also has high affinity to other borderline bases such as histidine, asparagine, glutamine and tryptophan (see Table 1). The high CN of 6 for Cr^{3+} elucidates its negative $\Delta R/R_f$ values for all proteins, except for MB. In this case, a positive $\Delta R/R_f$ value was obtained and probably refers to the number of the borderline functional groups available at the binding sites which tend to coordinate with Cr^{3+} instead of the surrounding anions (e.g. Cl^-).

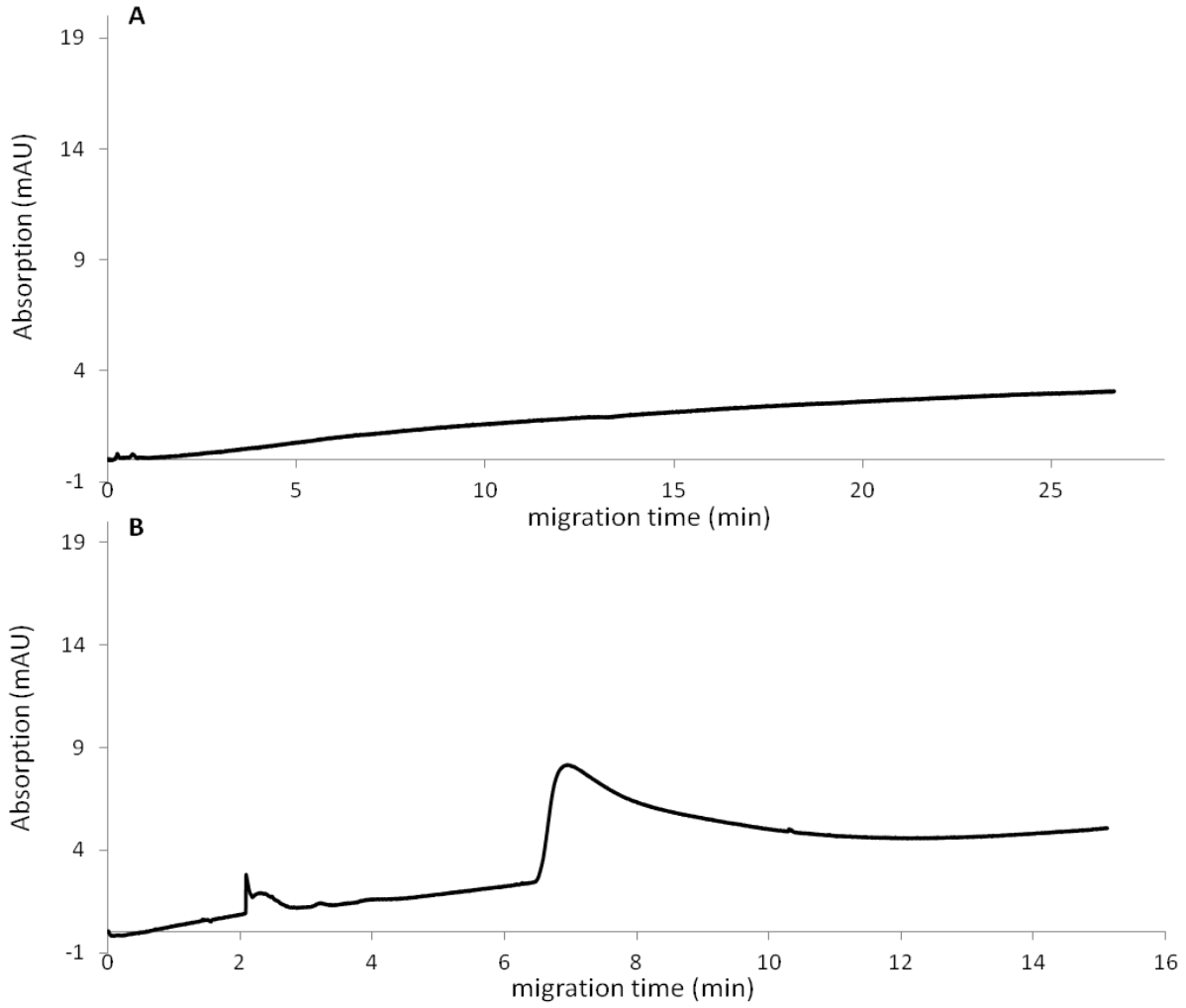

Figure 47. Electropherograms of acetanilide and OVA under the influence of Cr^{3+} (250 µmol/L) using two separation modes, A) normal mode (cathode at the

outlet end of the capillary and B) negative mode (anode at the outlet end of the capillary).

The metal ions Fe^{3+} and Fe^{2+} are involved in various biological complexes. Both oxidation states have different chemical properties which influence their binding site selectivity [51, 128]. The high oxidation state (Fe^{3+}) is favorable to bind at sites rich in amino acid residues containing hard functional groups such as glutamate, aspartate, tyrosine and possibly histidine [129]. On the other hand, Fe^{2+} favorably binds at sites containing borderline acids as the porphyrin site at hemoglobin which is a ring consisting of four pyrrole molcules connected together via methine bridges [51]. In general, both iron ions have significant interaction with all proteins, except MB since there are binding sites of iron ions at MB which are already naturally occupied. As shown in Figure 48, Fe^{3+} has stronger influence on the peak shapes of β-LG than Fe^{2+} since no peak was observed due to extreme broadening, and it was not possible to integrate them.

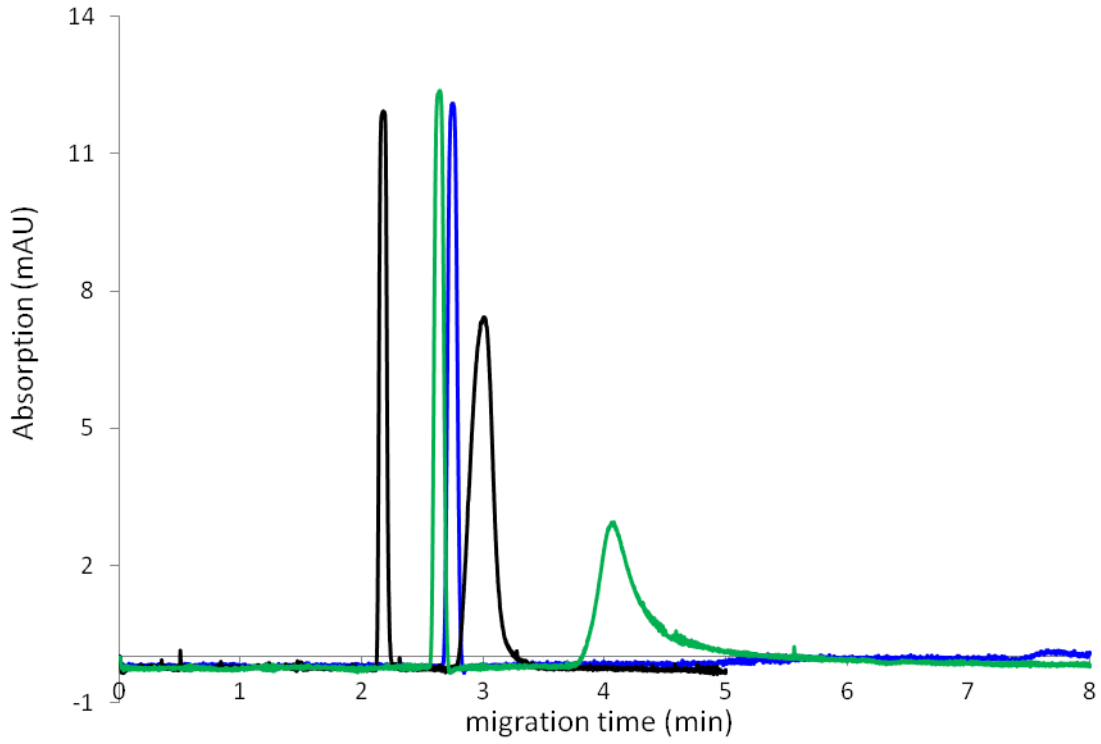

Figure 48. Three electropherograms of acetanilide (first migrated peak) and β-LG (second migrated peak). Black: without iron ions in the running buffer. Blue: with 100 µmol/L of ferric chloride in the running buffer. Green: with 100 µmol/L of ferrous chloride in the running buffer.

The interactions of HSA and the OVA isoforms with Fe^{3+} were weaker than those with Fe^{2+} ions. La^{3+} shows significant and strange influence on the EOF (similar to Cr^{3+}) using the concentration of 250 µmol/L. The EOF extremely decreased over the first three runs and then suddenly increased at the fourth run but then became stable over the subsequent two runs. Therefore, the 10 fold lower concentration of 25 µmol/L was used for further binding investigations. In principle, the interactions with most proteins were not significant, except the interactions with OVA isoforms which were small but significant since their $\Delta R/R_f$ values are more than 0.01. The V^{3+} tends to form complexes with ligands containing oxygen atoms whether neutral as water or anionic as glutamate and aspartate [51]. Therefore, positive values of the *cnf* ($\Delta R/R_f$) were obtained for the interaction of V^{3+} with most proteins, like for Al^{3+} and Ga^{3+} ions, this coordination behavior of V^{3+} using ACE being similar to that obtained on x-ray crystallography studies [130].

3.2.1.3 Anion complexes containing metal and semimetal ions

The essential trace metal ion Mo^{6+} and the cation Se^{4+} are transported and taken up by cell as anion complexes; MoO_4^{2-} and SeO_3^{2-} [131, 132]. The SeO_3^{2-} is formed quickly when dissolving $SeCl_4$ in tris buffer. As shown in Figure 44, both complexes can show significant interactions with BSA and HSA but with different signs of $\Delta R/R_f$ values. Negligible interactions were observed between MoO_4^{2-} and either β-LG or OVA isoforms as well as between both metal complexes (MoO_4^{2-} and SeO_3^{2-}) and MB. However, the mobility of the OVA isoforms was shifted by SeO_3^{2-} indicating significant binding.

4. Summary

4.1 Developing the mobility shift-ACE method

ACE is becoming more popular interested especially for protein-metal ion investigation. For further purposes, a fast, precise and reliable ACE method is highly important. In this work, the ACE method has been successfully optimized and accelerated by using a short capillary, a proper rinsing protocol, a low sample concentration and a small injection volume.

The ACE method transfer has been studied as well. Intra-instrument ACE transfer from the long to the accelerated method using a short capillary was successfully achieved on the same CE instrument without challenges. Transfers between different instruments showed different results due to the variation in the capillary cooling system designs. However, a successful inter-instrument ACE method transfer was achieved by adjusting the temperature setting of the capillary cooling system. The variation in the concentration of sodium hydroxide in the rinsing protocol and the room temperature can also affect the ACE method transfer.

Precision has been further improved by considering a short rinsing protocol, sample pushing, extra flushing procedures after several subsequent runs and refreshing inlet and outlet buffer solutions. The use of 0.1 M EDTA within the rinsing protocol has been found to be highly useful to succeed in long-term good precision.

The obtained optimum conditions of the accelerated ACE method are as following: sample injection at 50 mbar for 4.5 s followed by buffer sample pushing at 50 mbar for 2.5 s, a short rinsing protocol at 2.5 bar with solution consisting of 0.1 N sodium hydroxide and 0.1 M EDTA for 2.5 min, water for 1 min, and running buffer for 1.5 min. Extra flushing at 2.5 bar with 0.1 N sodium hydroxide for 10 min and water for 5 min after each 60 subsequent runs and refreshing the buffer solutions after each 30 subsequent runs should also be employed to improve the repeatability of the results. Excellent precision for mobility ratios was achieved for all protein-metal ion interactions (RSD% of 0.05-1.0%, $n > 324$). This method has several advantages such as fast screening, easy transfer between different instruments and moderate costs. Furthermore, it offers simultaneously investigation for metal ion interactions with a number of proteins in one sample due to the high separation power of the technique. Therefore, it can be now used for routine screening to investigate different interesting protein-metal ion interactions by ACE.

4.2 Applications

The accelerated ACE method has been successfully used for investigating a wide range of metal ions (28 metal ions) with five proteins, BSA, β-LG, HSA, MB and OVA. All results have been summarized as $\Delta R/R_f$ chart. This chart is very useful for deep and precise comparisons. All of the observed interaction results were successfully discussed in view of the properties of the metal ions and proteins, and the HSAB theory as well. For a given metal ion, the oxidation state, its coordination numbers and its geometry have high impact on the interaction with the various proteins. The $\Delta R/R_f$ values of the interaction of the comprehensive set of metal ions with a selection of relevant test proteins provide a preliminary knowledge about the general binding properties of these metal ions with different proteins. The $\Delta R/R_f$ values became interesting when increasing the valency and the ionic radius of the metal ions of groups aI and aII. In general, most of the tested protein-metal ion interactions showed negative $\Delta R/R_f$ values. These could probably be due to the coordination capability of the metal ions and positions of their binding sites. For example, binding sites at the surface of the protein could facilitate coordination with the background anions leading to negative $\Delta R/R_f$, while binding sites inside the protein could facilitate coordination with potential ligands (amino acid residues) leading to positive $\Delta R/R_f$. Furthermore, metal ions such as Al^{+3}, Ga^{+3} and V^{+3} possibly prefer to coordinate with the neutral molecule containing oxygen such as water. Accordingly, positive $\Delta R/R_f$ values were obtained in case Al^{+3}, Ga^{+3} and V^{+3}. These results confirm the capability of the accelerated mobility shift-ACE method to preliminary characterize certain protein-metal ion interactions. Furthermore, some metal ions have specific behaviours such as Rh^{3+}, Cr^{3+}, which showed strong interaction even at low concentration. Furthermore, Ir^{3+} showed strong influence on the overall charge and confirmation of serum albumins, BSA and HSA. Other future in-vitro studies using this mobility-shift ACE method for the binding of different metal ions to enzymes (such as some redox enzymes) could offer preliminary insight about enzyme selectivity to different metal ions. This might probably be helpful for the first stage development of new organometallic compounds for the treatment of certain diseases.

5. References

[1] H. Lodish, A. Berk, P. Matsudaira, C. A. Kaiser and M. Krieger, *Molecular Cell Biology*, W. H. Freeman, New York, 5th Edn., **2003**.

[2] D. L. Nelson and M. M. Cox, in *Lehninger Principles of Biochemistry*, W. H. Freeman, New York, 4th Edn., **2005**.

[3] N. Gregersen, P. Bross, S. Vang, J. H. Christensen, *Annu. Rev. Genomics Hum. Genet.*, **2006**, 7, 103–24.

[4] V. Bellotti, M. Stoppini, *Open Biol. J.,* **2009**, *2,* 228-234.

[5] M. Hung, W, Link, *J. Cell Sci.*, **2011**, 124, 3381–3392.

[6] L. C. Walker, H. LeVine, *J. Biol. Chem.*, **2012**, 287, 33109 –33115.

[7] L. Breydo , J. W. Wu, V. N. Uversky, *Biochim. Biophys. Acta*, **2012**,1822, 261–285.

[8] F. M. LaFerla, K. N. Green, S. Oddo, *Nat. Rev.*, **2007**, 8, 499-509.

[9] M.J. Stuart, R. L. Nigel, *Lancet*, **2004**, 364, 1343–1360.

[10] N. Rifai, M. A. Gillette, S. A. Carr, *Nat. Biotechnol.*, **2006**, 24, 971-983.

[11] I. M Tomlinson, *Nat. Biotechnol.*, **2004**, 22, 521-522.

[12] J. M. Ritter, L. D. Lewis, T. G. Mant and A Ferro, *A Textbook of Clinical Pharmacology and Therapeutics*. Hodder Arnold, London, 5th edn., **2008**.

[13] R. A. Lewis, *CRC dictionary of agricultural sciences*, CRC Press LLC, Florida, 1st edn., **2002**.

[14] B. Kuhlman, G. Dantas, G. C. Ireton, G. Varani, B. L. Stoddard, D. Baker, *Science*, **2003**, 302,1364-8.

[15] C. Dennison, *A Guide to Protein Isolation*, Kluwer Acad., Pub., New York, **2002**.

[16] W. Wang, S. Nema, D. Teagarden, *Int. J. Pharm.*, **2010**, 390, 89–99.

[17] W. Bal, M. Sokołowska, E. Kurowska, P. Faller, *Biochim. Biophys. Acta*, **2013**, 1830, 5444–5455.

[18] X. M. He, D. C. Carter, Nature, **1992**, 358, 209-215.

[19] C. D. Carter and J. X. Ho, *Structure of serum albumin. In Advances in Protein Chemistry*, Academic Press, New York, 153–203, **1994**.

[20] B. X. Huang, H. Kim, C. Dass, *J. Am. Soc. Mass Spectrom*, **2004**, 15, 1237–1247.

[21] N. El Kadi, N. Taulier, J. Y. Le Huérou, M. Gindre, W. Urbach, I. Nwigwe, P. C. Kahn, M. Waks, *Biophys. J.*, **2006**, 91, 3397–3404.

[22] J. Steinhardt, J. Krijn, J. G. Leidy, Biochemistry , **1971**, 10, 4005-4014.

[23] T. peters, *All about albumin, biochemistry, genetics and medical applications*, Academic Press, California, **1992**.

[24] M. R. Duff, C. V. Kumar, *Metallomics*, **2009**, 1, 518–523.

[25] D. Abd El-Hady, H.M. Albishri, *J. Chromatogr. B.*, **2012**, 911, 80– 185.

[26] G. Kontopidis, C. Holt, L. Sawyer, J Dairy Sci., **2004**, 87, 785-96.

[27] B. Y. Qin, M. C. Bewley, L. K. Creamer, H. M. Baker, E. N. Baker, G. B. Jameson, *Biochemistry*, **1998**, *37,* 14014-14023.

[28] S. Brownlow, J. H. M. Cabral, R. Cooper, D. R. Flower, S. J. Yewdall, I. Polikarpov, L. Sawyer, *Structure*, **1997**, 5, 481–495.

[29] J. B. Wittenberg, B. A. Wittenberg, *J. Exp. Biol.*, 2003, 206, 2011-2020.

[30] T. Suzuki، K. Imai, *Cell. Mol. Life Sci.*, **1998**, 54, 979–1004.

[31] G. A. Ordway, D. J. Garry, *J. Exp. Biol.*, **2004**, 207, 3441-3446.

[32] C. A. Nesbitt, K. Yeung, *Analyst*, **2009**, 134, 65–71

[33] J. A. Huntington, P. E. Stein, *J. Chromatogr. B*, **2001**, 756, 189 –198.

[34] A. D. Nisbet, R. H. Saundry, A. J. G. Moir, L. A. Fothergill, John E. Fothergill, Eur J. Biochem.,**1981**, 115, 335-345.

[35] E. R. B. Smith, *J. Biol. Chem.*, **1935**, 108, 187-194.

[36] A. C. C. Alleoni, Sci. Agric., **2006**, 63, 291-298.

[37] C. Swart, Anal. Bioanal. Chem., **2013**, 405, 5697–5723.

[38] S. Mounicou, J. Szpunar, R. Lobinski, *Chem. Soc. Rev.*, **2009**, 38, 1119–1138.

[39] C. Andreini, I. Bertini, G. Cavallaro, G. L. Holliday, J. M. Thornton, *J, Biol. Inorg. Chem.*, **2008**, 13, 1205–1218.

[40] H. Sun, Z. Chai, *Annu. Rep. Prog. Chem. Sect. A*, **2010**, 106, 20–38.

[41] C. M. L. Carvalho, E. Chew, S. I. Hashemy, J. Lu, A. Holmgren, *J. Biol. Chem.*, **2008**, 283, 11913-11923.

[42] I. Romero-Canelon, P. J. Sadler, *Inorg. Chem.*, **2013**, 52, 12276−12291.

[43] M. Frezza, S. Hindo, D. Chen, A. Davenport, S. Schmitt, D. Tomco, Q. P. Dou, *Curr. Pharm. Des.*, **2010**, 16, 1813–1825.

[44] D. Chen, V. Milacic, M. Frezza, Q. P. Dou, *Curr. Pharm. Des.*, **2009**, 15, 777–791.

[45] M. J. Hannon, *Pure Appl. Chem.*, **2007**, 79, 2243–2261.

[46] B. Desoize, *Anticancer Res.*, **2004**, 24, 1529-1544.

[47] T. Dudev, C. Lim, *Chem. Rev.*, **2014**, 114, 538−556.

[48] T. Dudev, C. Lim, *Annu. Rev. Biophys.*, **2008**, 37, 97–116.

[49] J. P. Glusker, A. K. Katz, C. W. Bock., *Rigaku J.*, **1999**. 16, 8-17.

[50] D. R. Gamer, N. Gresh, *J. Am. Chem. SOC.*, **1994**, 116, 3556-3567.

[51] A. F. Holleman, E. Wiberg, *in inorganic chemistry*, Academic press, California, , 1st English edn., **2001**.

[52] C. W. Bock, A. K. Katz, J. P. Glusker, *J. Am. Chem. SOC.*, **1995**, 117, 3754-3765

[53] R. G. Pearson, *J. Am. Chem. SOC.*, **1963**, 85, 3533-3539.

[54] J. A. Lemire, J. J. Harrison, R. J. Turner, *Nature Rev. Microbiol.*, **2013**, 11, 371–384.

[55] R. M. LoPachin, T. Gavin, A. DeCaprio, D. S. Barber, *Chem. Res. Toxicol.*, **2012**, 25, 239–251.

[56] J. D. Hoeschele, J. E. Turner, M. W. England, *Sci Total Environ.*, **1991**, 109/110, 477-492

[57] Y. S. Babu, C. E. Bugg, W. J. Cook, *J. Mol. Biol*., **1988**, 204, 191-204.

[58] H. M. Greenblatt, H. Feinberg, P. A. Tucker, G. Shoham, *Acta Cryst.*, **1998**, D54, 289-305.

[59] S. K. Singh, S. A. Roberts, S. F. McDevitt, A. Weichsel, G. F. Wildner, G. B. Grass, C. Rensing, W. R. Montfort, *J. Biol. Chem.*, **2011**, 286, 37849-37857.

[60] G. Kuppuraj, M. Dudev, C. Lim, *J. Phys. Chem. B*, **2009**, 113, 2952–2960.

[61] M. Dudev, J. Wang, T. Dudev and C. Lim. *J. Phys. Chem. B*, **2006**, 110, 1889-1895.

[62] R. D. Shannon, *Acta Cryst.*, **1976**, A32, 751-767.

[63] S. E. Harding, B. Z. Chowdhry, *Protein-Ligand Interactions: A Practical Approach Volume 1: Hydrodynamics and Calorimetry*, Oxford Univ. press Inc., New York, **2001**.

[64] G. Grasso, G. Spoto, *Anal. Bioanal. Chem.*, **2013**, 405, 1833–1843.

[65] Y. Cao, K. S. Er, R. Parhar, H. Li, *ChemPhysChem*., **2009**, 10, 1450 –1454.

[66] M. R. Jensen, M. A. S. Hass, D. F. Hansen, J. J. Led, *Cell. Mol. Life Sci*., **2007**, 64, 1085 – 1104.

[67] P. Gourdon, X. Liu, T. Skjørringe, J. P. Morth, L. B. Møller, B. P. Pedersen, P. Nissen, *Nature*, **2011**, 475, 59–65.

[68] X. Zhang, H. Tang, C. Ye, M. Liu., *Drug Discov. Today Technol.*, **2006**, 3, 241-245.

[69] R. Bauer, A. Muller, M. Richter, K. Schneider, J. Frey, W. Engelhardt, *Biochim. Biophys. Acta.*, **1997**, 1334, 98–108.

[70] S. Dudal, D. Baltrukonis, R. Crisino, M. J. Goyal, A. Joyce, K. Österlund, J. Smeraglia, Y. Taniguchi, J. Yang, *AAPS J.*, **2014**,16, 194–205.

[71] D. S. Hage, *Clin. Chem.*, **1999**, 45, 5593–5615.

[72] S. Lin, L. R. Drake, G. D. Rayson, Anal. Chem., **1996**, 68, 4087-4093.

[73] S. Redweik, Y. Xu, H. Wätzig, Electrophoresis, **2012**, 33, 3316–3322.

[74] S. Redweik, C, Cianciulli, M. Hara, Y. Xu, H. Wätzig, Electrophoresis, **2013**, 34, 1812–1819.

[75] Y. Xu, S. Redweik, D. A. El-Hady, H. M. Albishri, L. Preu, H. Wätzig, Electrophoresis, **2014**, 34, 2203–2212.

[76] S. El Deeb, H. Wätzig, D. A. El-Hady, *Trends Anal. Chem.*, **2013**, 48, 112-131.

[77] M. Zhang, D. R. Gumerov, I. A. Kaltashov, A. B. Mason, *J. Am. Soc. Mass. Spectrom.*, **2004**, 15, 1658–1664.

[78] P. Hu, Q. Ye, J. A. Loo, *Anal. Chem*. **1994**, 66, 4190-4194.

[79] W.D. Lehmann, J. Wei, C. Hung, H. Gabius, D. Kirsch, B. Spengler, D. Kbüler, *Rapid Commun. Mass Spectrom.*, **2006**, 20, 2404–2410.

[80] J. Yang, D. S. Hage, *J. Chromatogr. A*, **1997**, 766, 15–25.

[81] A. Chattopadhyay, T. Tian, L. Kortum, D. S. Hage, *J. Chromatogr. B*, **1998**, 715, 183–190.

[82] Y. T. Oester, S. Keresztes-Nagy, R.F. Mais, J. Becktel, J.F. Zaroslinski, *J. Pharm. Sci.* **1976**, 65,1673-7.

[83] G. G. Mironov, J. Logie, V. Okhonin, J. B. Renaud, P. M. Mayer, M. V. Berezovski, *J. Am. Soc. Mass Spectrom*., **2012**, 23, 1232-1240.

[84] N. H. H. Heegaard, S. Nilsson, N. A. Guzman, J. Chromatogr. B, **1998**, 715, 29–54.

[85] D. El-Hady, S. Kühne, N. El-Maali, H. Wätzig. *J. Pharm. Biomed. Anal.*, **2010**, 52, 232–241.

[86] H. Wätzig, S. Günter, *Clin. Chem. Lab. Med.*, **2003**, 41, 724–738.

[87] S. Ahuja, M. I. Jimidar, *Capillary Electrophoresis Methods in Pharmaceutical Analysis*, Academic Press, Burlington, **2008**.

[88] European Pharmacopoeia, **2005**, Suppl. 5.1, 74–79.

[89] A. S. Erin, R. J. Doherty, M. N. Meagher, A. E. B. Albarghouthi, *Electrophoresis*, **2003**, 24, 34–54.

[90] J. E. Melanson, N. E. Baryla, C. A. Lucy, *Trends Anal. Chem.*, **2001**, *20*, 365–374.

[91] J. Znaleziona, J. Petr, R. Knob, V. Maier, J. Sevcik, *Chromatographia*, **2008**, *67*, S5–S12.

[92] T. Takayanagi, E. Wada, S. Motomizu, *Analyst*, **1997**,122, 57–62.

[93] R. H. H., Neubert, H. H. Rüttinger, *Affinity Capillary Electrophoresis in Pharmaceutics and Biopharmaceutics*, Marcel Dekker Inc., New York, **2003**.

[94] S. M.Lunte, D. M.Radzik, *Pharmaceutical and Biomedical Applications of Capillary Electrophoresis*, Elsevier Science Ltd, Boulevard, 1st Edn., **1996**.

[95] H. Wätzig, M. Degenhardt, A. Kunkel, *Electrophoresis*, **1998**, 19, 2695-2752.

[96] H. M Albishri, S. El Deeb, N. AlGarabli, R. AlAstal, H. A. Alhazmi, M. Nachbar, D. Abd El-Hady, H, Wätzig, Bioanalysis, **2014**, 6, 3369-3392.

[97] Y. Chu, L. Z. Avila, J. Gao, G. Whitesides, *Acc. Chem. Res.*,**1995**, 28, 461-468.

[98] K. L. Rundlett, D. W. Armstrong, *Electrophoresis*, **2001**, 22, 1419-1427.

[99] Rundlett, K. L., Armstrong, D. W., *Electrophoresis,* **1997**, 18, 2194-2202.

[100] W. Tseng, H. Chang, S. Hsu, R. Chen, S. Lin, *Electrophoresis*, **2002**, 23, 836–846.

[101] N. H. H. Heegaard, *Electrophoresis*, **2003**, 24, 3879–3891.

[102] X. He, Y. Ding, D. Li, B. Lin, *Electrophoresis*, **2004**, 25, 697–711.

[103] C. Schou, N. H. H. Heegaard, *Electrophoresis*, **2006**, 27, 44–59.

[104] C. Jiang, D.W. Armstrong, *Electrophoresis*, **2010**, 31, 17–27.

[105] Z., Chen, S. G. Weber, *Trends Anal. Chem*., **2008**, 27, 738–748.

[106] X., He, Y. Ding, D. Li, B. Lin, *Electrophoresis*, **2004**, 25, 697–711.

[107] J. Towns, F. Regnier, *Anal. Chem.*, **1992**, 64, 2473-2478.

[108] J. Towns, F. Regnier, *Anal. Chem.*, **1991**, 63, 1132-1138.

[109] S. Ghosal, *Anal. Chem.*, **2002**, 74, 771-775.

[110] F., Gomez, L. Avila, Y. Chu, G. Whitesides, *Anal. Chem.*, **1994**, 66, 1785-179.

[111] R. Brechtel, W. Hohmann, H. Rüdiger, H. Wätzig, *J. Chromatogr. A,* **1995**, 716, 97-105.

[112] B. Verzola, C. Gelfi, P. G. Righetti, *J. Chromatogr. A*, **2000**, 868, 85–99.

[113] H. Wätzig, S. Kaupp, M. Graf, *Trends Anal. Chem.,* **2003**, 22, 588–604.

[114] R.H. Levy, D. Schmidt, *Epilepsia*, **1985**, 26, 199–205.

[115] K. L. Rundlett, D. W. Armstrong, *J. Chromatogr. A*, **1996**, 721, 173-186.

[116] J. Ermer, M. Limberger, K. Lis, H. Wätzig, *J. Pharm. Biomed. Anal.*, **2013**, 85, 262–276.

[117] M. E. Bohlin, L. G. Blomberg, N. H. H. Heegaard, Electrophoresis, **2011**, 32, 728–737.

[118] M. U. Musheev, Y. Filiptsev, S. N. Krylov, *Anal. Chem.*, **2010**, 82, 8692–8695.

[119] M. Berezovski, S. N. Krylov, *Anal. Chem.*, **2004**, 76, 7114-7117.

[120] C. Cianciulli, H. Wätzig, *Electrophoresis*, **2012**, 33, 1499-1508.

[121] C. J. Evenhuis, M. U. Musheev, S. N. Krylov, *Anal. Chem.*, **2011**, 83, 1808–1814.

[122] M. Geiger, A. L. Hogerton, M. T. Bowser, *Anal. Chem.*, **2012**, 84, 577−596.

[123] K. H. Patel, C. J. Evenhuis, L. T. Cherney, S. N. Krylov, *Electrophoresis*, **2012**, 33, 1079–1085.

[124] C. J. Evenhuis, M. U. Musheev, S. N. Krylov, *Anal. Chem.*, **2010**, 82, 8398–8401.

[125] H. W. Richardson, *Handbook of Copper Compounds and Applications*, Marcel Dekker Inc., New York, **1997**.

[126] T. Kumarevel, H. Mizuno, P. K. R. Kumar, *Nucleic Acids Res.*, **2005**, 33, 5494–5502.

[127] I. R. Loftin, S. Franke, N. J. Blackburn, M. M. Mcevoy, Protein Sci., **2007**, 16, 2287– 2293.

[128] S. H. Laurie, *J. Inher. Metab.*, **1983**, 6, 9–14.

[129] D. R. Hall, J. M. Hadden, G. A. Leonard, S. Bailey, M. Neu, M. Winn, P. F. Lindley, *Acta Cryst.*, **2002**, D58, 70–80.

[130] T. Lai, M. Wang, L. Wang, H. Sun, *J. Biol. Inorg. Chem.*, **2014**, 19, S833–S852.

[131] R. R. Mendel, T. Kruse, *Biochim. Biophys. Acta*, **2012**, 1823, 1568–1579.

[132] H. Zeng, M. I. Jackson, W. Cheng, G. F. C. Jr, *Biol. Trace Elem. Res.*, **2011**, 143, 1209–1218.

HASSAN AHMAD M. ALHAZMI, PhD student

Institute of Medicinal and Pharmaceutical Chemistry

Technical University of Braunschweig

Germany

Mob: (+49) 1-7670664816

Email: h.alhazmi@tu-braunschweig.de

PROFILE

- PhD student at Institute of Medicinal and Pharmaceutical Chemistry, Technical University of Braunschweig, Germany.
- One of the academic staff at Department of Pharmaceutical Chemistry, Jazan University, Saudi Arabia.
- Extensive R&D experience and outstanding teaching and laboratory capabilities.
- Proficient with operations and interpretations of HPLC-Triple Quadrupole Mass Spectrometer, HPLC-Ion Trap Mass Spectrometer, different modes of capillary electrophoresis and Spectrophotometric techniques.
- Proficient with interpretations the protein-ligand interaction data of different techniques such as Mass Spectrometer and affinity capillary electrophoresis.
- Extensive experience to work independently and to perform most research assignments.
- Proficient with different office and many chemistry related software's.
- Versatile and dynamic, able to work independently, if possible.
- Critical thinker, organizer-team player and self motivated.
- Ability to learn new techniques and to respond under pressure and maintain composure under difficult conditions.

LABORATORY EXPERIENCE

- Extensive experience in coordinating undergraduate courses and practical's.
- Analysis of ACE, LC-MS and HPLC results and provide supervisor with information for projects and application of analytical techniques to the solution of a wide variety of problems in field of drug quality control and protein-ligand interactions or any interesting interactions.

- Maintenance of laboratory equipment and supplies and promotes continuous improvement of workplace safety and environmental practices.
- Extensive method developments, optimization of entire protocols to investigate different protein-metal ion interactions by affinity capillary electrophoresis.
- Extensive method development, optimization of reaction protocols, related substances and impurity profiles in drug molecules by HPLC-UV, LC-MS and CE.
- Preparative HPLC and enrichment techniques like liquid-liquid extraction.
- Managing day to day operations of the laboratory, designing experiments to ensure data integrity, quality control, method development plans and protocol compliance.
- Responsible for setting up new instruments such as LC-MS and capillary electrophoresis as well as for maintenance and troubleshooting of the instrumentation. Maintained Standard operating procedures (SOP) for lab instrumentation.
- Performed inventory and samples record keeping as well as maintaining library.

TEACHING EXPERIENCE

- 2005–2007: Department of Pharmaceutical Chemistry, College of Pharmacy, Jazan University, Saudi Arabia.
- 3/2011–11/2011: Department of Pharmaceutical Chemistry, College of Pharmacy, Jazan University, Saudi Arabia.
- Supervising internship students in 2012, 2013 and 2014: Institute of Medicinal and Pharmaceutical Chemistry, Technical University of Braunschweig, Germany.

EDUCATION

Master's Degree M. Sc. in Pharmaceutical Chemistry (Analysis) – College of Pharmacy, King Saud University, Riyadh, Saudi Arabia (GPA: 4.67/5.0) (2011).

B. Sc. in Parmacy - Bachelor of Pharmacy (General pharmacy, very good) – College of Pharmacy, King Saud University, Riyadh, Saudi Arabia (GPA: 3.96/5.0) (2005).

OTHER CERTIFICATES & TRAININGS

- Hospital pharmacy training, Riyadh, Saudi Arabia, 2005.
- Community pharmacy training, 2005.

- Diploma of clinical instructor program (very good), General Directorate of the Health Colleges and Institutes, Ministry of Health, Saudi Arabia, 2007.
- Communication skills (Networking for maximum effect), Grade life program, Technical University of Braunschweig, Germany, 2012.
- Deutsche course, level A1, Languages center, Technical University of Braunschweig, Germany, 2013.
- Short course about fundamental of mass spectrometry, Amsterdam, Netherlands, 2013.
- User training on the PrinCE-C 760 instrument, Institute of Medicinal and Pharmaceutical Chemistry, Technical University of Braunschweig, Germany, 2013.
- Recent development in CE and CE-MS (Workshop), Drug analysis, Liege, Belgium, 2014.

PUBLICATIONS

- Alhazmi, H. A., Makeen H. & El Deeb, S. Determination of varenicline by capillary zone electrophoresis. Dig. J Nanomater Bios. 8: 295-301 (2013).
- Kadi, A. A., Kassem, M. G., Makeen H. A. & Alhazmi, H. A. Simultaneous determination of Phenytoin and Lamotrigine in Human Plasma using Hydrophilic Interaction Liquid Chromatography-Triple Quadrupole Mass Spectrometry. Dig. J Nanomater Bios. 8: 1113-1122 (2013).
- Alhazmi, H. A., Nachbar, M., Albishri H. M., Abd El-Hady, D., Redweik, S., El Deeb, S. & Wätzig, H. A comprehensive platform to investigate protein-metal ion interactions by affinity capillary electrophoresis. J. Pharm. Biomed. Anal. 107: 311–317 (2015).
- Albishri, H. M., El Deeb, S., AlGarabli, N., AlAstal, R., Alhazmi H. A., Nachbar, M., Abd El-Hady, D. & Wätzig, H. Recent advances in affinity capillary electrophoresis for binding studies, Bioanalysis 6: 3369-3392 (2014).
- Alhazmi, H. A., El Deeb, S., Nachbar, M., Redweik, S., Albishri H. M., Abd El-Hady, D. & Wätzig, H. Affinity capillary electrophoresis: acceleration, method transfer and precision improvement for protein-metal ion interactions. **Submitted to Journal of Separation science (2015).**
- Audioslides**:** Alhazmi, H. A., El Deeb, S. & Wätzig, H. A comprehensive platform to investigate protein-metal ion interactions by affinity capillary electrophoresis. Elsevier B. V. (2015).

PARTICIPATIONS

- Alhazmi, H. A. & Kadi, A. A.: The effect of different HILIC stationary phases on the ionization efficacy of some antiepileptic drugs. (Oral). 4th Portuguese Mass Spectrometry Meeting, Lisboa (2010).
- Alhazmi, H. A. & Kadi, A. A.: Simultaneous determination of Carbamazepine and Vigabatrin in Human Plasma using Hydrophilic Interaction Liquid Chromatography-Triple Quadrupole Mass Spectrometry. (poster). 4th Portuguese Mass Spectrometry Meeting, Lisboa (2010).
- Alhazmi, H. A. & Kadi, A. A.: Simultaneous determination of Phenytoin and Lamotrigine in Human Plasma using Hydrophilic Interaction Liquid Chromatography-Triple Quadrupole Mass Spectrometry. (poster). 4th Portuguese Mass Spectrometry Meeting, Lisboa (2010).
- Wätzig, H., Alhazmi, H. A., Nachbar, M., Abd El-Hady D. & Redweik, S.: Fast and validated Affinity Capillary Electrophoresis for routine binding screening assays. (poster) CEPH34-MO. HPLC 2013, Amsterdam (2013).
- Alhazmi, H. A., Nachbar, M., Albishri H. M., Abd El-Hady, D., El Deeb, S, Redweik, S. & Wätzig, H.: Investigation for successful ACE method transfer. (poster) P7. CE-Forum, Jena (2013).
- Alhazmi, H. A., Nachbar, M., Albishri H. M., Abd El-Hady, D., El Deeb, S., Redweik, S. & Wätzig, H.: Investigation for successful ACE method transfer. (poster) AC10. DPhG annual meeting, Freiburg (2013).
- Nachbar, M., Alhazmi, H. A., Abd El-Hady, D., Albishri H. M., Redweik, S. & Wätzig, H.: Fast screening for protein-ion interactions using affinity capillary electrophoresis. (poster) AC05. DPhG annual meeting, Freiburg (2013).
- Alhazmi, H. A., Nachbar, M., El Deeb, S., Abd El-Hady, D., Albishri H. M. & Wätzig, H.: Investigations of metalloproteins and their interactions by Affinity Capillary Electrophoresis. (oral) OC03. Drug analysis, Liege (2014).
- Alhazmi, H. A., Nachbar, M., El Deeb, S., Abd El-Hady, D., Albishri H. M. & Wätzig, H.: Affinity Capillary Electrophoresis (ACE) as Reliable Technique for Studying Protein-Metal Interactions. (poster) AS14. Drug analysis, Liege (2014).
- Alhazmi, H. A., Nachbar, M., Mozafari, M., Redweik, S., El Deeb, S., Abd El-Hady, D., Albishri H. M. & Wätzig, H.: A comprehensive platform to investigate protein-metal ion interactions by affinity capillary electrophoresis (ACE). (oral) OP 37. EuroBIC12, Zurich (2014).

- Alhazmi, H. A., Nachbar, M., El Deeb, S., Abd El-Hady, D., Albishri H. M. & Wätzig, H.: Affinity Capillary Electrophoresis (ACE) for Fast Prediction of Protein Selectivity to Metal Ions. (poster) P 295. EuroBIC12, Zurich (2014).
- Alhazmi, H. A., Nachbar, M., Mozafari, M., Redweik, S., El Deeb, S., Abd El-Hady, D., Albishri H. M. & Wätzig, H. Fast Estimation for Cellular Metal Ion Uptake Using Affinity Capillary Electrophoresis (ACE). (poster) MC 24. DPhG annual meeting, Frankfurt (2014).